Gori Yuri

Stable isotope dendrochronology in stressed trees: insights into plant-pest interactions and physiological functions during tree life

11/2014

Università degli Studi di Padova

GORI YURI

Stable isotope dendrochronology in stressed trees: insights into plant-pest interactions and physiological functions during tree life

Corso di Dottorato in Scienze delle Produzioni Vegetali

11/2014

UNIVERSITÀ
DEGLI STUDI
DI PADOVA

Dipartimento di *Agronomia Animali Alimenti Risorse Naturali e Ambiente (DAFNAE)*

CORSO DI DOTTORATO DI RICERCA IN SCIENZE DELLE PRODUZIONI VEGETALI
INDIRIZZO: PROTEZIONE DELLE COLTURE
CICLO: XXV

Stable isotope dendrochronology in stressed trees: insights into plant-pest interactions and physiological functions during tree life

Direttore del corso : Ch.mo Prof. Antonio Berti
Coordinatore d'indirizzo : Ch.mo Prof. Francesco Favaron
Supervisore : Ch.mo Prof. Andrea Battisti
Co-supervisori : Dr.ssa Federica Camin, Dr. Nicola La Porta

Dottorando : Yuri Gori

Gennaio, 2014

Declaration

I hereby declare that this submission is my own work and that, to the best of my knowledge and belief, it contains no material previously published or written by another person nor material which to a substantial extent has been accepted for the award of any other degree or diploma of the university or other institute of higher learning, except where due acknowledgment has been made in the text.

Yuri Gori, 16th January 2014

A copy of the thesis will be available at *http://paduaresearch.cab.unipd.it/*

Dichiarazione

Con la presente affermo che questa tesi è frutto del mio lavoro e che, per quanto io ne sia a conoscenza, non contiene materiale precedentemente pubblicato o scritto da un'altra persona né materiale che è stato utilizzato per l'ottenimento di qualunque altro titolo o diploma dell'università o altro istituto di apprendimento, a eccezione del caso in cui ciò venga riconosciuto nel testo.

Yuri Gori, 16 gennaio 2014

Una copia della tesi sarà disponibile presso *http://paduaresearch.cab.unipd.it/*

Index

Riassunto

Nonostante numerosi studi dimostrano una stretta relazione tra i meccanismi fisiologici delle piante e gli isotopi stabili presenti all'interno del legno dei loro anelli, ben poche sono le ricerche svolte in questo settore.

L'obiettivo generale di questa tesi è stato di esplorare e sviluppare nuovi metodi che permettano di identificare le risposte fisiologiche di piante stressate per la presenza di funghi patogeni o per la defogliazione causata da insetti. Il metodo che propongo con la presente tesi prevede l'analisi degli accrescimenti annuali (dendrocronologia) e degli isotopi stabili negli anelli del legno.

La tesi è suddivisa in quattro sessioni.

Nella prima sviluppo un metodo per stimare alcuni parametri climatici dai valori isotopici di *Picea abies*. Il metodo ha richiesto la calibrazione del clima sulla base delle cronologie isotopiche dell'ossigeno, del carbonio, e dell'idrogeno in differenti matrici del legno (legno intero, cellulosa e gruppi metilici della lignina). Il modello elaborato è stato in grado di ricostruire la temperatura media-annua nel sud-est delle Alpi. Il modello ha inoltre individuato le migliori componenti del legno e le migliori proxy isotopiche per la ricostruzione climatica.

La seconda parte ha lo scopo di studiare gli effetti dell'ambiente sull'abete rosso infetto da *Heterobasidion parviporum* per un lungo periodo. Nella conclusione di questo lavoro ipotizzo una maggiore aggressività del fungo alle quote più basse; in questo ambiente il fungo agisce molto più velocemente, portando spesso le piante all'arresto dell'accrescimento radiale e ad una maggiore sofferenza nei periodi secchi. Inoltre si è potuto stimare il periodo di inizio delle infezioni croniche e la perdita di accrescimento che hanno subito le piante infettate.

Nella terza parte dimostro che l'uso degli isotopi stabili può essere usato per evidenziare risposte fisiologiche dell'abete rosso infetto da *H. parviporum*. Ho avanzato l'ipotesi che a seguito dell'attacco del patogeno le piante di abete rosso a bassa quota possano aver accresciuto la conduttanza stomatica.

Nella quarta parte le analisi degli isotopi stabili e degli accrescimenti legnosi sono stati applicati per identificare eventuali risposte fisiologiche indotte da *Cephalcia arvensis* in

piante di abete rosso ripetutamente defogliate. Nelle conclusioni di tale lavoro viene ipotizzato che le piante, a causa di periodi aridi precedenti l'attacco dell'insetto, hanno attinto alle sostanze di riserva rendendosi così suscettibili agli attacchi dell'insetto a causa della conseguente maggiore concentrazione di zuccheri e amminoacidi negli aghi.

In generale si può affermare che l'applicazione congiunta di queste due tecniche costituisce un valido strumento di investigazione scientifica su tematiche eco-fisiologiche riguardati i processi di resilienza delle specie arboree a passati eventi di danni biotici o abiotici.

Summary

Although the links between plant physiological processes and stable isotopes in tree rings are well known, few studies have carried out stable isotope analyses in stressed plants.

The general objective of this thesis is to develop new tools able to identify the short- and long-term responses of plants to fungal attack and insect feeding. I propose a new methodology, which uses stable isotope values as indicators of physiological responses and which was tested on infected and defoliated Norway spruce trees sampled in the south-eastern Alps.

The thesis is divided into four main sections.

In the first section, I present a model designed to accurately estimate environmental proxies for *Picea abies*, which would serve as the basis for further analyses. This model required calibration and assessment of the effects of climate on the stable isotope signature in different wood components. For this purpose, I developed a simple model to reconstruct mean annual temperature in the south-eastern Alps. I found that $\delta^{18}O$ and $\delta^{2}H$ values in whole wood were the best signallers of climate.

The second section is aimed at clarifying the influence of environmental conditions on Norway spruce suffering from long-term infection by the white-rot fungus *Heterobasidion parviporum*. I found that at low elevations, where climatic conditions are unsuitable, *H. parviporum* was seemingly more aggressive, causing plants to decline more rapidly, decreasing the ability of host trees to cope with drought and, in some cases, arresting cambial activity.

In the third section, I propose using stable isotope ratios as a physiological indicator of Norway spruce affected by *H. parviporum* over a long period of time and put this forward as a novel way for providing insights into plant–pathogen relationships. I obtained evidence that stomatal conductance increases in *Picea abies* affected by *H. parviporum*.

The fourth section focuses on stable isotope ratios and tree-ring chronologies to investigate the short- and long-term effects of defoliation of *Picea abies* caused by *Cephalcia arvensis*. I found that drought stress prior to insect attack may have caused the

trees to mobilise reserves, making them more susceptible to *Cephalcia* attack as a result of increased soluble sugars and amino acids.

General Introduction

Li circuli delli rami degli alberi segati mostrano il numero delli anni suoi
e quali furono più umidi e più secchi secondo la maggiore o minore loro grossezza.
E così mostrano gli aspetti del mondo dov'essi erano volti;
perché più grossi sono a settentrione che a meridio;
e così il centro dell'albero per tal causa è più vicino alla scorza sua meridionale
che alla scorza settentrionale.

"Trattato della Pittura"
XVI secolo, Leonardo da Vinci

1Stable isotopes in plants

1.1Theory and nomenclature of stable isotopes

An isotope is one of two or more atoms of the same element containing different numbers of neutrons. The superscript number on the left of an element designation is called the "mass number", which is the sum of the number of neutrons and protons in the atomic nucleus. Isotopes can be radioactive or non-radioactive. The former disintegrate spontaneously over time to form other isotopes, while the latter don't decay to other isotopes and thus are also known as stable isotopes.

The three main elements in wood (carbon, oxygen and hydrogen) all have more than one stable (non-radioactive) isotope.

Carbon has two stable isotopes, ^{12}C and ^{13}C, each with six protons and with either six or seven neutrons. These isotopes have almost identical chemical properties but the difference in mass allows their physical, chemical and biological processes to be discriminated, thereby providing an environmental signal. By convention, the ratio of ^{13}C to ^{12}C is expressed in delta (δ) notation with reference to a standard material for which the isotopic ratio is known (Eq. 1). The carbon isotope ratio ($\delta^{13}C$) is expressed in parts per thousand (‰) as

$$\delta^{13}C = (R_{sample} / R_{standard} - 1)1000$$

Eq. 1

where R_{sample} and $R_{standard}$ are the $^{13}C/^{12}C$ ratios in a sample and a standard, respectively. The chosen standard in the case of carbon was a fossil belemnite from the Pee Dee formation of South Carolina, which is now exhausted and has been replaced by 'Vienna-PDB' or VPDB (Coplen, 1995). On this scale, the carbon isotopic ratio of CO_2 in air is about -8‰.

Oxygen has three natural stable isotopes, each with eight protons and between 8 and 10 neutrons. The $^{18}O/^{16}O$ ratio has traditionally been used in the environmental sciences. In the case of water, ice and plant material, the standard mean ocean water (SMOW) was adopted, now replaced by Vienna-SMOW or VSMOW. Water containing the lighter isotopes of oxygen will evaporate more easily than water containing the heavier isotopes, so source water is isotopically heavier than the moisture that evaporates from it. The effect is temperature dependent, so that cold air masses are isotopically lighter than warm air masses. When

moisture vapour condenses the opposite is true, with the heavier isotopes condensing more readily, and again the isotopic ratio depends on the temperature at which condensation takes place. Global variations in the $\delta^{18}O$ of precipitation are thus linked in a complex way to climate (Dansgaard, 1964).

Hydrogen has two stable isotopes, the heavier being deuterium (^{2}H or D). The $^{2}H/H$ ratio is also expressed relative to SMOW or VSMOW using the δ notation as δD (‰). Moisture vapour is lower in deuterium compared to the source. The δD ratio of precipitation also varies globally and is linked in a complex way to climate. Variations in $\delta^{18}O$ and δD of precipitation are also strongly correlated but differ in magnitude along a global meteoric water line (IAEA, 1981).

1.2 Stable isotopes in tree rings

All the carbon in each annual tree ring comes from CO_2 in air, while O and H come from soil water, hence precipitation. However, the isotopic composition of wood differs from that in either air or water because trees do not passively collect and store these elements. The carbon isotopic ratio of CO_2 in air is about -8‰ (VPDB), while wood yields much lower values (-20‰ to -30‰), showing that trees are depleted in ^{13}C compared to air. This change in ratio from air and water to wood compounds is known as fractionation, and the degree to which it occurs is controlled to some extent by climate and environmental conditions. Fractionation occurs during two physiological phases: i) when carbon dioxide diffuses through the stomata, and ii) when internal CO_2 is utilised by the photosynthetic enzyme RuBisCO (Fig. 1).

When air diffuses through the stomata, the lighter carbon dioxide molecules ($^{12}CO_2$) diffuse more easily than the heavier molecules ($^{13}CO_2$), simply because as molecules bounce off each other the lighter ones bounce furthest. The net effect is that internal air is depleted in ^{13}C relative to ambient air. When the stomatal opening is extremely small ($\leq$ 0.1μm), collisions with guard cells increase and fractionation is much higher.

Fractionation also occurs when internal CO_2 is utilised by RuBisCO. During carboxylation, the photosynthetic enzyme tends to use ^{12}C in preference to ^{13}C. Discrimination against ^{13}C during carbon fixation by trees can be expressed as:

$$\Delta‰ = a + (b - a)\,(c_i/c_a)$$

Eq. 2

where a is the discrimination against $^{13}CO_2$ during diffusion through the stomata (≈ – 4.4‰), b is the net discrimination due to carboxylation (≈ – 27‰), and c_i and c_a are intercellular and ambient CO_2 concentrations, respectively (Farquhar et al., 1982; McCarroll and Loader, 2004). The dominant environmental factors influencing stable carbon isotopic ratios in tree rings should, therefore, be those controlling the rate of stomatal conductance and the rate of photosynthesis.

^{18}O and ^{2}H stable isotopes come from soil water. Initial discrimination occurs within the soil: the lighter water evaporates more easily than the water containing the heavier isotopes, the net effect being that soil water is isotopically heavier (e.g. ^{18}O or ^{2}H enrichment) than air moisture. Fractionation does not occur during water uptake by roots (Wershaw et al., 1966), but instead during leaf transpiration. Evaporation leads to a loss of lighter isotopes and consequent ^{18}O enrichment (Saurer et al., 1998). The level of enrichment of leaf water above source water at the site of evaporation ($\Delta^{18}O_e$) is given by:

$$\Delta^{18}O_e = \varepsilon^* + \varepsilon_k + (\Delta^{18}O_v - \varepsilon_k)\, \varepsilon_a/\varepsilon_i$$

Eq. 3

where ε^* is the proportional depression of water vapour pressure by the heavier $H_2{}^{18}O$, ε_k is the fractionation as water diffuses through the stomata and leaf boundary layer, $\Delta^{18}O_v$ is the oxygen isotope composition of water vapour in the atmosphere (relative to source water), and ε_a and ε_i are the ambient and intercellular vapour pressures, respectively (McCarroll and Loader, 2004). As a consequence, evaporation raises the $\delta^{18}O$ of leaf water. The net effect depends on stomatal conductance and vapour pressure deficit, both of which are linked to relative humidity (RH), and the resulting fractionation is moderated by the $\delta^{18}O$ of moisture vapour outside the leaf (Roden et al., 2000; McCarrol and Loader, 2004).

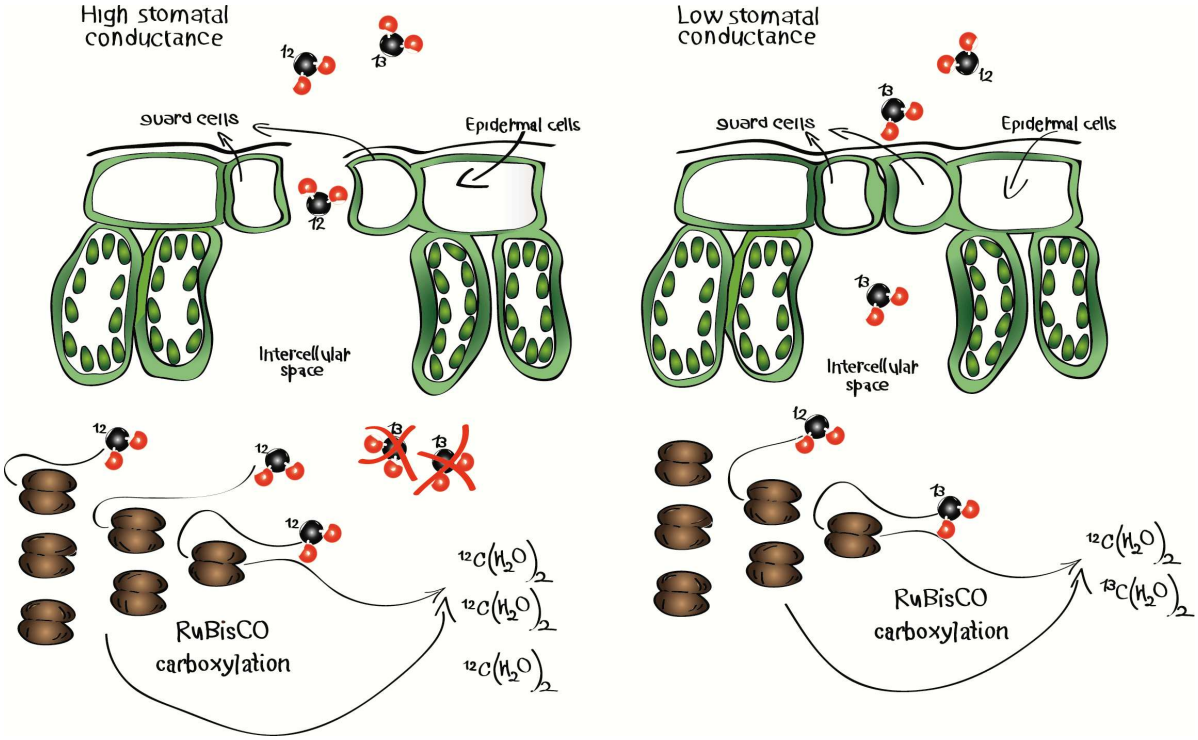

Fig. 1 Scheme of carbon isotope fractionation. High stomatal conductance leads to high discrimination; the activity of the RuBisCO is not limited by CO_2 concentration, thus it discriminates against ^{13}C. Low stomatal conductance leads to low discrimination; since the limiting factor of photosynthesis is a low stomatal conductance, RuBisCO fix a higher proportion of ^{13}C (From Ferrio, 2005, drawn by Gori Y.).

1.3 Isotope analysis and wood components

In order to determinate the stable isotope ratios of a tree-ring sample, the wood (tree-ring sample) must be pyrolysed. The gaseous form is currently the only one suitable for mass spectrometry. This first stage may be carried out ‘‘off-line’’, typically as single samples or small batches, or ‘‘on-line’’ as part of an integrated system involving quantitative combustion or pyrolysis of the sample.

The stable carbon, hydrogen and oxygen isotope ratios of the resulting sample gases are determined using a stable isotope ratio mass spectrometer (IRMS): an aliquot of sample gas is placed in the mass spectrometer where it is ionised. The charged particles are accelerated by high voltage and pass down a flight tube where a magnetic field deflects them according to differences in their mass towards Faraday cup detectors. The ratios from the detectors are compared with the results from standards of known isotopic composition. Reference materials of known isotopic compositions relative to an international standard are used to calibrate the sample isotopic compositions.

Stable isotope analyses may be performed using whole wood, cellulose or lignin (Leavitt and Long, 1986, 1984). Given that there is no material exchange and no further fractionation (Dellus et al., 1997), the isotope ratios of cellulose are often thought to be the most meaningful indicator of environmental conditions during tree growth (Ferrio and Voltas, 2005). Cellulose extraction, even by the simple bath method (Leavitt and Danzer, 1993; Gori et al., 2013a, see section 1), is still time-consuming and it has recently been suggested, at least for some tree species, that both carbon and oxygen isotope ratios in whole wood may yield as good a climatic signal as cellulose (Borella et al., 1999; Saurer et al., 2000), since stable isotope ratios differ according to site features and tree species. It has also been suggested that stable hydrogen isotope values of lignin methoxyl groups in tree rings may be a suitable paleoclimate proxy (Keppler et al., 2007). Stable isotopes have been measured in a huge number of tree species (Table 1, updated to December 2013) but , as far as ecological research is concerned, the issue of whether wood component extraction is necessary is still an open question.

Reference	**Species**	**Site**	**Wood component**	**Isotopes**	**Environmental or physiological signal**
Anderson et al. (1998)	*Abies alba*	Switzerland	Cellulose	$\delta^{13}C$, $\delta^{18}O$	Temperature, precipitation and RH
Anderson et al. (2002)	*Abies alba*	Switzerland	Cellulose	$\delta^{18}O$	Temperature, precipitation and RH
Barbour et al. (2001)	*Quercus* sp., *Pinus* sp.	Various	Wholewood, cellose, lignin	$\delta^{18}O$	Correlations between $\delta^{18}O$ of various wood constituents
Barszczowka et al. (2005)	*Pinus nigra*	Croatia, Spain	Needles	$\delta^{13}C$	$\delta^{13}C$ variations in needles
Battipaglia et al. (2008)	*Acer pseudoplatanus, Fagus sylvatica*	Italy	Cellulose, wholewood	$\delta^{18}O$	Climate signals in different wood components
Battipaglia et al. (2009)	*Abies alba, Picea abies*	Italy	Cellulose extraction	$\delta^{18}O$, $\delta^{13}C$	Temperature and precipitataion
Battipaglia et al., 2010	*Pinus pinea*	Italy	Cellulose	$\delta^{13}C$, $\delta^{15}N$	Influence of air pollution on trees.
Battipaglia et al., 2013	Various	Italy, North Carolina, Tennensee	Cellulose	$\delta^{18}O$, $\delta^{13}C$	CO_2 increases WUE
Becker et al. (1991)	*Quercus* sp., *Pinus sylvestris*	Central Europe	Nitrocellulose	$\delta^{13}C$, $\delta^{2}H$	Qualitative to Lateglacial–Holocene transition
Bert et al. (1997)	*Abies alba*	France	Holocellulose	$\delta^{13}C$	Possible age related trend, changing iWUE response to CO_2
Buhay and Edwards (1995)	Elm, pine maple	Canada	Cellulose	$\delta^{18}O$, $\delta^{2}H$	Modelled $\delta^{18}O$ of precipitation and air RH
Burk and Stuiver	Various	America	Cellulose	$\delta^{18}O$	RH and temperature

(1981)					
Chevillat et al. (2005)	Various	Central Europe	Various tissues	$\delta^{13}C$	Tissue-specific variation of $\delta^{13}C$
Craig (1954)	*Sequoia gigantea*	America	Whole wood	$\delta^{13}C$	Correlation between $\delta^{13}C$ and atmosphere
Cullen and Grierson (2006)	*Callitris glaucophylla*	Australia	Cellulose, wholewood	$\delta^{18}O$, $\delta^{13}C$	Climate signals in different wood components
Cullen and Macfarlane C. (2005)	Various	Controlled experiment	Various tissues	$\delta^{18}O$, $\delta^{13}C$	Various cellulose extraction methods
De Micco V. et al (2007)	*Pinus pinaster*	Italy	Wholewood	$\delta^{13}C$	$\delta^{13}C$ variations within-tree rings
Dubois (1984)	*Pinus sylvestris*	United Kingdom	Nitrocellulose	$\delta^{2}H$	Link to deuterium content of prec. and RH enrichment.
Dupouey et al. (1993)	*Fagus sylvatica*	France	Cellulose	$\delta^{13}C$	Correlation between $\delta^{13}C$ and soil moisture
Duquesnay et al. (1998)	*Fagus sylvatica*	France	Cellulose	$\delta^{13}C$	Long-term trend and age effect.
Edwards et al. (2000)	*Abies alba*	Germany	Cellulose	$\delta^{13}C$, $\delta^{2}H$	Correlation between $\delta^{13}C$-$\delta^{2}H$ and temperature
Epstein and Krishnamurthy (1990)	*Pinus aristata*	California	Nitrocellulose	$\delta^{13}C$, $\delta^{2}H$	Correlation with temperature
Epstein and Yapp (1976)	Various	Scotland and America	Wholewood	$\delta^{13}C$	Correlation with winter temperature
Farmer and Baxter (1974)	*Quercus robur*, *Larix decidua*	United Kingdom	Wholewood	$\delta^{13}C$	Changing atmospheric ^{13}C
February and Stock (1999)	*Widdringtonia* sp.	Africa	Cellulose	$\delta^{13}C$	Air $\delta^{13}C$
Feng and Epstein (1995)	*Pinus* sp., *Juniper* sp., *Quercus* sp.	America	Nitrocellulose	$\delta^{13}C$	Precipitation and $\delta^{13}C$ trend
Feng et al. (1999)	*Picea sp.*	China	Nitrocellulose	$\delta^{2}H$	Comparison of monsoon influence; recent vs. ancient period
Ferrio J.P. and Voltas (2005)	*Pinus halepensis*	Spain	Cellulose, wholewood, extracted wood, lignin	$\delta^{18}O$, $\delta^{13}C$	Precipitation, temperature and vapour pressure deficit in various wood components
Freyer (1979a,b)	*Various*	Northern emisphere	Cellulose	$\delta^{13}C$	Atmospheric $\delta^{13}C$ trend
Freyer and Belacy (1983)	*Quercus robur, Pinus sylvestris*	Germany and Sweden	Cellulose	$\delta^{13}C$	Temperature and precipitation
Gagen M. et al. (2006)	*Pinus sylvestris, Pinus uncinata*	French	Cellulose	$\delta^{13}C$	$\delta^{13}C$, ring width and wood density improve the climate signal
Gori et al. (2013a)	*Picea abies*	Italy	Wholewood, cellulose, lignin methoxyl groups	$\delta^{18}O$, $\delta^{13}C$, $\delta^{2}H$	Climate signals in different wood components
Gori et al. (2013c)	*Picea abies*	Italy	Wholewood	$\delta^{18}O$, $\delta^{13}C$	Physiological responses of infected plants
Gray and Se (1984)	*Picea glauca*	Canada	Nitrocellulose	$\delta^{2}H$	Temperature and source water
Gray and Thompson (1976)	*Picea glauca*	Canada	Cellulose	$\delta^{18}O$	Temperature
Gray and Thompson (1977)	*Picea glauca*	Canada	Wholewood, lignin and cellulose	$\delta^{18}O$	Temperature; cellulose preserve the best temperature signal
Guerrieri M.R. et	*Picea abies,*	Italy,	Wholewood	$\delta^{13}C$, $\delta^{15}N$,	Influence of different

al (2009)	*Quercus cerris*	Switzerland		$\delta^{18}O$	nitrogen emission sources on tree physiology
Hemming et al. (1998)	*Fagus sylvatica, Pinus sylvestris, Quercus robur*	United Kingdom	Various	$\delta^{18}O$, $\delta^{13}C$, $\delta^{2}H$	RH, temperature, precipitation and sunshine
Impa S.M. (2005)	*Orzyra sativa*	India	Various	$\delta^{13}C$	$\delta^{13}C$ and WUE
Jedrysek et al. (1998)	*Quercus* sp.	Poland	Nitrocellulose	$\delta^{13}C$, $\delta^{2}H$	Correlation between $\delta^{13}C$ and precipitation, no correlation with $\delta^{2}H$
Keppler et al., (2007)	Various	Various	Lignin methoxyl groups	$\delta^{2}H$	Geographical origin of wood
Kitagawa and Matsumoto (1995)	*Cryptomeria japonica*	Japan	Cellulose	$\delta^{13}C$	Temperature
Krishnamurthy (1996)	*Juniperus phoenica*	Sinai peninsula	Wholewood	$\delta^{13}C$	Air $\delta^{13}C$ trend
Krishnamurthy and Epstein (1985)	*Juniperus procera*	Kenya	Nitrocellulose	$\delta^{2}H$	Water stress
Lawrence and White (1984)	*Pinus strobus*	America	Wholewood	$\delta^{2}H$	Precipitation
Leavitt (1993)	*Pinus edulis*	America	Wholewood	$\delta^{13}C$	Moisture stress singals
Leavitt and Lara (1994)	*Fitzroya cupressoides*	Chile	Holocellulose	$\delta^{13}C$	Anthropogenic effect in southern Hemisphere
Leavitt and Long (1986)	*Juniperus sp.*	America	Cellulose	$\delta^{13}C$	Temperature and precipitation
Libby and Pandolfi (1974)	*Quercus petrea*	Germany	Wholewood	$\delta^{18}O$, $\delta^{13}C$, $\delta^{2}H$	Winter temperature reconstruction
Libby et al. (1976)	*Quercus petrea, Abies alba, Cryptomeria japonica*	Germany, Japan	Wholewood	$\delta^{18}O$, $\delta^{2}H$	Temperature
Lipp and Trimborn (1991)	*Picea abies, Abies alba*	Germany	Cellulose	$\delta^{13}C$, $\delta^{2}H$	Temperature
Loader and Switsur (1996)	*Pinus sylvestris*	United Kingdom	Cellulose	$\delta^{13}C$	Temperature
McCarroll and Pawellek (2001)	*Pinus sylvestris*	Finland	Cellulose	$\delta^{13}C$	Sunshine and temperature
McCormack et al. (1994)	*Quercus robur, Quercus petrea*	United Kingdom	Holocellulose	$\delta^{13}C$	Identified isotopic difference between land- and bog-grown oaks
Okada et al. (1995)	*Chamaecyparis* sp.	Japan	Cellulose	$\delta^{13}C$	No direct external forcing identified
Pendall (2000)	*Pinus edulis*	USA	Cellulose	$\delta^{2}H$	RH, latewood preserve best signal than earlywod
Pollastrini et al. (2013)	*Populus* sp.	Italy	Wholewood	$\delta^{18}O$, $\delta^{13}C$	$\delta^{18}O$, $\delta^{13}C$ are affected by water stress
Ramesh et al. (1985)	*Abies pindrow*	India	Cellulose and nitrocellulose	$\delta^{18}O$, $\delta^{13}C$, $\delta^{2}H$	Identified common forcing between radii
Ramesh et al. (1986)	*Abies pindrow*	India	Cellulose and nitrocellulose	$\delta^{18}O$, $\delta^{13}C$, $\delta^{2}H$	$\delta^{13}C$ with RH and cloud; $\delta^{2}H$ with precipitation and temperature
Robertson et al. (1997)	*Quercus robur*	Finland	Cellulose	$\delta^{13}C$	Prec.>RH>Temperature
Saurer and Siegenthaler (1989)	*Fagus sylvatica*	Switzerland	Cellulose	$\delta^{13}C$	Temperature and preicipitation
Saurer et al. (1995)	*Fagus sylvatica*	Switzerland	Cellulose	$\delta^{13}C$	Soil moisture, total precipitation
Saurer et al. (1998)	*Fagus sylvatica*	Switzerland	Cellulose	$\delta^{13}C$, $\delta^{18}O$	Temperature and precipitation
Saurer et al.	*Larix* sp., *Picea*	Eurasia	Wholewood	$\delta^{18}O$	Spatial analysis with

(2002)	sp., *Pinus* sp.				precipitation $\delta^{18}O$
Scheidegger et al. (2000)	*Festuca rubra, Potentilla aurea, Achillea millefoliuìm*	Controlled experiment	Wholewood	$\delta^{18}O$, $\delta^{13}C$	Relationship between stable isotopes and physiological mechanisms
Schiegl (1974)	*Picea abies*	Germany	Wholewood	$\delta^{2}H$	Summer temperature
Schleser et al. (1999)	*Picea abies*	Germany	Wholewood, cellulose	$\delta^{13}C$	Temperature
Sheu et al. (1996)	*Abies kawakamii*	Taiwan	Cellulose	$\delta^{13}C$	Temperature
Simard et al., 2008	*Pinus banksiana, Picea mariana, Abies balsama*	Canada	Cellulose	$\delta^{18}O$, $\delta^{13}C$	Identification of past defoliations and physiological change in field
Simard et al., (2012)	*Abies balsamea*	Canada, controlled experiment	Cellulose	$\delta^{18}O$, $\delta^{13}C$	Identification of past defoliations and physiological change in controlled exeperiment
Sonninen and Jungner (1995)	*Pinus sylvestris*	Finland	Cellulose	$\delta^{13}C$	Temperature
Stuiver and Braziunas (1987)	Various	America	Cellulose	$\delta^{13}C$	Latitudinal trend. RH>Temperature
Switsur et al. (1994)	*Quercus robur*	United Kingdom	Cellulose	$\delta^{18}O$, $\delta^{13}C$, $\delta^{2}H$	$\delta^{13}C$ and $\delta^{18}O$ with temperature and RH
Switsur et al. (1996)	*Quercus robur*	United Kingdom	Cellulose	$\delta^{18}O$, $\delta^{13}C$, $\delta^{2}H$	Temp($\delta^{18}O$, $\delta^{13}C$, $\delta^{2}H$); RH($\delta^{18}O$, $\delta^{13}C$); Prec($\delta^{18}O$)
Tang et al. (1999)	*Pinus longeva*	California	Cellulose	$\delta^{13}C$	WUE increases with CO_2
Tang et al. (2000)	*Pseudotsuga menziesii*	USA	Nitrocellulose	$\delta^{2}H$	Source-water signal dominates, temperature signal is weak
Tans and Mook (1980)	*Oak, Fagus sylvatica*	Netherlands	Cellulose	$\delta^{13}C$	Mean summer temperature, mean annual temperature
Tardif et al. (2008)	*Picea glauca*	Canada	Cellulose	$\delta^{13}C$	Influence of climate
Treydte et al. (2001)	*Picea abies*	Swiss Alps	Cellulose	$\delta^{13}C$	Temperature, precipitation and RH
Waterhouse et al. (2000)	*Pinus sylvestris*	Russia	Cellulose	$\delta^{13}C$	Correlation with moisture stress
Wingate et al. (2007)	*Picea sitchensis*	United Kingdom	CO_2 gas exchange	$\delta^{13}C$	Variations in ^{13}C discrimination during CO_2 exchange
Yapp and Epstein (1982)	*Various*	America	Nitrocellulose	$\delta^{2}H$	Mean annual temperature
Zimmermann et al. (1997)	*Juniperus tibetica*	Tibetan plateau	Cellulose	$\delta^{13}C$	Soil moisture stress

Table 1. A summary of paper focused on tree-ring isotope for environmental research (from McCarrol and Loader, 2004, updated to December 2013).

2 Tree-ring and stable isotopes as environmental signals

2.1 Comparison of tree rings and stable isotopes

Trees are wonderful, annually-resolved archives of tree history stretching back for thousands of years. Annual variability in width, density and stable isotope ratios in tree rings provides a record of climate and physiological signals (photosynthetic capacity and stomatal conductance) (Scheidegger et al., 2000; Simard et al., 2012, 2008).

The relationship between ring widths or stable isotope ratios and ecological signals may be quantified using regression-based techniques or "bootstrap" approaches based on multiple random resampling from the same data set (Cook, 1990). Although it is possible to extract high-resolution paleoclimatic data from ring width (Briffa et al., 1998), a number of limitations restrict their potential. One problem is known as the "segment length curse": as trees grow, their ring widths tend to decline (Cook et al., 1995) and regression-based techniques, usually fitting a negative exponential curve, must be used to remove this trend. However, this helpful data treatment unfortunately also removes other data on low-frequency long-term changes in climate that are often of most importance. Another problem is that the correlation between ring widths and climate may not be very strong. Since individual trees in a stand are likely to respond in different ways to climate in a given year, the widths of the rings they form individually will vary greatly. Tree-ring widths and tree-ring densities in different stands may also differ greatly due to local microclimate conditions. To some extent, the problem of between-tree and between-stand variability may be overcome by using a large number of trees to remove noise and enhance the common signal. Naturally, the greater the variability, the greater the number of trees required.

On the other hand, using stable isotopes may avoid the necessity to statistically de-trend the isotope series, thus retaining high (year-to-year variations) and low (long-term variations) frequencies and removing the "segment length" effect. This is why fewer trees are required for carbon and oxygen stable isotope analyses than for classical tree-ring width analyses. Stable carbon isotope ratios also have the advantage that the physiological factors influencing their variation are reasonably well understood and relatively simple compared with the multiple factors influencing annual growth increment.

Variations in tree-ring isotope ratios have been interpreted in many different ways (Table 1): as inferred palaeoclimatic signals (temperature, RH and precipitation) or as stomatal

conductance and photosynthetic capacity. None of the isotopes has a single controlling factor, so the dominant control will change according to tree species and ecological conditions (McCarroll and Loader, 2004).

2.2 A novel unexplored method

Scheidegger et al. (2000) developed a conceptual model based on measurements of $\delta\ ^{18}O$ and $\delta^{13}C$ in organic matter, that provides insights into the long-term effects of environmental factors on CO_2 and H_2O gas exchange. According to this model, simultaneous measurement of carbon and oxygen isotopes in tree rings allows estimates to be made of changes in stomatal conductance and photosynthetic rate during the tree life and under different ecological conditions (Fig. 2). This model may be helpful in investigating physiological responses under different climate conditions and during abiotic or biotic stress. It is well known that plants can modify their physiological processes in different ways in the course of a stress event (e.g. by altering water relations or photosynthetic capacity). These physiological responses are thought to be defensive mechanisms of resistance (Little et al., 2003). For example, previous studies have reported significant variations in photosynthetic rate and stomatal activity as a consequence of insect defoliation (Chen et al., 2001; Ozaki et al., 2004; Pataki et al., 1998; Quentin et al., 2011). Nevertheless, most research has focussed on the physiological responses of plants during insect outbreak and, so far, much less attention has been given to adaptive mechanisms in plants infected by pathogenic fungi or defoliated by insects in the long-term.

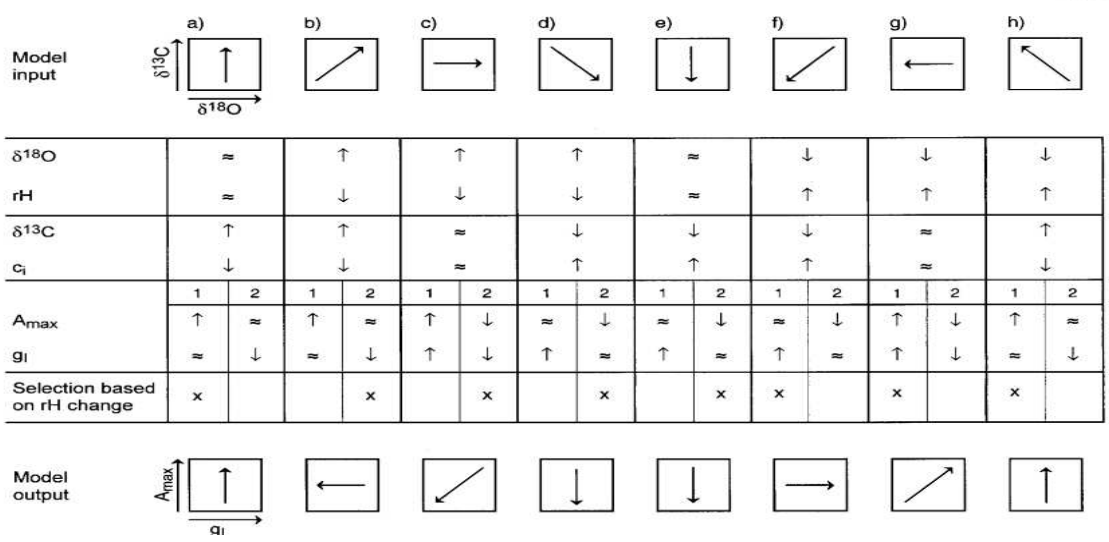

Fig.2 Theoretical development, the changes between $\delta^{13}C$ and $\delta^{18}O$ are shown by arrows. Relative humidity (rH) comes from $\delta^{18}O$, CO_2 in the leaf intercellular spaces (c_i) from $\delta^{13}C$ (up-or downward arrows represent increasing or decreasing values, ≈ indicates insignificant changes). For each scenario there are two possible cases, denoted as 1 and 2, with corresponding changes in average maximum net photosynthesis (A_{max}) and stomatal conductance (g_l). The model output is determined by the selection based on the rH change (from Scheidegger et al., 2000).

2.3 Potential of a multi-proxy approach

Extracting environmental signals from tree-ring widths or stable isotopes requires a full understanding of both isotope theory and of the ecophysiology of the sampled trees. It is often easy to find a good correlation between a tree-ring chronology and a climate parameter but it should be born in mind that correlation does not necessarily imply causation.

Since the dominant controls on $\delta^{13}C$ are photosynthetic rate and stomatal conductance, the environmental signal at a certain site will be linked to the relative strengths of these two factors. For example, at a dry site such as in the western Alps, the dominant control is stomatal conductance and the likely environmental signals are precipitation and air humidity (Gagen et al., 2004). On the other hand, where water is not a limiting factor, the dominant control may be photosynthetic rate, which may be regulated by either temperature or the amount of sunlight (McCarroll and Loader, 2004). Where trees are growing under mild conditions, tree-ring widths and isotope ratios may not carry strong environmental signals.

Trees are a physical archive, and this allows for a multi-proxy approach (McCarrol and Pawellwek, 2001) to dendroecology, including the measurement of stable isotopes, which improves the amount of environmental information that can be extracted from trees. Using

several proxies, some of the noise associated with each of the measures may be removed, enhancing the climate or physiological signal (Gori et al.,2013a, 2013b, 2013c; Simard et al., 2012, 2008; Scheidegger et al., 2000). The most important consideration is that the sources of error (noise) for each of the proxies are not the same.

In the south-eastern Alps, for example, a combination of eight different isotope chronologies from *Picea abies* allowed us to reduce non-climate noise and to reconstruct the past climate of this region (Gori et al., 2013a; see section 1). The potential of this approach was also tested in three other studies (sections 2,3,4) forming part of this thesis.

Using a combination of maximum latewood density and stable carbon isotope ratios, McCarrol and Pawellwek (2001) were able to identify dry summers, even in a region where trees are rarely moisture stressed (Fig. 3).

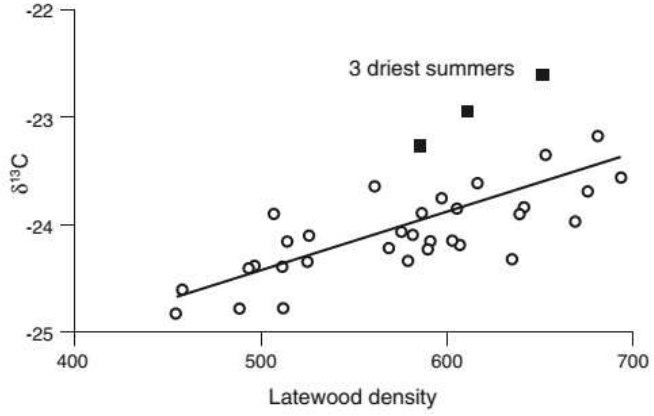

Fig. 3 Regression between $\delta^{13}C$ values and latewood density values, the residuals show the dry summers (from McCarrol and Pawellwek, 2001).

2.4 Influence of fungi and insects on tree rings and stable isotopes

Dendrochronology is the science of dating annual growth layers (rings) in woody plants. Two sub-disciplines are dendroclimatology, which uses the information in tree rings to study anomalies in present and past climates, and dendroecology, which includes all branches of science involved in drawing environmental information from tree-ring sequences, e.g.:

- geomorphology (dendrogeomorphology)
- tectonics (dendrotectonis)
- glaciology (dendroglaciology)
- snow research (dendroniveology)

Recently, dendrochronology has moved into the realm of plant pests and tree-ring analyses can be used to reconstruct the temporal processes of diseases caused by pests (Schweingruber, 1996). Abrupt, periodic growth reductions in oaks in northern Germany were investigated dendrochronologically by Hartmann and Blank (1992), who reported the possible causes as budmoth and *Pezicula cinnamomea*. Other researchers have been able to reconstruct outbreaks over the past 300 years by analysing tree rings in *Picea englemannii* in Colorado's Rocky Mountains (Veblen et al., 1991).

Growth reduction is common after a mass insect outbreak or during fungal infection, but tree-ring analyses are rarely carried out in this context (Schweingruber, 1996).

Recently, Simard et al. (2008; 2012) proposed using carbon and oxygen stable isotopes as indicators of spruce budworm outbreak (*Choristoneura fumiferana* Cem.), but no further studies have since been carried out.

3 Sampling, measurement and statistical treatments

3.1 Sampling strategies

When the aim is to enhance a climate signal on tree growth, it should be born in mind that the most useful trees are those growing under extreme conditions. As a rule, relatively isolated trees (i.e. without competition), potentially limited by the factor under investigation, are the material of choice (Ferrio, 2005). For example, when we need good inferences on precipitation, isolated trees in a dry stand located on a slope are the best choice.

3.2 Sampling resolution

Samples may be acquired by felling trees and removing a disk or by using increment borers (Fig.4). Early tree-ring isotope analyses used disks because a lot of wood material was needed, but as sample preparation techniques have become faster and mass spectrometers have improved, small samples have become feasible. The minimum number of trees required for ecology purposes necessarily depends on intra-site and intra-tree heterogeneity. In dendroclimatology, as a rule, 20 trees per site may be enough (Schweingruber, 1996), although Leavitt and Long (1984) have suggested that pooling four cores from four trees will yield an accurate absolute ^{13}C value, a proposal that has been disputed (McCarrol and Pawellek, 1998).

3.3 Core preparation

Even in conifers, where most boundaries are clear to see on the unsurfaced core, there is a risk of overlooking very tiny rings or misidentifying false rings. For dendrochronology purposes, it is usually sufficient to prepare the cores with sandpaper to obtain a surface similar to a cut surface and thereby facilitating identification of indistinct ring boundaries (Fig. 4)

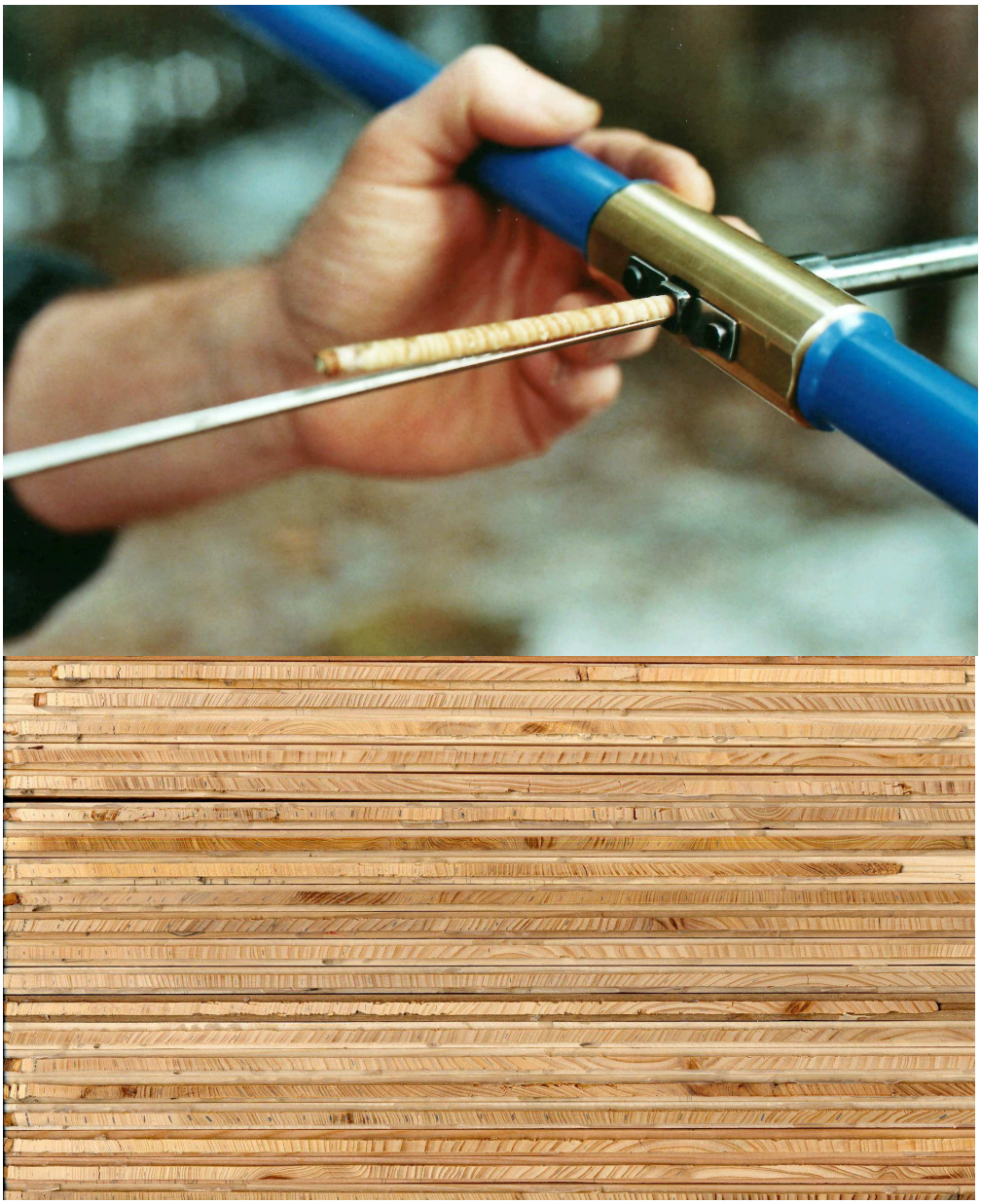

Fig. 4 Pressler's increment borer (on the top; Gori Y.) and cores from *Cupressus sempervirens* (on the bottom; Nicola La Porta, photo credits).

However, to prevent isotopic contamination, no lubricants, markers or sandpaper must be used during field sampling and dendrochronological measurement. A simple solution, proposed by Gärtner and Nievergelt (2010), to make the features of the rings clearly visible under magnification, is to use a sliding microtome blade (Fig. 5). Properly sliced surfaces have another advantage over sanded surfaces in that the vessels are left open and are not filled with sawdust (Fig. 6).

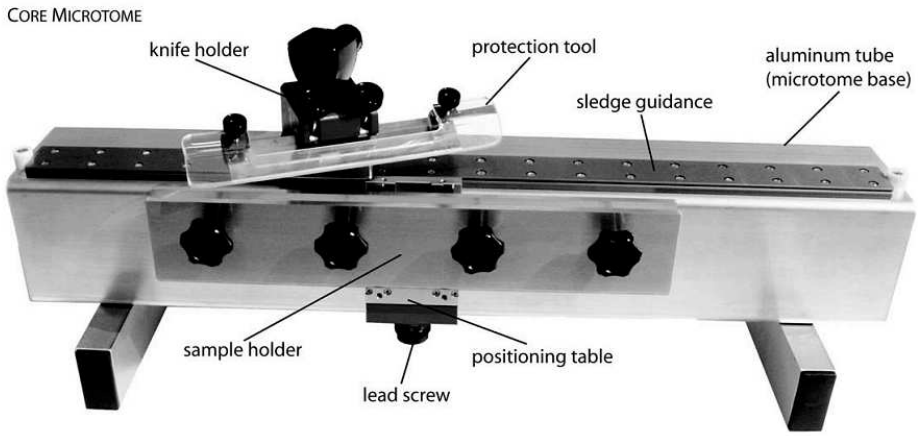

Fig. 5 The core-microtome and its components. The protection tool is designed to be placed on the microtome knife to avoid injuries while handling the microtome (from Gaertner and Nievergelt, 2010).

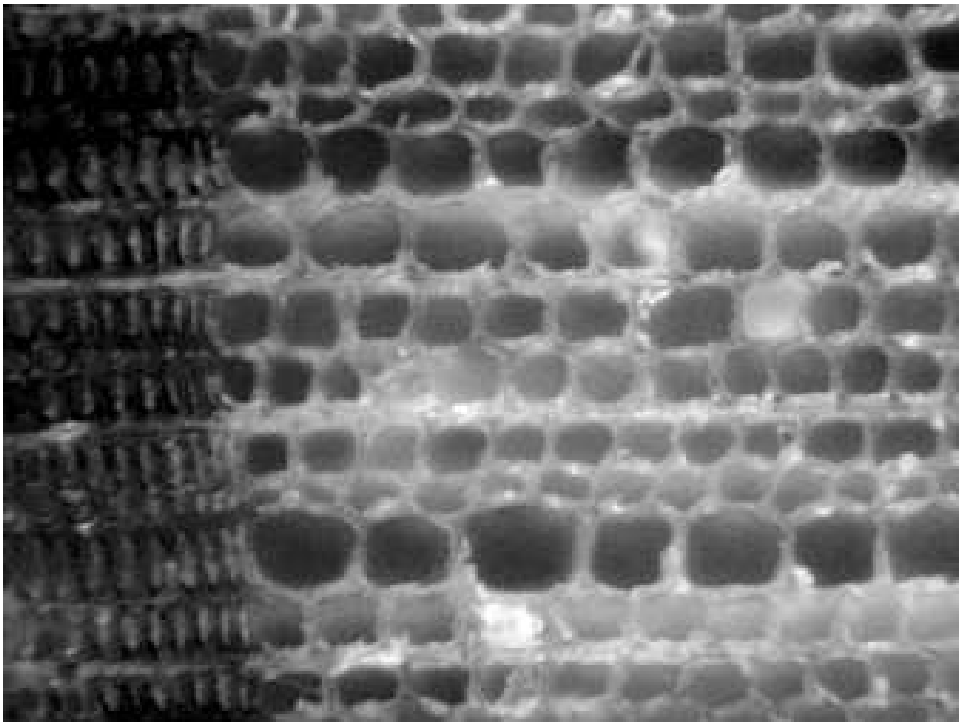

Fig. 6 *Picea abies* cross-section after core-microtome preparation (Fonti P., unpublished data)

3.4 Cross-dating and de-trending of ring widths

Ring widths are the amount of wood formed in a given year. Comparing the ring widths of a tree with dated master chronology allows the exact year in which each tree ring was formed to be identified (cross-dating).

This is the basis of "dendrochronology". Nevertheless, tree growth may also be affected by other, non-climatic, factors such as tree age (see section 2). For example, ring width may greatly increase after a neighbouring tree is cut. To some extent, this undesired noise should be statistically removed through standardisation. This involves fitting a curve to the tree-ring series, then dividing each ring-width value by the corresponding curve value. In an ideal tree, fitting an exponential curve would be enough, but in most cases a second de-trending is performed through a cubic smoothing spline (Cook and Peters, 1981). The spline acts as a high-pass filter and is defined by a cut-off wavelength. In some cases, further de-trending is performed using autoregressive models (Monserud, 1986). To enhance the climate signal, the series obtained from several trees at a given site may be averaged using a biweight robust mean estimation (Cook and Holmes, 1986). As already mentioned, the main problem with statistical treatments lies in the risk of removing low-frequency climate variability (Cook et al., 1995).

3.5 Sample grinding

After cross-dating, tree rings are usually separated using a razor. In order to obtain homogeneous wood samples, most researchers dry samples at 60°C then grind them (<0.1 mm) in a centrifugal mill. During a previous phase of this thesis, I found that cooling the samples in liquid nitrogen was the best way of obtaining a homogeneous sample (Gori Y., unpublished data).

3.6 Atmospheric CO_2 correction

Because fossil fuels are depleted in ^{13}C, anthropogenic increases in CO_2 concentrations in the atmosphere have lowered the $\delta^{13}C$ values in air by about 1.5%. Since fractionation is an additive process, this trend is reflected in tree rings. Indeed, most of the tree-ring $\delta^{13}C$ series show this trend. A simple solution to remove this noise without weakening the climate signal has been proposed by Francey et al. (1999). They have compiled a high precision record of atmospheric $\delta^{13}C$ based on Antarctic ice cores which, for the purposes of correcting tree-ring data, can be summarised by two consecutive segments, one between 1850 and 1961 with an annual decline of 0.0044%, and one between 1962 and 1980 with a steeper annual decline of 0.0281% (Table 2).

Year	$\delta^{13}C$	Δ	CO_2	Year	$\delta^{13}C$	Δ	CO_2	Year	$\delta^{13}C$	Δ	CO_2
1850	-6.41	0.01	285.2	1901	-6.64	0.24	297	1952	-6.86	0.46	312.8
1851	-6.42	0.02	285.3	1902	-6.64	0.24	297.3	1953	-6.87	0.47	313.2
1852	-6.42	0.02	285.4	1903	-6.65	0.25	297.6	1954	-6.87	0.47	313.6
1853	-6.43	0.03	285.5	1904	-6.65	0.25	297.9	1955	-6.88	0.48	314.1
1854	-6.43	0.03	285.6	1905	-6.66	0.26	298.2	1956	-6.88	0.48	314.6
1855	-6.43	0.03	285.7	1906	-6.66	0.26	298.5	1957	-6.89	0.49	315.1
1856	-6.44	0.04	285.8	1907	-6.66	0.26	298.9	1958	-6.89	0.49	315.7
1857	-6.44	0.04	285.9	1908	-6.67	0.27	299.2	1959	-6.90	0.5	315.8
1858	-6.45	0.05	286	1909	-6.67	0.27	299.6	1960	-6.90	0.5	316.8
1859	-6.45	0.05	286.2	1910	-6.68	0.28	299.9	1961	-6.90	0.5	317.5
1860	-6.46	0.06	286.3	1911	-6.68	0.28	300.2	1962	-6.92	0.52	318.3
1861	-6.46	0.06	286.5	1912	-6.69	0.29	300.5	1963	-6.95	0.55	318.8
1862	-6.47	0.07	286.6	1913	-6.69	0.29	300.9	1964	-6.98	0.58	319.4
1863	-6.47	0.07	286.8	1914	-6.70	0.3	301.2	1965	-7.01	0.61	319.9
1864	-6.47	0.07	287	1915	-6.70	0.3	301.5	1966	-7.03	0.63	321.2
1865	-6.48	0.08	287.2	1916	-6.70	0.3	301.8	1967	-7.06	0.66	322
1866	-6.48	0.08	287.4	1917	-6.71	0.31	302.2	1968	-7.09	0.69	322.9
1867	-6.49	0.09	287.6	1918	-6.71	0.31	302.5	1969	-7.12	0.72	324.5
1868	-6.49	0.09	287.8	1919	-6.72	0.32	302.9	1970	-7.15	0.75	325.5
1869	-6.50	0.1	288	1920	-6.72	0.32	303.2	1971	-7.17	0.77	326.2
1870	-6.50	0.1	288.2	1921	-6.73	0.33	303.5	1972	-7.20	0.8	327.3
1871	-6.51	0.11	288.4	1922	-6.73	0.33	303.9	1973	-7.23	0.83	329.5
1872	-6.51	0.11	288.7	1923	-6.74	0.34	304.2	1974	-7.26	0.86	330.1
1873	-6.51	0.11	288.9	1924	-6.74	0.34	304.6	1975	-7.29	0.89	331
1874	-6.52	0.12	289.1	1925	-6.74	0.34	304.9	1976	-7.32	0.92	332
1875	-6.52	0.12	289.4	1926	-6.75	0.35	305.2	1977	-7.34	0.94	333.7
1876	-6.53	0.13	289.7	1927	-6.75	0.35	305.6	1978	-7.37	0.97	335.3
1877	-6.53	0.13	289.9	1928	-6.76	0.36	305.9	1979	-7.40	1	336.7
1878	-6.54	0.14	290.2	1929	-6.76	0.36	306.2	1980	-7.43	1.03	338.5
1879	-6.54	0.14	290.5	1930	-6.77	0.37	306.5	1981	-7.46	1.06	339.8
1880	-6.55	0.15	290.8	1931	-6.77	0.37	306.8	1982	-7.48	1.08	341
1881	-6.55	0.15	291.1	1932	-6.78	0.38	307.1	1983	-7.51	1.11	342.6
1882	-6.55	0.15	291.4	1933	-6.78	0.38	307.4	1984	-7.54	1.14	344.3
1883	-6.56	0.16	291.7	1934	-6.78	0.38	307.7	1985	-7.57	1.17	345.7
1884	-6.56	0.16	292	1935	-6.79	0.39	308	1986	-7.60	1.2	347
1885	-6.57	0.17	292.3	1936	-6.79	0.39	308.3	1987	-7.62	1.22	348.8
1886	-6.57	0.17	292.6	1937	-6.80	0.4	308.5	1988	-7.65	1.25	351.3
1887	-6.58	0.18	292.9	1938	-6.80	0.4	308.8	1989	-7.68	1.28	352.8
1888	-6.58	0.18	293.1	1939	-6.81	0.41	309.1	1990	-7.71	1.31	354
1889	-6.58	0.18	293.4	1940	-6.81	0.41	309.3	1991	-7.74	1.34	355.5
1890	-6.59	0.19	293.7	1941	-6.82	0.42	309.5	1992	-7.77	1.37	356.3
1891	-6.59	0.19	294	1942	-6.82	0.42	309.8	1993	-7.79	1.39	357
1892	-6.60	0.2	294.3	1943	-6.82	0.42	310	1994	-7.82	1.42	358.9
1893	-6.60	0.2	294.6	1944	-6.83	0.43	310.2	1995	-7.85	1.45	360.9
1894	-6.61	0.21	294.9	1945	-6.83	0.43	310.5	1996	-7.88	1.48	362.7
1895	-6.61	0.21	295.2	1946	-6.84	0.44	310.8	1997	-7.91	1.51	363.8
1896	-6.62	0.22	295.5	1947	-6.84	0.44	311	1998	-7.93	1.53	365.5
1897	-6.62	0.22	295.8	1948	-6.85	0.45	311.3	1999	-7.96	1.56	367
1898	-6.62	0.22	296.1	1949	-6.85	0.45	311.7	2000	-7.99	1.59	368.5
1899	-6.63	0.23	296.4	1950	-6.86	0.46	312	2001	-8.02	1.62	370
1900	-6.63	0.23	296.7	1951	-6.86	0.46	312.4	2002	-8.05	1.65	371.5

Table 2. Annual values for the $\delta^{13}C$ of the atmospheric CO_2 and the correction factor to quote tree-ring $\delta^{13}C$ values relative to a pre-industrial value of -6.4‰ (McCarrol and Loader, 2004).

4 *Heterobasion annosum*: ecology, symptoms and damage in infected forests

Heterobasidion annosum (Fr.) Bref. sensu lato, which causes root and butt rot and tree mortality, is regarded as one of the most destructive diseases of conifers in northern boreal conifer forests, particularly in weakening root systems and increasing the risk of windfall (Woodward et al., 1998). Economic losses attributable to *Heterobasidion* infection in Europe only as wood decay agent were estimated at 800 million euros per year (Woodward et al., 1998). These losses take several forms:

- Wood decay of the lower part of the inner stem of living trees (normally for 2-5 meters, but can reach also 12-15 meters), usually without external symptoms (at least in *Picea abies*) , it is assessed in field only at harvesting time.
- Potential growth loss caused by chronic root infection that interferes with the plant physiology.
- Increasing windfall susceptibility for weakening the root system, especially in case of moderate storms with heavy snowing.
- Indirect costs (increased logging costs for forest planning disturbance, diagnosis, application of control measures, research).

In 1978, Korhonen (1978) divided *H. annosum* sensu lato into two intersterility groups (proto-species) according to main host preference, spruce or pine. Subsequently, Capretti et al., (1990) added a third group with a preference for silver fir. The three intersterility groups eventually received species status and were named *H. annosum* sensu stricto, *H. parviporum* and *H. abietinum*, with preferences respectively for pine species, Norway spruce and silver fir (Niemelä and Korhonen, 1998).

For Norway spruce external symptoms of *H. annosum* s.l. root rot are often hidden and with not clearly characteristic traits, hardly distinguishable from those caused by other root diseases. Some older Norway spruces display reduced crown density with yellowish foliage and resin exudation during the last stage of infection. However, other root pathogens, such as honey fungus (*Armillaria* spp.), may cause similar symptoms. The last stage of decline may last for up to ten years before a tree dies, and during this phase the crown becomes rounded and very transparent and the root system may be reduced by up to two-thirds.

Presence of *H. annosum* may be confirmed by the presence of the imperfect state, *Spininger meineckellus* (A.J. Olson) Stalpers, according to the methods described by Stalpers (1978).

During the first stage of infection, a stain may be observed on the butt of felled trees, varying in colour according to the host tree species. Incipient decay is normally pale pink, developing into a light brown spongy decay to then become a white pocket rot with black flecks in its advanced stage.

4.1 Ecological requirements of *Heterobasidion annosum*

H. annosum grows in a wide range of temperatures according to isolate. Mycelial growth take place above 0-2°C, with an optimum of 22-28°C; growth stops above 32-37°C and under 0-2°C, depending on the strain (Korhonen and Stenlid, 1998; La Porta et al., 2008). The temperature range for the production and germination of basidiospores and conidiospores is similar to that for mycelia growth: 22-28°C (Asiegbu et al., 2005).

The pH range for growth of *H. annosum* varies according to isolate with different isolates varying considerably in their reaction to pH. The optimum is between 4 and 5.7, depending on the strain (Korhonen and Stenlid, 1998).

In the Alpine region, *H. annosum* is particularly harmful to *P. abies*. Several researchers have reported that the pathogen is more active in conifer reforestation on former agricultural or pasture land, where the soil mycoflora do not inhibit its growth.

4.2 Reduced standing timber volume caused by *Heterobasidion annosum*

While the most evident detrimental effect of *H. annosum* s.l. is decay of the lower part of the inner stem and subsequent depreciation for timber use, this pathogen also causes indirect volume reduction as a consequence of physiological disorder. The three main mechanisms causing growth loss brought about by root rot are: i) death of most major roots, ii) reduced ability of trees to take up water and nutrients (Cherubini et al., 2002; Benz-Hellgren and Stenlid, 1995; Joseph et al.,1998), and iii) the formation of a reaction zone (Benz-Hellgren and Stenlid, 1995; Hietala et al., 2009; Oliva et al., 2010), an energy-costly defence mechanism whereby necrotic tissue is enriched with antifungal phenolic extractives (Shain, 1979).

The impact of root disease is manifested on two principal levels: the first is the readily observable and quantifiable rot columns, while the second, indirect volume reduction, is more difficult to identify and quantify (Manion, 1991).

Periodic growth reduction was observed in infected *P. abies* by Bendz-Hellgren and Stenlid (1995), who reported volume increment losses of 23% due to *H. annosum* infection 17 years after initial thinning. However, they detected no increment loss at a second location 8 years after initial thinning, highlighting the need for long-term studies of these effects. They hypothesized that about 50% of the periodic increment reductions in decayed trees could be due to resources being allocated to building the reaction zone in order to compartmentalize the decay column, instead of being invested in secondary growth.

5 *Cephalcia arvensis* ecology and outbreak

The web-spinning sawfly *Cephalcia* Panzer (Hymenoptera, Pamphillidae) is a monophagous defoliator of the *Picea* genus and endemic to the spruce range in Eurasia (Battisti et al. 2000). Some species of the genus *Cephalcia* have caused intense defoliation in *Picea abies* Karst. in European forests (Fig. 7). These species are characterized by long periods of latency and eruptive outbreaks (Eichhorn, 1990).

During the 1980s, two areas of the Venetian Pre-Alps were dramatically infested by *Cephalcia arvensis* Panzer and over 200 ha of forest were killed (Fig. 8). *Cephalcia arvensis* outbreaks had been previously reported in spruce forests in Sweden (Trägårdh, 1939), Denmark (Boas, 1934) and Czechoslovakia, always in mature plantations. However, *C. arvensis* had never before been reported as a spruce pest in Italy (Battisti and Stergulc, 1988). As it is well-known, this region is at the southern edge of the area of natural distribution of Norway spruce, where climatic conditions tend to be less favourable, giving rise to long vegetative periods and frequent drought stresses (Schmidt-Vogt, 1977). Nonetheless, foresters have used spruce in reforestation programmes in these areas because of its high productivity. There are a few conflicting hypotheses regarding the possible causes of these outbreaks, with climatic and pedological factors seeming to predominate (Marchisio et al., 1994). Schwenke (1963) proposed that the increase in needle sugar levels resulting from drought stress may have contributed to the exceptional outbreak in southern Germany. In fact, drought could facilitate insect growth by modifying the chemical composition of leaves. In the case of *Cephalcia alpina (=fallenii* Dalman) in Central Europe, pollution has also been shown to be a factor contributing to the outbreak (Capecki, 1982; Martinek, 1987). It is not easy to identify which environmental factor could have triggered these intense outbreaks, which are likely to have resulted from the interaction of various factors, both biological (e.g. insect growth and tree resistance) and abiotic (e.g. climate variability and soil characteristics).

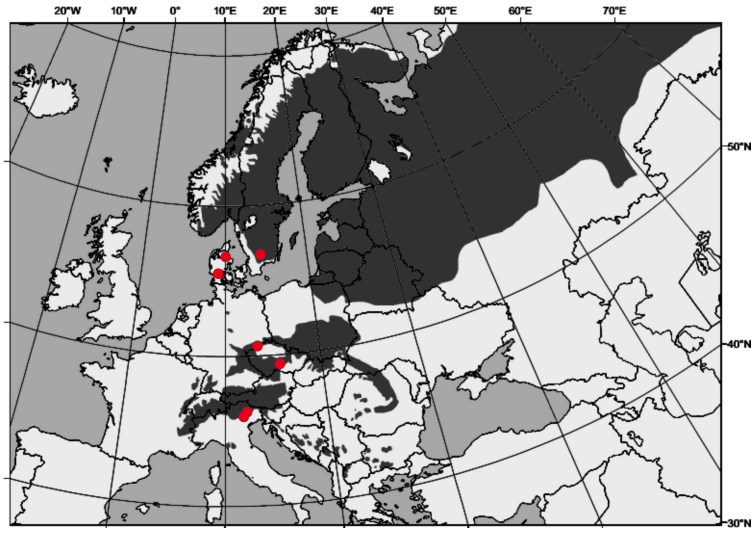

Fig. 7. Outbreak areas of *Cephalcia arvensis* in Europe (red circles) and natural range of the Norway spruce (*Picea abies*) according to Schmidt-Vogt (1977). Adapted from Marchisio et al. (1994).

Fig. 8 Norway spruce stand in the Cansiglio plateau during the *Cephalcia arvensis* outbreak (Battisti A., photo credits).

6 Climate change and forest pests

Climate change could alter the geographical range of pests and hosts (Lonsdale and Gibbs, 1996) and modify host resistance (Desprez-Loustau et al., 2006). Some authors have suggested that one outcome of climate warming could be changes in the occurrence and intensity of tree diseases (Linares et al. 2010; Fischlin et al., 2007; La Porta et al., 1997; La Porta et al., 2008). An increase in summer droughts would probably favour diseases caused by *Heterobasidion spp*. or other facultative biotrophic pathogens and increase tree mortality (Linares et al., 2010; Henry et al., 2009).

It has been shown that warmer temperatures correlate strongly with the incidence rate of *Heterobasidion* spp. (Thor et al., 2005; Mattila and Nuutinen, 2007). Moreover, the combined effect of warmer temperatures and drought conditions predispose conifers to *Heterobasidion* attack by reducing the trees' endogenous defence mechanisms (Gori et al., 2013 b,c; La Porta et al., 2008; Lindberg and Johansson, 1992). On the other hand, increased temperatures can also benefit the *Heterobasidion* antagonist *Phlebiopsia gigantean* (Fr.) Jülich, where this fungus is used as a control method (Thor et al., 1997).

It has been claimed that climate change (rises in temperature and CO_2 levels) is responsible for the northward and upward expansion of the range of several insect species of northern temperate forests (Battisti, 2006). In the case of *Cephalcia arvensis*, it seems likely that increases in temperature in June and July 1983-85 was the major factor in prompting the outbreaks (Battisti, 2006; Marchisio et al., 1994).

Accordingly, further investigation into the effects of the interactions of environmental factors and pests on forest trees will be necessary in order to throw light on these complex mechanisms (Desprez-Loustau et al., 2006).

Objectives

As already stated in the general introduction, the overall objective of this thesis is to investigate the impact of pests on tree growth and tree physiological responses over the long term by means of tree-ring and stable isotope analyses. Due to the interdisciplinary nature of this work, I have grouped the objectives into four different topics, each of which was developed in a separate paper with its own introduction and conclusions, thus making exposition clearer.

The outline of this thesis, as reported in the sections which follow, is summarised below:

Method and overall goal:	**Questions to be answered:**
1. Eight different stable isotope ratio analyses of *Picea abies* (Preliminary study). **Title of the paper**: Carbon, hydrogen and oxygen stable isotope ratios of whole wood, cellulose and lignin methoxyl groups of *Picea abies* as climate proxies. **Aim**: to develop a model able to accurately estimate environmental proxies from stable isotope ratios in *Picea abies* tree rings.	1.1 Is wood component extraction necessary for climate reconstruction from *P. abies*? 1.2 What is the best wood component? 1.3 What environmental information does each proxy contain? 1.4 Does combining proxies improve the model?
2. Dendroecological analyses. Tree-ring analysis of *Picea abies* affected by *Heterobasidion parviporum*. **Title of the paper**: Fungal root pathogen (*Heterobasidion parviporum*) increases drought stress in Norway spruce stand at low elevation in the Alps. **Aim**: to gain insights into plant-pathogen interactions under different climate conditions	2.1 Do climatic conditions influence fungal behaviour? 2.2 How long can a tree survive after a fungal attack? 2.3 Is dendrochronology helpful in dating the onset of fungal attack? 2.4 To what extent is growth reduction due to the prolonged presence of the fungus in the wood?
3. Isotope analyses. Carbon and oxygen isotope analyses of *Picea abies* affected by *Heterobasidion parviporum.* **Title of the paper**: Tree-ring isotope analyses of Norway spruce suffering from long-term infection by the pathogenic white-rot fungus *Heterobasidion parviporum*. **Aim**: to gain insights into the physiological responses of infected trees.	3.1 Can isotopic signals identify the physiological responses of long-term fungal infection? 3.2 What physiological mechanisms can be altered by a fungal attack?
4. Dendroecological and isotope analyses. Tree-ring and stable isotope analyses of *Picea abies* defoliated by *Cephalica*	4.1 Does defoliation caused by the insect give rise to physiological compensation? Do any of the physiological

arvensis. **Title of the paper**: Tree rings and stable isotopes reveal the short- and long-term effects of insect defoliation of Norway spruce (*Picea abies*). **Aim**: to gain insights into the physiological responses of defoliated trees.	adaptation processes persist after defoliation and full recovery of the tree? Can isotopic signals identify physiological responses during defoliation? 4.2 Can isotopic signals explain the high growth rate of *Cephalcia* populations in the infested area? 4.4 Can isotopic signals date the onset of insect defoliation better than tree-ring width chronologies?

List of original papers

This doctoral thesis is based on the following four articles:

I. Gori Yuri, Wehrens Ron, Greule Markus, Frank Keppler, Ziller Luca, La Porta Nicola, Camin Federica (2013). Carbon, hydrogen and oxygen stable isotope ratios of whole wood, cellulose and lignin methoxyl groups of *Picea abies* as climate proxies. Rapid Communications in Mass Spectrometry. 27, 265-275. DOI: 10.1002/rcm.6446

II. Gori Yuri, Cherubini Paolo, Camin Federica, La Porta Nicola (2013). Fungal root pathogen (*Heterobasidion parviporum*) increases drought stress in Norway spruce stand at low elevation in the Alps. European Journal of Forest Research. 132, 4:607-619. DOI: 10.1007/s10342-013-0698-x

III. Gori Yuri, La Porta Nicola, Camin Federica (2013). Tree-ring isotope analysis of Norway spruce suffering from long-term infection by the pathogenic white-rot fungus *Heterobasidion parviporum*. Forest Pathology. DOI: 10.1111/efp.12089

IV. Gori Yuri, Camin Federica, La Porta Nicola, Carrer Marco, Battisti Andrea. Tree rings and stable isotopes reveal the short- and long-term effects of insect defoliation on Norway spruce (*Picea abies*). Manuscript submitted to Forest Ecology and Management on 27 October 2013.

I was primarily responsible for planning the study, designing and carrying out the experiments, analysing the data and writing the papers. Laboratory work for papers I and II was carried out together with Anne Verstege (WSL, Birmensdorf, Switzerland), and for paper IV with Dr. Raffaella Dibona (Centre for Studies of the Alpine Environment, San Vito di Cadore, Italy) and Anna Rova. Stable isotope measurements were made together with Luca Ziller (FEM-IASMA, S. Michele all'Adige, Italy). Other co-authors of the papers contributed mainly by providing valuable comments on the manuscripts.

Section 1

Carbon, hydrogen and oxygen stable isotope ratios of whole wood, cellulose and lignin methoxyl groups of *Picea abies* as climate proxies.

Rapid Communications in Mass Spectrometry 2013. 27, 265-275

Research Article

Rapid Communications in Mass Spectrometry

Received: 10 August 2012 Revised: 10 October 2012 Accepted: 19 October 2012 Published online in Wiley Online Library

Rapid Commun. Mass Spectrom. **2013**, *27*, 265–275
(wileyonlinelibrary.com) DOI: 10.1002/rcm.6446

Carbon, hydrogen and oxygen stable isotope ratios of whole wood, cellulose and lignin methoxyl groups of *Picea abies* as climate proxies

Y. Gori[1]*, R. Wehrens[1], M. Greule[2], F. Keppler[2], L. Ziller[1], N. La Porta[1] and F. Camin[1]

[1]IASMA Research and Innovation Centre – Fondazione Edmund Mach, Via E. Mach 1, 38010 San Michele all'Adige, Italy
[2]Max Planck Institute for Chemistry, Department of Atmospheric Chemistry, Hahn-Meitner-Weg 1, DE 55128 Mainz, Germany

RATIONALE: Carbon, hydrogen and oxygen (C, H and O) stable isotope ratios of whole wood and components are commonly used as paleoclimate proxies. In this work we consider eight different proxies in order to discover the most suitable wood component and stable isotope ratio to provide the strongest climate signal in *Picea abies* in a southeastern Alpine region (Trentino, Italy).
METHODS: $\delta^{13}C$, $\delta^{18}O$ and $\delta^{2}H$ values in whole wood and cellulose, and $\delta^{13}C$ and $\delta^{2}H$ values in lignin methoxyl groups were measured. Analysis was performed using an Isotopic Ratio Mass Spectrometer coupled with an Elemental Analyser for measuring $^{13}C/^{12}C$ and a Pyrolyser for measuring $^{2}H/^{1}H$ and $^{18}O/^{16}O$. The data were evaluated by Principal Component Analysis, and a simple Pearson's correlation between isotope chronologies and climatic features, and multiple linear regression were performed to evaluate the data.
RESULTS: Each stable isotope ratio in cellulose and lignin methoxyl differs significantly from the same stable isotope ratio in whole wood, the values begin higher in cellulose and lignin except for the lignin $\delta^{2}H$ values. Significant correlations were found between the whole wood and the cellulose fractions for each isotope ratio. Overall, the highest correlations with temperature were found with the $\delta^{18}O$ and $\delta^{2}H$ values in whole wood, whereas no significant correlations were found between isotope proxies and precipitation.
CONCLUSIONS: $\delta^{18}O$ and $\delta^{2}H$ values in whole wood provide the best temperature signals in *Picea abies* in the northern Italian study area. Extraction of cellulose and lignin and analysis of other isotopic ratios do not seem to be necessary.

Reconstruction of past climates is of great importance since instrumental climatic records rarely extend beyond the 20th century. More comprehensive knowledge of past climate changes and weather extremes is useful for determining the extent to which current global warming is anthropogenic and for improving predictive models.[1,2] Information about past climates can be obtained from indirect proxy indicators, such as tree-ring widths and stable isotope ratios in tree rings.[3,4] Although tree-ring width is the easiest and most commonly used measurement for extracting climate data, it should be borne in mind that tree growth is not only determined by climatic conditions, but is also affected by other, non-climatic, factors. Competition for resources, disturbance events and other long-term trends related to tree age could alter the climate signal in tree-ring width. Moreover, tree-ring widths may vary considerably between sites, even those located in the same area.[1,5] Stable isotope ratios, on the other hand, are less influenced by non-climatic factors and are therefore more useful for obtaining information on trends in rainfall, temperature and relative humidity, and are hence a powerful tool for paleoclimatic studies.[9–11]

* *Correspondence to:* Y. Gori, IASMA Research and Innovation Centre – Fondazione Edmund Mach, Via E. Mach 1, 38010 San Michele all'Adige, Italy.
E-mail: yuri.gori@fmach.it

The three main stable isotopes present in wood (carbon, oxygen and hydrogen) provide access to very long chronologies with annual resolution and yield quantitative estimates useful for ecophysiological research and climate reconstruction.[6,4,7,8,58,59]

Following the findings by Wilson and Grinsted[12] that tree-ring components have different isotopic ratios, most research has been carried out on single components, usually cellulose, and on single isotope proxies (usually carbon or oxygen). Given that there is no material exchange and no further fractionation,[4,13,14] the isotope ratios of cellulose are often thought to be the most meaningful indicator of environmental information during tree growth.[7,8] Since the physiological process leading to fractionation differs substantially between isotopes, a multi-proxy approach based on the three main isotopes and a range of components would appear to be the best method for improving climate reconstruction and ecophysiological research.[15]

Cellulose extraction, even by the simple bath method,[16–18] is still time-consuming, especially in view of the need to analyse long-term chronologies for paleoclimatic reconstruction. It has recently been suggested for some tree species that both carbon and oxygen isotope ratios in whole wood may yield as good a climatic signal as cellulose.[19–21,58] However, according to other authors, cellulose separation is essential, at least for $\delta^{18}O$ values, given that the $\delta^{18}O$ value of cellulose provides the strongest and most stable climatic signal.[7,8] Yet other authors[19,22] consider cellulose

extraction to be necessary only for some tree species, since stable isotope ratios differ according to site features and tree species.

A further problem with cellulose is that some of the hydrogen atoms undergo exchange with xylem water and then with the atmosphere. Most investigations have therefore focused on nitrocellulose, which contains only non-exchangeable hydrogen, although the extraction and preparation method is even more time-consuming and labour-intensive. The development of any new methods to simplify sample preparation would therefore be of great help.

Recently, it was suggested that stable hydrogen isotope values of lignin methoxyl groups in tree rings might be a source of climate information and could serve as a paleoclimate proxy.[23] Conspicuous ^{2}H depletion of wood methoxyl groups relative to source water has been observed with a uniform isotopic fractionation (mean -216 ± 19‰) recorded with respect to meteoric water over a range of δ^2H values from +20 to −110‰, indicating that the methoxyl groups reflect the isotope values of the meteoric source water of woody plants. Lignin methoxyl groups are considered to be stable, i.e. the hydrogen atoms of the methoxyl moiety do not exchange with those of plant water during metabolic reactions in the plant. Thus, the initial δ^2H value of the methoxyl groups of lignin in woody tissue at formation is retained throughout the lifetime of the tree and in preserved tissue.[25–27]

The main aim of this study is to develop a simple model to accurately estimate climate proxy information from *Picea abies* (L.) Karst. in the south-eastern Alps. We used a series of δ^{13}C, δ^{18}O and δ^2H values of bulk wood and two wood constituents (cellulose and methoxyl groups of lignin) in order to find the most suitable combination of wood component and stable isotope ratio for obtaining the strongest climate signal. The originality of our study lies mainly in the simultaneous analysis of eight different proxies in ten trees at three different sites with annual resolution. We consider this multi-proxy to be a powerful technique for extracting climatic information from tree-ring isotope chronologies.[15]

Our main questions are:

(1) Is wood component extraction necessary for climate reconstruction from *P. abies* in the south-eastern Alps and, if so, what is the best wood component?
(2) How strong are the various climate proxy signals?
(3) Can the proxies be combined to build a better model for estimating climate?

EXPERIMENTAL

Samples, field sampling and dendrochronological methods

Field sampling was carried out on mature Norway spruce stands at three different elevations in the south-eastern Alps: Baselga (900 m a.s.l.; 46°4′48"N, 11°3′3"E), Val Maggiore (1300 m a.s.l.; 46°17′32"N, 11°36′49"E) and Cermis (1900 m a.s.l.; 46°15′0"N, 11°29′43"E).

The climate features are typical of the southern alpine region with cold winters, mild summers and frequent precipitation mostly concentrated in the summer months (June to September). The climate is cold temperate[57] and the vegetation season depends on elevation and date of snow melt, varying between 120 days (at the Cermis stand) and 150 days (at the Baselga stand).

All the sites are located on slopes ranging from 30% to 50%, have a northern aspect, and are within a distance of 25 km from each other (Fig. 1). The bedrock is porphyric granite, partially covered with morainic material and podzolic soils. The three stands are dense and homogeneous. All the forests within which they lie are characterised by several large, even-aged, homogeneous group of trees.

A total of ten mature *P. abies* trees were selected at each site. Care was taken to select only dominant trees growing in similar light and soil moisture conditions in plots measuring 100 m × 100 m. Four cores were extracted at 90° from each other using a 0.5 cm diameter Pressler increment borer; the pith was reached in at least one of the four cores. To prevent isotopic contamination, no lubricants, markers or sandpaper were used during field sampling and dendrochronological measurements.

The cores of all trees were prepared with a core-microtome[28] and standard dendrochronological methods were used to cross date.[56] Ring-width measurements on each core were made to the nearest 0.01 mm using LINTAB measuring equipment (Frank Rinn, Heidelberg, Germany). Raw Tree-Ring-Widths (TRW) of all curves were plotted, cross-dated visually and then cross-dated statistically by: (a) Gleichläufigkeit, i.e. the percentage agreement in the signs of first-differences of two time series; and (b) a t-test, which determines the degree of correlation between the curves. Cross-dating quality was checked using the COFECHA programme[29] as a standard dendrochronological protocol for quality control.

Average tree ages at the sites were over 100 years at Baselga, 150 years in Val Maggiore and 230 years at Cermis.

Sample preparation

After being dated, all the cores were prepared for isotopic analysis. Although some authors argue that latewood gives the strongest climatic signal,[30,31] others have found good signals using the whole tree ring, especially with conifer.[19,32,33,58] As the *P. abies* growing at Cermis presented very narrow rings with indistinguishable latewood bands, whole annual ring was used for all wood samples. Annual rings from each core were carefully separated with a razor under a binocular microscope at the early and late-wood border. To minimise the juvenile effect observed in young trees,[34,35] only rings formed during the mature growth phase were analysed (e.g. after 60 years at the high elevation site at Cermis, after 40 years at medium elevation in Val Maggiore, and after 30 years at low elevation at Baselga).[36]

Since isotopic signals vary around the circumference of the tree, we pooled the ring samples from the four radii.[37] Finally, all rings from a given year at each site (ten sampled trees per site) were pooled to reduce isotope variability between trees.[38] Care was taken to use the same dry weight in order to prevent the isotopic value being biased by the relative mass contribution of the tree rings (larger tree rings affect isotope values more than small ones).[39] Overall, we separated 150 tree rings at Cermis (from 1860 to 2009), 110 in Val Maggiore (from 1900 to 2009) and 75 at Baselga (from 1935 to 2009).

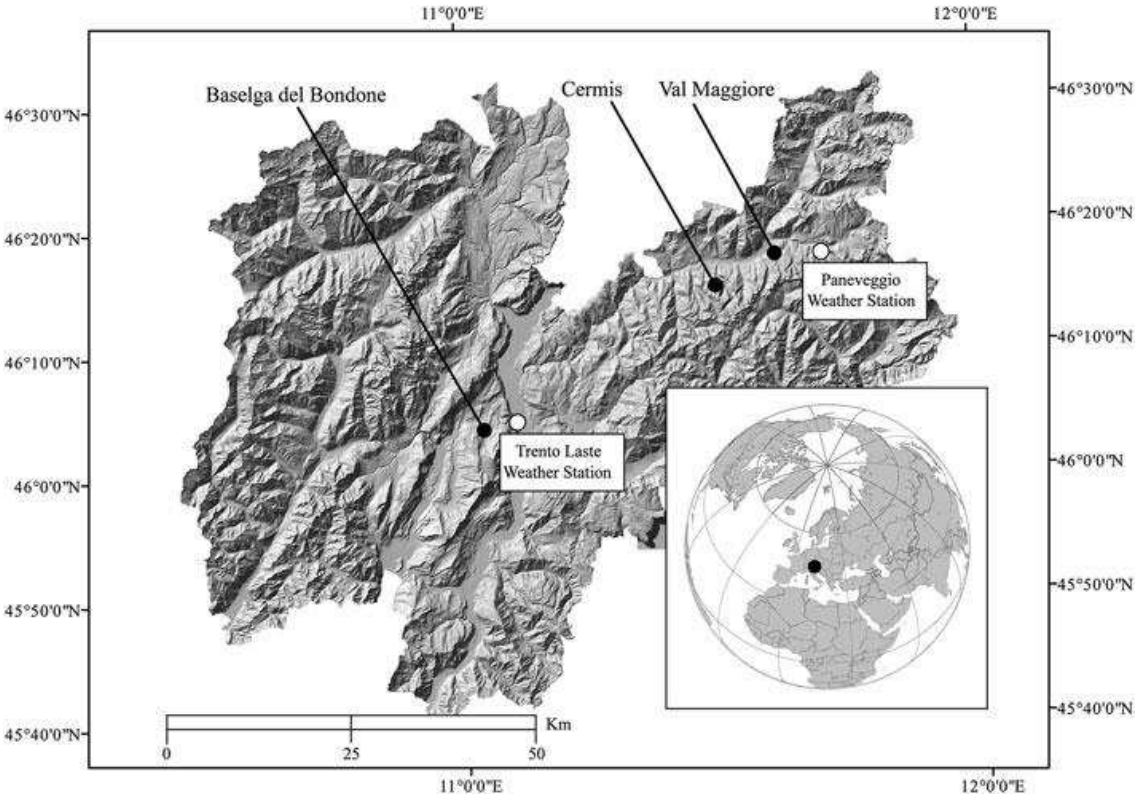

Figure 1. Location of the study sites. White dots represent the two weather stations at Paneveggio and Trento Laste.

Dried samples of whole wood were ground (<0.1 mm) in a centrifugal mill (ZM200, Retsch®, Hann, Germany) and all wood samples were split into three subsamples. The first group of subsamples did not undergo any treatment (whole wood); the second was used for cellulose extraction, and the third for lignin methoxyl group extraction. Cellulose was extracted according to a slightly modified version of the method described by Loader and co-authors.[17] In brief, the samples were washed twice in 5% NaOH solution for 2 h at 60°C in order to remove fats, oils, resins and hemicellulose. In a second step, the lignin was removed with a 7% $NaClO_2$ solution for a minimum of 36 h at 60°C. Since this solution is only reactive for about 10 h, it was changed and refilled daily as necessary.[8] After each treatment the samples were washed three times with boiling distilled water and dried for 48 h at 60°C.

No further preparation was needed to measure the stable carbon and hydrogen isotope values of the lignin methoxyl groups. The dried and ground wood samples were analysed directly using the HI method as described below and by Keppler *et al.*[23] and Greule *et al.*[25,26]

Isotope analysis

Overall, we analysed eight isotopic proxies for each sample: $\delta^{13}C$, $\delta^{18}O$ and $\delta^{2}H$ values in whole wood, $\delta^{13}C$, $\delta^{18}O$ and $\delta^{2}H$ values in cellulose and $\delta^{13}C$ and $\delta^{2}H$ values in lignin methoxyl groups. No analysis of $\delta^{2}H$ values in lignin methoxyl groups for the years 1900–1932 in Val Maggiore was performed due to the small amount of wood material. Sub-samples of 0.3–0.35 mg of cellulose and whole wood were weighed and placed in tin capsules for $\delta^{13}C$ analysis and in silver capsules for $\delta^{18}O$ and $\delta^{2}H$ analysis. All the samples were then oven-dried (80°C) to remove water vapour, and stored in a desiccator until analysis. The analysis was performed using Isotope Ratio Mass Spectrometry (IRMS) with a Finnigan DELTA XP isotope ratio mass spectrometer (Thermo Scientific, Bremen, Germany) coupled with an Elemental Analyser (Flash EA™1112, Thermo Scientific) to measure $^{13}C/^{12}C$ ratios, and a Pyrolyser (Finnigan™ TC/EA, High-Temperature Conversion Elemental Analyser, Thermo Scientific) to measure $^{2}H/^{1}H$ and $^{18}O/^{16}O$ ratios. To separate the gases, the EA was fitted with a Porapack QS GC column (3 m; 6 × 4 mm, o.d./i.d.) and the Pyrolyser with a molecular sieve 5 Å (0.6 m) GC column. The devices were interfaced with the isotope ratio mass spectrometer through a dilutor (Conflo III, Thermo Scientific) for dosing the sample and reference gases, and fitted with an autosampler (Finnigan AS 200, Thermo Scientific). An appropriate cover on the pyrolyser autosampler allowed continuous flushing with nitrogen to guarantee dryness of the samples during measurement.

For $^{13}C/^{12}C$ measurements, the tin capsules were inserted into the EA where they were quantitatively burnt to CO_2 and H_2O (H_2O removed using a $Mg(ClO_4)_2$ filter in the presence of O_2 and CuO). The CO_2 was flushed into the mass spectrometer through the ConFlo III device, where the content of the different isotopomers (m/z 44 and 45) was determined. For $^{18}O/^{16}O$ and $^{2}H/^{1}H$ analysis, the capsules were dropped into the pyrolyser tube where at a temperature of 1450°C the oxygen and hydrogen atoms of the sample were quantitatively converted into CO and H_2, respectively, at a temperature of 1450°C, then flushed into the mass spectrometer. The isotope ratio mass spectrometer first measured

$^{2}H/^{1}H$ and then, following the magnet jump, $^{18}O/^{16}O$. The H_3 factor, which allows correction of the contribution of $[H_3]^+$ to the m/z 3 signal,[40] was checked and found to be lower than 9. The isotope ratio values are expressed in δ‰ (= $[(R_{sample} - R_{standard})/R_{standard}]$ * 1000, where R is the ratio between the heavier isotope and the lighter one) against international standards (Vienna-Pee Dee Belemnite (V-PDB) for $\delta^{13}C$ values, and Vienna-Standard Mean Ocean Water (V-SMOW) for $\delta^{2}H$ and $\delta^{18}O$ values). To calculate the δ‰ values, working in-house standards for proteins were used calibrated against international reference materials: L-glutamic acid USGS 40 (IAEA – International Atomic Energy Agency, Vienna, Austria), fuel oil NBS-22 (IAEA), and sugar IAEA-CH-6 (IAEA) for $^{13}C/^{12}C$; and benzoic acid (IAEA-601) for $^{18}O/^{16}O$ in casein.

The $^{2}H/^{1}H$ values of whole wood and cellulose were corrected against an internal standard with an assigned value of $\delta^{2}H$ (−113‰), according to the comparative equilibration technique.[41]

The hydrogen and carbon isotope signatures of lignin methoxyl groups were measured using CH_3I released following treatment of the dried and ground wood samples with HI, as previously described by Greule and co-authors (for $\delta^{2}H$ measurements, see,[25] for $\delta^{13}C$ measurements, see[26]). In brief, hydriodic acid (0.5 mL, 55-58%) was added to the sample in a crimp glass vial (1.5 mL). The vials were sealed with crimp caps containing PTFE-lined butyl rubber septa (thickness 0.9 mm) and incubated for 30 min at 130°C. After being heated, the vials were allowed to equilibrate at room-temperature (22 ± 0.5°C, air-conditioned room) for at least 30 min before a headspace sample (10–90 µL) was removed and directly injected directly into the gas chromatography–combustion/thermal conversion–isotope ratio mass spectrometry (GC-C/TC-IRMS) system.

To determine the $\delta^{13}C$ and $\delta^{2}H$ values we used an HP 6890N gas chromatograph (Agilent, Santa Clara, CA, USA) equipped with an A200S autosampler (CTC Analytics, Zwingen, Switzerland), coupled to a Delta^{PLUS}XL isotope ratio mass spectrometer (ThermoQuest Finnigan, Bremen, Germany) via an oxidation reactor (for $\delta^{13}C$ values) [ceramic tube (Al_2O_3), length 320 mm, 0.5 mm i.d., with Cu/Ni/Pt wires inside (activated by oxygen), reactor temperature 960°C] or via a pyrolysis reactor (for $\delta^{2}H$ values) [ceramic tube (Al_2O_3), length 320 mm, 0.5 mm i.d., reactor temperature 1450°C] and a GC Combustion III interface (ThermoQuest Finnigan). The gas chromatograph was fitted with a ZB-5 ms capillary column (Phenomenex, Torrance, CA, USA) (30 m × 0.25 mm i.d., d_f 1.0 mm). The GC conditions for $\delta^{13}C$ analysis were: split injection (split ratio 10:1), injector temperature 200°C; initial oven temperature at 30°C for 3.8 min, ramp at 30°C/min to 100°C. The carrier gas was helium at a flow rate of 1.8 mL/min.

The GC conditions for $\delta^{2}H$ analysis were as follows: split injection (split ratio 4:1), injector temperature 200°C; initial oven temperature 30°C for 7 min, ramp at 40°C/min to 120°C with helium carrier gas at a constant flow rate of 0.6 mL/min. All the $\delta^{13}C$ and $\delta^{2}H$ values were normalised relative to V-PDB or V-SMOW using a CH_3I standard. The $\delta^{13}C$ value of CH_3I was calibrated against international reference substances (IAEA-CH-6, IAEA-CH-7, NBS-22) using an offline elemental analyser (EA)/IRMS system (IsoAnalytical Ltd., Sandbach, UK). The calibrated $\delta^{13}C$ value vs. V-PDB for CH_3I was −69.27 ± 0.05‰ (n = 15, 1σ).

The $\delta^{2}H$ value of CH_3I was also calibrated against international reference substances (IA-R002, IAEA- CH-7, NBS-22) using the EA/IRMS system described above. The calibrated $\delta^{2}H$ value vs. V-SMOW was −179.0 ± 2.9‰ (n = 15, 1σ).[24] The standard was measured after every fourth sample injection.

The analytical precision (1 standard deviation) was <0.2‰ for $\delta^{13}C$ values, 0.4‰ for $\delta^{18}O$ values, and <2‰ for $\delta^{2}H$ values.

Atmospheric CO_2 correction

Because fossil fuels are depleted in ^{13}C, anthropogenic increases in CO_2 concentrations in the atmosphere have lowered the $\delta^{13}C$ values of air by about 1.5‰. Since fractionation is an additive process, this trend is reflected in most of the tree-ring $\delta^{13}C$ series. The motive behind adjusting data for climate research is to remove this noise without weakening the climate signal, since these trends are unrelated to past climates.[4]

In our study, all the tree-ring $\delta^{13}C$ series measurements were corrected to preindustrial atmospheric $\delta^{13}C$ values by simple addition using data provided by Francey *et al.*[4,42] Since we pooled the tree rings formed during the mature growth phase, no other data treatment was necessary.[54,55]

Meteorological data

Meteorological data were supplied by two weather stations located near the sites: (a) Paneveggio weather station: 1415 m a.s.l.; 46° 18′33″N, 11°44′50″E, about 5 km from the Val Maggiore stand and 15 km from the Cermis stand; and (b) Trento Laste weather station: 312 m a.s.l.; 46°04′19″N, 11°08′8″E, about 6 km from the Baselga stand[60] (Fig. 1). Homogenised and corrected climate data from 1958 onwards for temperature and precipitation obtained from these two weather stations[43] were used to remove undesired effects (e.g. long-term error or changes in metering practices) and to increase the strength of the climate signal.

Finally, to check for potential climatic divergence we compared the homogenised temperature data from the two weather stations with the high-resolution MODIS LST (Moderate Resolution Imaging Spectroradiometer Land Surface Temperature). MODIS LST data have been collected since 2002 and have been further developed by Neteler.[44,45] This dataset provides very accurate daily minimum and maximum temperatures in a GIS (Geographic Information System) format with a high resolution of 200 m pixels.Since the recorded temperature data were consistent between the two datasets (r = 0.80 at Cermis; r = 0.83 at Val Maggiore; r = 0.79 at Baselga; p <0.05) we assumed the homogenised temperatures from the two weather stations to be representative of our three stands.

For the study, we used mean monthly, seasonal (winter: 21 December to 20 March; spring: 21 March to 20 June; summer: 21 June to 20 September; autumn: 21 September to 20 December) and annual temperature and precipitation at each site during the 1958-2009 period.

During the study period, the mean annual precipitation was 1196 mm at the Paneveggio weather station and 931 mm at Trento Laste, while the mean annual temperatures were 6°C and 12°C, respectively. The coolest and warmest months were January and July, with mean minimum temperatures of

Rapid Communications in Mass Spectrometry

−7°C and −3°C at the Paneveggio and Trento Laste weather stations, respectively, and mean maximum temperatures of 25°C and 29°C.

Statistical analysis

Descriptive statistics and stable isotope time series were carried out for all the data: Cermis from 1860 to 2009; Val Maggiore from 1900 to 2009 (except for the δ^2H values of the lignin methoxyl group); and Baselga from 1936 to 2009. The Pearson's correlation coefficient (Cermis from 1860 to 2009; Val Maggiore from 1933 to 2009; and Baselga from 1936 to 2009) was calculated and used as the basis for exploring the relationships between the stable isotope chronologies.

The reliability of the isotopic parameters as climate proxies was only tested against the 1958–2009 period. Principal component analysis (PCA) was performed as a clustering technique to identify isotope values with similar patterns and to determine whether and how isotope values from the same wood component are related. PCA was performed on mean-centred and autoscaled data.

A simple Pearson's correlation coefficient was calculated to determine the relationships between the isotope chronologies and climatic features, taking mean monthly, seasonal and annual temperatures and precipitation into account.

Multiple linear regression models were used to predict mean annual temperature. Six different models were built to discover which wood component (whole wood, cellulose, lignin methoxyl groups) best explains climate variation. Model parameters were the three isotope chronologies ($\delta^{13}C$, $\delta^{18}O$ and δ^2H values) and the three different wood components. The models were: (1) the full model, with all eight isotope proxies in all three wood components ($Model_{WLC}$);(2) a model excluding cellulose, with five isotope proxies in whole wood and lignin methoxyl fraction ($Model_{WL}$); (3) a model excluding lignin methoxyl, with six isotope proxies in whole wood and cellulose fraction ($Model_{WC}$); (4) only the three isotope proxies in whole wood ($Model_W$); (5) only the three isotope proxies in cellulose fraction ($Model_C$); and (6) only the two isotope proxies in lignin methoxyl ($Model_L$). An ANOVA (analysis of variance) was performed to compare $Model_{WLC}$ with the other simpler models (i.e. $Model_{WL}$, $Model_{WC}$, $Model_W$, $Model_C$ and $Model_L$) in order to identify the simplest efficient model.

Finally, in order to obtain the minimal adequate model, a further simplification was made by reducing the isotopic variable from the selected models by means of step-wise variable selection ($p < 0.01$). All statistical analyses were carried out with the R 2.11.0. programme.[46]

RESULTS AND DISCUSSION

Stable isotope chronologies

The time series of each isotope parameter for each of the three sites are shown in Fig. 2. The ANOVA showed that, for each isotope, the mean stable isotope ratio in extracted cellulose and lignin methoxyl groups differed significantly ($p < 0.001$) from that in whole wood. With the exception of the most recent period at Baselga, the $\delta^{13}C$ values in extracted cellulose ($\delta^{13}C_C$) and lignin methoxyl ($\delta^{13}C_L$) were higher than the values in whole wood ($\delta^{13}C_W$). On average, the $\delta^{13}C$ values for whole wood were about 1.4‰ lower than those for cellulose at all three sites. Similar results have been reported by other authors.[16,47]

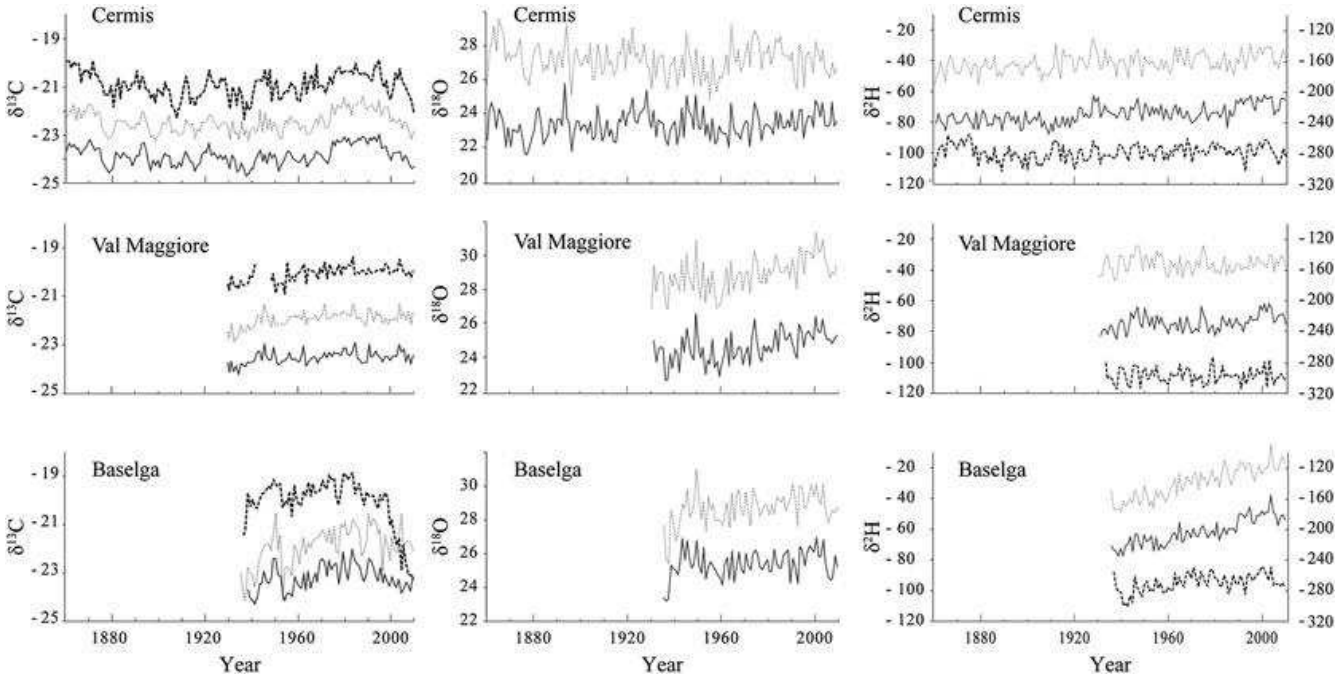

Figure 2. Stable isotope time series for the three spruce stands for the periods 1860-2009 at Cermis, 1933-2009 in Val Maggiore and 1936–2009 at Baselga. Cellulose, light grey dotted line; whole wood, continuous dark grey line; lignin methoxyl groups, broken black line. Hydrogen isotope values in lignin methoxyl groups are reported in a second ordinate axis on the right hand side.

The $\delta^{18}O$ values in cellulose ($\delta^{18}O_C$) were always higher than those reported for whole wood ($\delta^{18}O_W$), by an average of 3.9‰ at Cermis, 4.0‰ in Val Maggiore and 3.30‰ at Baselga. These results are consistent with the differences ranging from ca. 3‰[19] to 5.21‰; reported by other researchers.[8]

The δ^2H values in lignin methoxyl (δ^2H_L) are always lower than in wood (δ^2H_W) and cellulose (δ^2H_C), the mean values begin at −300‰ at Cermis and Baselga and −308‰ in Val Maggiore. The highest values are found for cellulose fraction (δ^2H_C). These findings are consistent with previous results, where the δ^2H_L values ranged from −325‰ to −153‰, and the δ^2H_W values from 141‰ to −29‰.[23]

The differences between the stable isotope values for cellulose and lignin and those in whole wood are a consequence of the isotopic fractionations involved in the pathways that lead to their biosynthesis.[23,48,49]

The relationship between the stable isotope ratio of each bioelement in whole wood and in the two subfractions across the three sites was explored by means of the Pearson's correlation coefficient. Table 1 summarises these results. The strongest correlations are between whole wood and the cellulose fraction for each isotope ratio.

In agreement with previous studies,[7,8,39,47,50,51,58] we found that the $\delta^{13}C$ values in whole wood were highly positively correlated with the $\delta^{13}C$ values in the cellulose fraction, suggesting similar sources of variability for these proxies. The $\delta^{13}C$ values in lignin methoxyl groups correlate to a lesser extent with $\delta^{13}C$ values in cellulose and $\delta^{13}C$ values in whole wood.

For the stable oxygen isotope ratios, the $\delta^{18}O_W$ and $\delta^{18}O_C$ values were highly ($p < 0.001$) correlated in Val Maggiore ($r = 0.75$) and at Baselga (0.78) but less so at Cermis ($r = 0.67$), the correlation coefficients being much higher than those found by other authors.[7,8,39] Our results agree with data published by Barbour and co-authors[19] and Sidorova and co-authors.[58] They reported a significant positive relationship between *Pinus* and *Quercus*[19] ($r = 0.89$, $p < 0.001$) and *Larix cajandery* Mayr.[58] (0.63, $p < 0.05$, during the 1904–2004 period), suggesting that similar climatic information is stored in these different wood components.

The coefficients of correlation between the δ^2H_C and δ^2H_W values were always positive, and higher than those calculated for δ^2H_Lvalues: the r values ranged from 0.66 (Val Maggiore, $p < 0.001$) to 0.88 (Baselga, $p < 0.001$).

Relationship between climate data and stable isotope values

To obtain a general insight into the explanatory variables, a PCA analysis was performed on data from the stable isotope series within the common period (1958–2009). The loading

Table 1. Correlation matrix of the eight proxies at each site. Isotope chronologies were: 1860–2009 at Cermis, 1933–2009 in Val Maggiore, 1936–2009 at Baselga

	$\delta^{13}C_C$	$\delta^{13}C_W$	$\delta^{13}C_L$	$\delta^{18}O_W$	$\delta^{18}O_C$	δ^2H_C	δ^2H_L
			CERMIS				
$\delta^{13}C_W$	0.91***						
$\delta^{13}C_L$	0.72***	0.78***					
$\delta^{18}O_W$	0.28***	0.28***	0.22**				
$\delta^{18}O_C$	0.41***	0.38***	0.40***	0.67***			
δ^2H_C	0.12	−0.10	−0.15	0.43***	0.32***		
δ^2H_L	0.30***	0.25**	0.32***	0.18	0.38***	0.49***	
δ^2H_W	0.23**	0.22**	0.17	0.44***	0.13	0.70***	0.38***
			VAL MAGGIORE				
$\delta^{13}C_W$	0.88***						
$\delta^{13}C_L$	0.57***	0.50***					
$\delta^{18}O_W$	0.19	0.18	0.00				
$\delta^{18}O_C$	0.21	0.12	0.27*	0.75***			
δ^2H_C	−0.27*	−0.47***	0.11	0.03	0.38***		
δ^2H_L	−0.01	−0.06	−0.05	0.23	0.28**	0.39***	
δ^2H_W	−0.24	−0.41	0.11	0.20	0.53***	0.66***	0.42***
			BASELGA				
$\delta^{13}C_W$	0.83***						
$\delta^{13}C_L$	0.24**	0.48***					
$\delta^{18}O_W$	0.39***	0.49***	0.17				
$\delta^{18}O_C$	0.61***	0.65***	0.22	0.78***			
δ^2H_C	0.63***	0.47***	−0.29*	0.38***	0.55***		
δ^2H_L	0.38**	0.30*	0.00	0.35**	0.48***	0.62***	
δ^2H_W	0.55***	0.35**	−0.36**	0.42***	0.53***	0.88***	0.58***

*$p < 0.05$; **$p < 0.01$; ***$p < 0.001$

$\delta^{13}C_W$: carbon isotope values in whole wood; **$\delta^{13}C_C$**: carbon isotope values in cellulose; **$\delta^{13}C_L$**: carbon isotope values in lignin methoxyl groups; **$\delta^{18}O_W$**: oxygen isotope values in whole wood; **$\delta^{18}O_C$**: oxygen isotope values in cellulose; **δ^2H_W**: hydrogen isotope values in whole wood; **δ^2H_C**: hydrogen isotope values in cellulose; **δ^2H_L**: hydrogen isotope values in lignin methoxyl groups

plot is given in Fig. 3: the variance explained by the first principal component is 39.2% (PC 1), while the second principal component (PC 2) accounts for 29.6% of the variance. The $\delta^{18}O$, $\delta^{13}C$ and $\delta^{2}H$ values of the various wood components clustered together; within each isotope series, cellulose and whole wood have the closest relationship. These findings agree with the good relationship found between the $\delta^{13}C$ and $\delta^{18}O$ values in different wood components for the complete time series (Table 1). The stable isotope values in lignin methoxyl are less highly correlated with the other components and therefore appear to be influenced by different environmental and biochemical factors.

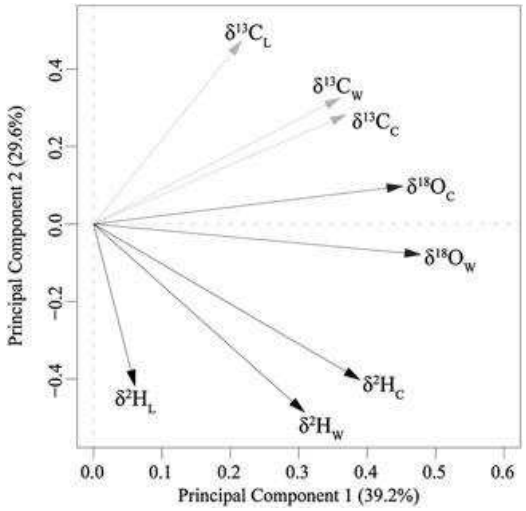

Figure 3. Biplot of the PCA analysis reporting the isotope proxies in whole wood ($\delta^{13}C_W$, $\delta^{18}O_W$, $\delta^{2}H_W$ values), cellulose ($\delta^{13}C_C$, $\delta^{18}O_C$, $\delta^{2}H_C$ values) and lignin methoxyl groups ($\delta^{13}C_L$, $\delta^{2}H_L$ values) for the period 1958-2009. Axis labels report the percentage of variance expressed by each component.

In order to test their reliability as climate proxies, each stable isotope value of each component was separately correlated to the mean temperature and precipitation at each site. We accepted only a significance level of $p < 0.01$. The mean annual and mean seasonal climate variables are shown as predictors. For precipitation, we report only the mean autumn precipitation at Cermis because we found no correlations ($p < 0.01$) in the other cases. The coefficients of correlation between climate variables and isotope series are given in Table 2. Looking at the results from the three sites, we can see that the correlation is significant ($p < 0.01$) for all the proxies, with the exception of the $\delta^{13}C_W$ and $\delta^{2}H_L$ series. The strongest correlation was obtained using the $\delta^{2}H_W$ value as a predictor for annual temperature ($p < 0.001$). Significant relationships were also found between the $\delta^{2}H_C$ and $\delta^{18}O_W$ series and various seasonal temperatures. The $\delta^{18}O_C$ series are related only to mean annual and mean seasonal temperature in Val Maggiore and to mean annual temperature at Baselga, but the correlation coefficients are always lower than those of the $\delta^{18}O_W$ series with the same climate proxies.

The $\delta^{13}C_L$ series are only negatively correlated with annual and some seasonal temperatures at Baselga. We do not have an explanation for this but it should be borne in mind that stable isotope values of different wood fractions depend not only on the species, but also on climatic features at the stand

Table 2. Coefficients of correlation between isotope proxies and climate features for the three sites with respect to the 1958–2009 period

Site	C.F.	Period¶	$\delta^{13}C_W$	$\delta^{13}C_C$	$\delta^{13}C_L$	$\delta^{18}O_W$	$\delta^{18}O_C$	$\delta^{2}H_W$	$\delta^{2}H_C$	$\delta^{2}H_L$
CERMIS	t	ANNUAL				0.57***		0.69***	0.36**	
		WINTER						0.63***	0.46***	
		SPRING				0.48***		0.46***		
		SUMMER				0.38**		0.49***		
	p	AUTUMN		−0.37**						
VAL MAGGIORE	t	ANNUAL				0.60***	0.57***	0.62***	0.45***	
		WINTER					0.37**	0.43***	0.47***	
		SPRING				0.45***	0.42**	0.54***		
		SUMMER				0.53***	0.44***	0.39**		
BASELGA	t	ANNUAL			−0.61***	0.43***	0.37**	0.75***	0.69***	
		WINTER						0.52***	0.45***	
		SPRING			−0.61***			0.47***	0.40**	
		SUMMER				0.38**		0.59***	0.59***	
		AUTUMN			−0.48***					

**$p < 0.01$; ***$p < 0.001$

$\delta^{13}C_W$: carbon isotope values in whole wood; **$\delta^{13}C_C$**: carbon isotope values in cellulose; **$\delta^{13}C_L$**: carbon isotope values in lignin methoxyl groups; **$\delta^{18}O_W$**: oxygen isotope values in whole wood; **$\delta^{18}O_C$**: oxygen isotope values in cellulose; **$\delta^{2}H_W$**: hydrogen isotope values in whole wood; **$\delta^{2}H_C$**: hydrogen isotope values in cellulose; **$\delta^{2}H_L$**: hydrogen isotope values in lignin methoxyl groups; **C.F.**: Climatic factor; t: temperature; p: precipitation

¶Average daily temperatures and precipitation were used for the periods: 21 December to 20 March (winter), 21 March to 20 June (spring), 21 June to 20 September (summer), 21 September to 20 December (autumn).

level and on the geographical origin of the wood.[19,23] Contrary to what would be expected from previous reports,[4,8] we found no significant correlations between stable isotope ratios and precipitation (p <0.01), except for the $\delta^{13}C_C$ values and mean autumn precipitation at Cermis (−0.37, p <0.01), but it is not strong enough to suggest precipitation as a primary control. This is consistent with the findings of Warren *et al.*[53] who demonstrated that $\delta^{13}C$ values are highly correlated with precipitation only at dry sites. It should remembered that the $\delta^{13}C$ values in tree rings are not directly linked with precipitation but are instead influenced by those environmental factors which affect plant physiological processes (e.g. stomatal conductance and the rate of photosynthesis), with stomatal conductance having the greatest influence.[4] We therefore focused on temperature as the primary environmental/climatic factor affecting the stable isotope values of tree rings in this region.

Although correlations vary in strength between sites, the patterns are quite similar, suggesting the absence of a strong influence at stand level. Overall, the highest correlations between temperature and the eight stable isotope series/components were found for the δ^2H_W and $\delta^{18}O_W$ values, suggesting that these two parameters are a suitable source of climate information. The δ^2H_W values are related to mean annual temperature and mean winter, spring and summer temperatures, while the $\delta^{18}O_W$ values exhibit a similar correlation only during the growing season (spring and summer). Even if the variability in δ^2H values is controlled by the same factors influencing the $\delta^{18}O$ values,[4,52] and is mainly determined by the isotopic composition of the soil water and by leaf water, it appears that other fractionation effects are also involved. Although hydrogen isotope behaviour has been modelled,[52] very few data are available for this proxy[4] and further studies are required.

To enhance the common climate signal and reduce non-climate noise,[4] a multi-proxy approach was taken which made use of multiple linear regression models using the eight isotopic chronologies as variables. In order to define the best wood component for climate reconstruction in this region, six models were built using either isotope proxies in single wood components or in combinations of different wood components. Only mean annual temperature was used as a variable since this parameter exhibited the strongest correlations with the stable isotope data. The results are reported in Table 3. Each multivariate model was assessed using all the normal procedures, including checks on the homoscedasticity of the residuals, and leverages. In all cases, assumptions of linear regression were met. Scatter graphs (Fig. 4) show the relationship between the predicted mean annual temperature and the measured mean annual temperature for the three sites.

Table 3. R^2 values of the multiple linear regression. Mean annual temperature was used as a predictor variable at the three sites

Site	$\mathbf{Model_{WLC}}$	$\mathbf{Model_{WL}}$	$\mathbf{Model_{WC}}$	$\mathbf{Model_{W}}$	$\mathbf{Model_{C}}$	$\mathbf{Model_{L}}$
CERMIS	0.54***	0.53***	0.54***	0.50***	0.16**	not at $p < 0.05$
VAL MAGGIORE	0.42***	0.42***	0.42***	0.42***	0.33***	not at $p < 0.05$
BASELGA	0.74***	0.74***	0.57***	0.55***	0.50***	0.38***

**$p < 0.01$; ***$p < 0.001$

Each model was run with $\delta^{13}C$, $\delta^{18}O$ and δ^2H values in the various wood components.

$\mathbf{Model_{WLC}}$: full model with 3 kinds of wood components (whole wood, cellulose and lignin methoxyl groups);
$\mathbf{Model_{WL}}$: two wood components (whole wood and lignin methoxyl groups);
$\mathbf{Model_{WC}}$: two wood components (whole wood and cellulose);
$\mathbf{Model_{W}}$: single wood component (whole wood);
$\mathbf{Model_{C}}$: single wood component (cellulose);
$\mathbf{Model_{L}}$: single wood component (lignin methoxyl groups).

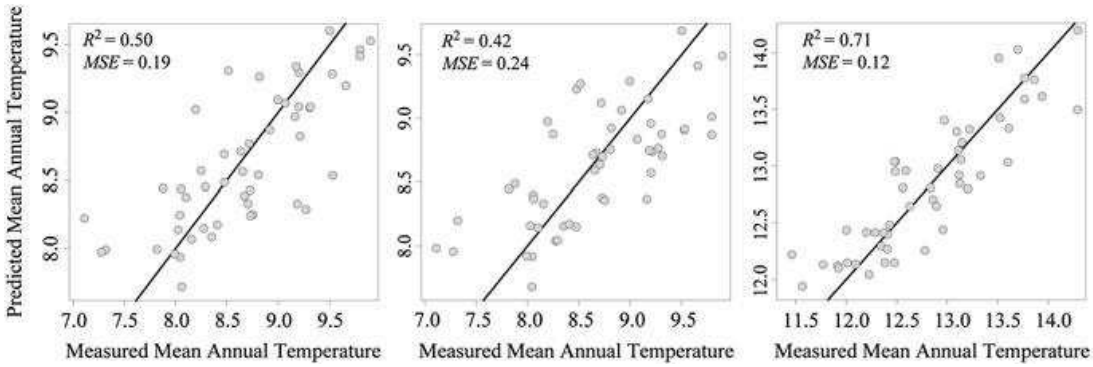

Figure 4. Scatter graphs of the predicted mean annual temperature *vs* measured mean annual temperature of Minimal Adequate Model at Cermis (a), Val Maggiore (b), and Baselga (c). The equation for the line of the best fit is computed from a multiple linear regression. R^2 and MSE are reported for each plot.

As reported in a previous study,[15] we found that a multi-proxy approach enhanced the climate signal. McCarroll and co-authors[15] state that the key to this lies in combining independent proxies or proxies that are not very similar. This leads to an improved estimate of climate signal since the proxies are not subject to similar sources of 'error'. In our study, we improved the effective correlation by combining the proxies, but the best result was obtained at the Baselga stand (Table 3). It is worth noting that this stand yields the best predictive model when both wood and lignin methoxyl groups are used (the R^2 value rises from 0.55 to 0.74). Therefore, combining these proxies improves temperature prediction.

The best temperature prediction was found at Baselga: both $Model_{WLC}$ and $Model_{WL}$ have an R^2 of 0.77 ($p < 0.001$). At each site, both $Model_{WLC}$ and the simpler $Model_{WL}$ have the same adjusted R^2 value and, in Val Maggiore, the simplest $Model_W$ has the same adjusted R^2 as $Model_{WLC}$. When single wood components are examined, $Model_W$ is found to have higher R^2 values than those of the combined wood fractions.

In order to more efficiently test the difference between the models, an ANOVA was performed to compare $Model_{WLC}$ with the other simpler models. The results of the ANOVA are shown in Table 4 and they clearly show the absence of differences between $Model_{WLC}$ and $Model_{WL}$ at any site ($p < 0.001$). The simpler $Model_{WL}$ could therefore save two degrees of freedom without being significantly worse than the more complex model. Moreover, the simplest $Model_W$ does not differ from $Model_{WLC}$ in Val Maggiore or at Cermis, while $Model_L$ and $Model_C$ always differed significantly from $Model_{WLC}$ ($p < 0.05$) at all three sites. Therefore, we selected $Model_W$ at Cermis and in Val Maggiore, and $Model_{WL}$ at Baselga, as adequate models to predict mean annual temperature.

The selected models were further simplified in order to obtain minimal adequate models. The results are reported in Table 5. An ANOVA confirmed that model simplification was completely justified at Cermis and in Val Maggiore, where it was possible to build the minimal adequate model using only the δ^2H_W and $\delta^{18}O_W$ series for both sites. On the other hand, only the $\delta^{13}C_W$ series was not significant at Baselga, and the minimal adequate model had four proxies ($\delta^{18}O_W$; δ^2H_W; $\delta^{13}C_L$; and δ^2H_L values).

CONCLUSIONS

We can conclude from our results that the stable isotope ratios in whole wood samples preserve the best temperature signal and that it is not necessary to include cellulose, at least as far as temperature reconstruction with *P. abies* in the south-eastern Alpine study area is concerned.

Our findings appear to disagree with those of many other studies which report that the stable isotope values of cellulose (mainly for $\delta^{18}O$) yield the best temperature information.[7,8,39]

For lignin methoxyl groups, only the $\delta^{13}C$ values (and only at at the low altitude site) turned out to improve temperature prediction, although it has been suggested that the δ^2H values of lignin methoxyl groups could be used as a paleoclimate

Table 4. ANOVA comparing the full model (**$Model_{WLC}$**) with the simpler models in the three study areas

Site	**$Model_{WL}$**	**$Model_{WC}$**	**$Model_W$**	**$Model_C$**	**$Model_L$**
CERMIS	not at $p < 0.05$	not at $p < 0.05$	not at $p < 0.05$	***	***
VAL MAGGIORE	not at $p < 0.05$	not at $p < 0.05$	not at $p < 0.05$	*	***
BASELGA	not at $p < 0.05$	***	***	***	***

*$p < 0.05$; **$p < 0.01$; ***$p < 0.001$

Each model was run with $\delta^{13}C$, $\delta^{18}O$ and δ^2H values in the various wood components.

$Model_{WLC}$: full model with three kinds of wood components (whole wood, cellulose and lignin methoxyl groups);
$Model_{WL}$: two wood components (whole wood and lignin methoxyl groups);
$Model_{WC}$: two wood components (whole wood and cellulose);
$Model_W$: single wood component (whole wood);
$Model_C$: single wood component (cellulose);
$Model_L$: single wood component (lignin methoxyl groups).

Table 5. Minimal Adequate Model for the study areas after removing any non-significant explanatory variables from the linear regression.

Site	Minimal adequate model	Adjusted R^2	ANOVA test
CERMIS	$\delta^{18}O_W + \delta^2H_W$	0.50	not at $p < 0.01$
VAL MAGGIORE	$\delta^{18}O_W + \delta^2H_W$	0.42	not at $p < 0.01$
BASELGA	$\delta^{18}O_W + \delta^2H_W + \delta^{13}C_L + \delta^2H_L$	0.71	not at $p < 0.01$

The ANOVA shows the p values between the selected models ($Model_W$ for Cermis and Val Maggiore, $Model_{WL}$ for Baselga). The p-value threshold was 0.01

proxy.[23] One possible explanation for the different results might be that our study was carried out in a cold temperate region where precipitation is not an environmental constraint, whereas most previously published studies were carried out in Mediterranean areas where precipitation is a limiting factor. Our trees may therefore have responded in a different way to the climate variables and we are aware that our results may not be reproducible in other regions with different climatic conditions.

With respect to isotope proxies, δ^2H values in wood have the highest correlations with seasonal and mean annual temperatures, $\delta^{18}O$ values correlate highly only with mean annual temperature, and $\delta^{13}C$ values in lignin methoxyl groups correlate with mean annual temperature at the lower altitude location.

Proxy selection allowed us to find the best-fit model to predict mean annual temperature: combining the $\delta^{18}O$ and δ^2H values in whole wood we obtained the minimal adequate model to reconstruct mean annual temperature at two of the three sites, while at the other site the $\delta^{13}C$ and δ^2H values of lignin methoxyl groups are also necessary. The current results will be useful in the selection of appropriate wood components and stable isotope proxies for future paleoclimate isotopic research. Moreover, our simplified model saves a considerable amount of time given that extraction of lignin methoxyl groups is simpler and faster than cellulose extraction.

Further studies are required to improve our knowledge of the complex mechanisms of fractionation, especially where the physiological processes determining the origin of isotope signatures in the different wood components are concerned, as has already been pointed out.[4,8]

Acknowledgements

This study was partly supported and co-funded by the Fondazione CARITRO – Cassa di Risparmio di Trento e Rovereto – as part of the ISOCHANGE project. F. Keppler and M. Greule were supported by the German Science Foundation (KE 884/6-1). The authors wish to thank Magdalena Nötzli (WSL, Birmensdorf, Germany) for valuable laboratory assistance, Anne Verstege (WSL, Birmensdorf) for assistance with measuring, Tessa Say for revision of the English text, and the Magnifica Comunità di Fiemme for allowing us to sample the trees. We would also like to thank Emanuele Eccel, Annalisa Piazzi and Luca Delucchi (FEM, S. Michele all'Adige) for their suggestions concerning the meteorological analysis. The authors wish to thank two anonymous reviewers for their insightful and helpful comments on a previous version of the manuscript.

REFERENCES

[1] J. P. Ferrio. Reconstruction of climatic and crop conditions in the past based on the isotope signature of archeobotanical remains. *Thesis dissertation*, Barcelona, Spain, **2005**.
[2] G. Battipaglia, D. Frank, U. Büntgen, P. Dobrovolný, R. Brázdil, C. Pfister, J. Esper. Five centuries of Central European temperature extremes reconstructed from tree-ring density and documentary evidence. *Glob. Planet. Change* **2010**, *72*, 182.
[3] F. H. Schweingruber. *Tree Rings. Basics and Applications of Dendrochronology.* Kluwer, Dordrecht, **1988**.
[4] D. McCarroll, N. J. Loader. Stable isotopes in tree rings. *Quat. Sci. Rev.* **2004**, *23*, 771.
[5] W. J. Robinson, E. Cook, J. R. Pilcher, D. Eckstein, L. Kairiukstis, S. Shiyatov, D. A. Norton, in *Methods of Dendrochronology*, (Eds: E. R. Cook, L. A. Kairiukstis). Kluwer, Dordrecht, **1990**, pp. 1–21.
[6] R. Switsur, J. S. Waterhouse, in *Stable Isotopes: Integration of Biological, Ecological and Geochemical Processes*, (Ed.: H. Griffiths). BIOS, Oxford, **1998**, pp. 303–321.
[7] P. J. Ferrio, J. Voltas. Carbon and oxygen isotope ratios in wood constituents of *Pinus halepensis* as indicators of precipitation, temperature and vapor pressure deficit. *Tellus Ser. B* **2005**, *10*, 164.
[8] G. Battipaglia, M. Jäggi, M. Saurer, R. T. W. Siegwolf, M. F. Cotrufo. Climatic sensitivity of $\delta^{18}O$ in the wood and cellulose of tree rings: Results from a mixed stand of *Acer pseudoplatanus* L. and *Fagus sylvatica* L. *Palaeogeogr., Palaeoclimatol., Palaeoecol.* **2008**, *261*, 193.
[9] J. Gray, P. Thompson. Climatic information from $^{18}O/^{16}O$ analysis of cellulose lignin and whole wood from tree rings. *Nature* **1977**, *270*, 708.
[10] S. W. Leavitt, A. Long. Drought indicated in carbon-13/carbon-12 ratios of south-western tree rings. *Water Res. Bull.* **1989**, *25*, 341.
[11] T. W. D. Edwards, W. Graf, P. Trimborn, W. Stichler, J. Lipp, H. D. Payer. $\delta^{13}C$ response surface resolves humidity and temperature signals in trees. *Geochim. Cosmochim. Acta* **2000**, *64*, 161.
[12] A. T. Wilson, M. J. Grinsted. $^{12}C/^{13}C$ in cellulose and lignin as palaeothermometers. *Nature* **1977**, *265*, 133.
[13] V. Dellus, I. Mila, A. Scalbert, C. Menard, V. Michon, C. L. M. Herve du Penhoat. Douglas-fir polyphenols and heartwood formation. *Phytochemistry* **1997**, *45*, 1573.
[14] A. M. Taylor, B. L. Gartner, J. J. Morrell. Co-incident variations in growth rate and extractive concentration in Douglas-fir. *For. Ecol. Manag.* **2003**, *186*, 257.
[15] D. McCarroll, R. Jalkanen, S. Hicks, M. Tuovinen, F. Pawellek, M. Gagen, D. Eckstein, U. Schmitt, J. Autio, O. Heikkinen. Multi-proxy dendroclimatology: a pilot study in northern Finland. *The Holocene* **2003**, *13*, 829.
[16] S. W. Leavitt, S. R. Danzer. Method for batch processing small wood samples to holocellulose for stable-carbon isotope analysis. *Anal. Chem.* **1993**, *65*, 87.
[17] N. J. Loader, I. Robertson, A. C. Barker, V. R. Switsur, J. S. Waterhouse. An improved technique for the batch processing of small whole wood samples to alpha-cellulose. *Chem. Geol.* **1997**, *136*, 313.
[18] K. T. Rinne, T. Boettger, N. J. Loader, I. Robertson, V. R. Switsur, J. S. Waterhouse. On the purification of alpha-cellulose from resinous wood for stable isotope (H, C and O) analysis. *Chem. Geol.* **2005**, *222*, 75.
[19] M. M. Barbour, T. J. Andrei, G. F. Farquhar. Correlation between oxygen isotope ratios of wood constituents of *Quercus* and *Pinus* samples from around the world. *Aust. J. Plant Physiol.* **2001**, *28*, 335.
[20] M. Saurer, P. Cherubini, T. R. W. Siegwolf. Oxygen isotopes in tree rings of *Abies alba*: the climatic significance of interdecadal variations. *J. Geophys. Res. [Atmos.]* **2000**, *105*, 12461.
[21] N. J. Loader, I. Robertson, D. McCarroll. Comparison of stable carbon isotope ratios in the whole wood, cellulose and lignin of oak tree rings. *Palaeogeogr., Palaeoclimatol., Palaeoecol.* **2003**, *196*, 395.
[22] S. Borella, M. Leuenberger, M. Saurer. $\delta^{18}O$ analysis in tree rings: wood–cellulose comparison and method dependence sensitivity. *J. Geophys. Res., [Atmos.]* **1999**, *104*, 19267.
[23] F. Keppler, D. B. Harper, R. M. Kalin, W. Meier-Augenstein, N. Farmer, S. Davis, H. L. Schmidt. Stable hydrogen isotope ratios of lignin methoxyl groups as a paleoclimate proxy and constraint of the geographical origin of wood. *New Phytol.* **2007**, *176*, 600.

[24] S. Zeisel. Über ein Verfahren zum quantitativen Nachweise von Methoxyl. *Monatshefte für Chemie* **1885**, *6*, 989.
[25] M. Greule, A. Mosandl, J. T. G. Hamilton, F. Keppler. A rapid and precise method for determination of D/H ratios of plant methoxyl groups. *Rapid Commun. Mass Spectrom.* **2008**, *22*, 3983.
[26] M. Greule, A. Mosandl, J.T.G. Hamilton, F. Keppler. A simple rapid method to precisely determine $^{13}C/^{12}C$ ratios of plant methoxyl groups. *Rapid Commun. Mass Spectrom.* **2009**, *23*, 1710.
[27] M. Greule, F. Keppler. Stable isotope determination of ester and ether methyl moieties in plant methoxyl groups. *Isot. Environ. Health Stud.* **2011**, *47*, 470
[28] H. Gärtner, D. Nievergelt. The core-microtome. A new tool for surface preparation on cores and time series analysis of varying cell parameters. *Dendrochronologia* **2010**, *28*, 85.
[29] R. L. Holmes. Computer-assisted quality control in tree-ring dating and measurement. *Tree-ring Bull.* **1983**, *43*, 69.
[30] V. R. Switsur, J. S. Waterhouse, E. M. Field, A. H. C. Carter, in *Tree Rings, Environment and Humanity; Proceedings of the International Conference*, (Eds: J. S. Dean, D. M. Meko, T. W. Swetnam). Dept of Geosciences, University of Arizona, **1996**, pp. 637–645.
[31] M. Jäggi, M. Saurer, J. Fuhrer, T. R. W. Siegwolf. Seasonality of $\delta^{18}O$ in needles and wood of *Picea abies*. *New Phytol.* **2003**, *158*, 51.
[32] S. A. Hill, J. S. Waterhouse, E. M. Field, V. R. Switsur, T. Ap Rees. Rapid recycling of triose phosphates in oak stem tissue. *Plant Cell Environ.* **1995**, *18*, 931.
[33] G. H. Schleser, J. Frielingsdorf, A. Blair. Carbon isotope behaviour in wood and cellulose during artificial aging. *Chem. Geol.* **1999**, *158*, 121.
[34] R. J. Francey, G. D. Farquhar. An explanation of C-13/C-12 variations in tree rings. *Nature* **1982**, *297*, 28.
[35] D. McCarroll, F. Pawellek. Stable carbon isotope ratios of *Pinus sylvestris* from northern Finland and the potential for extracting a climate signal from long Fennoscandian chronologies. *The Holocene* **2001**, *11*, 517.
[36] M. G. Tjoelker, A. Boratynski, W. Bugala. *Biology and Ecology of Norway Spruce*, Springer, Poznan, Poland, **2007**.
[37] S. W. Leavitt, A. Long. Sampling strategy for stable carbon isotope analysis of tree rings in pine. *Nature* **1984**, *311*, 145.
[38] K. Treydte, G. H. Schleser, F. H. Schweingruber, M. Winiger. The climatic significance of $\delta^{13}C$ in subalpine spruces (Lötschental, Swiss Alps). *Tellus* **2001**, *53B*, 593.
[39] L. E. Cullen, P. F. Grierson. Is cellulose extraction necessary for developing stable carbon and oxygen isotopes chronologies from *Callitris glaucophylla*? *Palaeogeogr., Palaeoclimatol., Palaeoecol.* **2006**, *236*, 206.
[40] A. L. Sessions, T. W. Burgoyne, J. M. Hayes. Determination of the H_3 factor in hydrogen isotope ratio monitoring mass spectrometry. *Anal. Chem.* **2001**, *73*, 200.
[41] L. I. Wassenaar, K. A. Hobson. Comparative equilibration and online technique for determination of non-exchangeable hydrogen of keratins for animal migration studies. *Isot. Environ. Health Stud.* **2003**, *39*,1.
[42] R. J. Francey, C. E. Allison, D. M. Etheridge, C. M. Trudinger, I. G. Enting, M. Leuenberger, R. L. Langenfelds, E. Michel, L. P. Steele. A 1000-year high precision record of $\delta^{13}C$ in atmospheric CO_2. *Tellus* **1999**, *51B*, 170.
[43] E. Eccel, P. Cau, R. Ranzi. Data reconstruction and homogenization for reducing uncertainties in high-resolution climate analysis in Alpine regions. *Theor. Appl. Climatol.* **2012**.
[44] M. Neteler. Time series processing of MODIS satellite data for landscape epidemiological applications. *Int. J. Geoinf.* **2005**, *1*, 133.
[45] M. Neteler. Estimating daily Land Surface Temperatures in mountainous environments by reconstructed MODIS LST data. *Remote Sens.* **2010**, *2*, 333.
[46] R Development Core Team. *R: A Language and Environment for Statistical Computing*. R Foundation for Statistical Computing, Vienna, Austria, **2011**. Available: http://www.R-project.org.
[47] S. Borella, M. Leuenberger, M. Saurer, R. Siegwolf. Reducing uncertainties in $\delta^{13}C$ analysis of tree rings: pooling, milling, and cellulose extraction. *J. Geophys. Res. [Atmos.]* **1998**, *103*, 19519.
[48] H. L. Schmidt, R. A. Werner, R. Andreas. ^{18}O Pattern and biosynthesis of natural plant products. *Phytochemistry* **2001**, *58*, 32.
[49] H. L. Schmidt, R. A. Werner, W. Eisenreich. Systematics of ^{2}H patterns in natural compounds and its importance for the elucidation of biosynthetic pathways. *Phytochem. Rev.* **2003**, *2*, 61.
[50] S. W. Leavitt, A. Long. Seasonal stable isotope variability in tree rings: possible paleoenvironmental signals. *Chem. Geol.* **1991**, *87*, 59.
[51] N. J. Livingston, D. L. Spittlehouse. Carbon isotope fractionation in tree ring early and late wood in relationship to intra-growing season water balance. *Plant, Cell Environ.* **1996**, *19*, 768.
[52] J. S. Roden, G. Lin, J. R. Ehleringer. A mechanistic model for interpretation of hydrogen and oxygen isotope ratios in tree-ring cellulose. *Geochim. Cosmochim. Acta* **2000**, *64*, 21.
[53] C. R. Warren, J. F. McGrath, M. A. Adams. Water availability and carbon isotope discrimination in conifers. *Oecologia* **2001**, *127*, 476.
[54] N. J. Loader, D. McCarroll, M. H. Gagen, I. Robertson, R. Jalkanen, in *Stable Isotopes as Indicators of Ecological Change*, (Eds: T. Dawson, R. Siegwolf). Terrestrial Ecology Series. Elsevier, **2007**, pp. 27–48.
[55] J. Esper, D. C. Frank, G. Battipaglia, U. Büentgen, C. Holert, K. Treydte, R. Siegwolf, M. Saurer. Low-frequency noise in $\delta^{13}C$ and $\delta^{18}O$ tree-ring data: A case study of *Pinus uncinata* in the Spanish Pyrenees. *Global Biogeochem. Cycles* **2010**, *24*, GB4018.
[56] F. H. Schweingruber, *Tree Rings and Environment Dendroecology*, Paul Haupt Publishers Berne, Stuttgart, Vienna, **1996**.
[57] C. Sboarina, A. Cescatti. Il clima del Trentino. Distribuzione spaziale delle principali variabili climatiche. Report N. 33. Centro di Ecologia Alpina, Trento, **2004**.
[58] O. V. Sidorova, R. T. W. Siegwolf, M. Saurer, M. M. Naurzbaev, E. A. Vaganov. Isotopic composition ($\delta^{13}C$, $\delta^{18}O$) in wood and cellulose of Siberian larch trees for early Medieval and recent periods. *J. Geophys. Res. [Biogeosciences]* **2008**, *113*, G02019.
[59] A. A. Knorre, T. R. W. Siegwolf, M. Saurer, O. V. Sidorova, E. A. Vaganov, A. V. Kirdyanov. Twentieth century trends in tree rings stable isotopes ($\delta^{13}C$ and $\delta^{18}O$) of *Larix sibirica* under dry conditions in the forest steppe in Siberia. *J. Geophys. Res. [Biogeosciences]* **2010**, *115*, G03002.
[60] Available: http://www.meteotrentino.it/dati-meteo/info-dati.aspx?ID=3.

Section 2

Fungal root pathogen (*Heterobasidion parviporum*) increases drought stress in Norway spruce stand at low elevation in the Alps.

European Journal of Forest Research 2013. 132, 4:607-619

Eur J Forest Res (2013) 132:607–619
DOI 10.1007/s10342-013-0698-x

ORIGINAL PAPER

Fungal root pathogen (*Heterobasidion parviporum*) increases drought stress in Norway spruce stand at low elevation in the Alps

Yuri Gori · Paolo Cherubini · Federica Camin · Nicola La Porta

Received: 10 August 2012 / Revised: 16 January 2013 / Accepted: 20 March 2013 / Published online: 23 April 2013

Abstract Tree-ring patterns of *Picea abies* (L.) Karst. both unaffected and affected by *Heterobasidion parviporum* were analysed in three mature stands located at different elevations in the Eastern Alps. The main objectives were (1) to clarify the role of climatic conditions on infected trees; (2) to estimate indirect volume losses due to the prolonged presence of the fungus within the wood. The low elevation site showed the highest growth decline in the last decade, whereas all infected trees at medium and high elevation showed a slow growth decline over many decades. We hypothesise that infection could be dated over 80 years at the highest site. Fungal attack made *P. abies* more susceptible to drought stress at low elevation site. Both infected and healthy *P. abies* at medium and high elevation showed similar climate–growth relationships, suggesting that the same driving environmental factors influence their growth. At low elevation, *H. parviporum* was seemingly more aggressive, causing a more rapid decline, decreasing the ability of host trees to cope with drought and, in some cases, inducing cambial activity to stop. *P. abies* at higher elevation, however, exhibited a very slow decline and no sign of increasing water stress since the influence of climate on tree growth was the same for both infected and healthy trees.

Communicated by R. Matyssek.

Y. Gori (✉) · F. Camin · N. La Porta
FEM-IASMA Edmund Mach Foundation, Via E. Mach 1, 38010 San Michele all' Adige, Italy
e-mail: yuri.gori@fmach.it

P. Cherubini
Swiss Federal Institute for Forest, Snow and Landscape Research WSL, 8903 Birmensdorf, Switzerland

Keywords Dendroecology · Drought stress · Climate–growth relationship · Fungal infection · Growth reduction · PDSI

Introduction

Heterobasidion annosum (Fr.) Bref. sensu lato causes root and butt rot and tree mortality, and is regarded as the most economically serious threat to northern boreal conifer forests, being particularly dangerous in weakening root systems and increasing the risk of windfall (Woodward et al. 1998).

Since 1978, *H. annosum* has been divided into two intersterility groups (ISG) by Korhonen (1978) according to the main host preference, spruce and pine. Later, Capretti (Capretti et al. 1990) added a third one specialised for Silver fir. Finally, the three ISG received the status of species and were called *H. annosum* s.s., *H. parviporum* and *H. abietinum* specialised, respectively, for pine species, Norway spruce and Silver fir (Niemelä and Korhonen 1998).

Some authors report that its distribution depends largely on stand type and history, forest composition and soil properties (Korhonen and Stenlid 1998). All these pathogens cause significant economic losses in different ways: increasing tree mortality, increasing susceptibility to windthrow, decreasing wood quality as a result of wood decay and indirect loss caused by growth reduction. Up to now, economic losses have often been underestimated as they are usually limited to the assessment of the decay of the lower part of the inner stem and its consequential estimation in terms of loss of wood volume, while indirect losses such as growth reduction have often been overlooked. Benz-Hellgren and Stenlid (1995) demonstrated

that Norway spruce infected by *H. annosum* for 17 years accumulated, on average, 23 % less volume over the last 5 years. Oliva et al. (2010), in a research carried out in Sweden, found a 12.5 % losses per year in terms of volume in Norway spruce with reaction zones infected for more than 13 years. Moreover, stands affected by *H. annosum* are more likely to suffer from windthrow (Korhonen and Stenlid 1998; Stenlid and Johansson 1987) and are more susceptible to bark beetle (*Scolytus spp*., *Ips spp*.,) (Schmitt et al. 2000).

Three main mechanisms can be involved in growth losses by root rot: death of most major roots, reduced ability of trees to take up water and nutrients (Cherubini et al. 2002; Benz-Hellgren and Stenlid 1995; Joseph et al. 1998) and the formation of a reaction zone (Benz-Hellgren and Stenlid 1995; Hietala et al. 2009; Oliva et al. 2010), a energy costly defence which consists of necrotic tissue enriched with antifungal phenolic extractives (Shain 1979).

Many climate change models predict increased drought throughout Europe with a likely substantial alteration in the structure and functioning of terrestrial ecosystems. Climate change could alter the incidence and geographical range of pathogens and hosts (Lonsdale and Gibbs 1996) therefore modifying host resistance and resulting in changes in the physiology of tree–pathogen interactions (Desprez-Loustau et al. 2006). Some investigators have even suggested that a significant outcome of climate change could be changes in the occurrence and intensity of tree diseases (Linares et al. 2010; Fischlin et al. 2007; La Porta et al. 1997; La Porta et al. 2008). An increase in summer droughts would probably favour diseases caused by *Heterobasidion* spp. or other facultative biotrophic pathogens and enhance tree mortality (Linares et al. 2010; Henry et al. 2009). As the host defence responses are strongly influenced by the climate, understanding the influences of the infection to abiotic stresses, such as a drought stress, will be of increasing importance. To date, however, despite several studies have investigated interactive effects of environmental factors and fungi on forest trees in controlled environment or plantation, not enough has been done to evaluate these effects under natural condition (Desprez-Loustau et al. 2006).

Dendrochronology has proven to be a valuable tool for analysing tree growth history for various purposes, not the least of which is better understanding of the effects of environment on disease incidence (Cherubini et al. 2002; Manion 1991; Kozlowski 1969; Kozlowski et al. 1991; Pedersen and McCune 2002). The combination of increasing air temperature and occurrence of summer drought at warmer sites, usually located at the lowest elevations, could decrease host resistance and trigger a widespread increase in tree mortality caused by *H. parviporum* (Puddu et al. 2003; La Porta et al. 2008). To test this hypothesis, we evaluated the effect of diseases at different elevations by analysing the tree-ring growth patterns of three *Picea abies* (L.) Karst. mature stands infected by *H. parviporum*. Specifically, the objectives were as follows: (1) to analyse the climate–growth at different elevations in infected and not infected trees; (2) to estimate the indirect volume losses due to the prolonged presence of the fungus within the wood.

Materials and methods

Study site and climate data

Three Norway spruce [*Picea abies* (L.) Karst.] mature stands infected by *H. parviporum* were selected in the Eastern Alps: Baselga, a low elevation site ('LOW'); Val Maggiore, a medium elevation site ('MED') and Cermis, a high elevation site ('HIGH'). All the sites were located within a distance of 25 km from each other (Fig. 1).

The LOW stand is located at an elevation ranging from 850 to 900 m a.s.l. (46° 4′ 48″N, 11° 3′ 3″E), with 30–50 % slopes and northerly exposure. The prevailing geological substrate is limestone and marly limestone. The soil is a brown forest soil, deep and clay-rich, with litter rich in nutrients. The forest is an old plantation of Norway spruce (about 80 years old) but the abundant regeneration of this specie confers a natural like aspect to the stand. The site is classified as *Adenostylo glabrae-Abietetum* (Weber et al. 2000).

The stand is dominated by mature *P. abies* (over 80 %) with sporadic European larch (*Larix decidua* Mill.) and beech (*Fagus sylvatica* L.). The forest is homogeneous. The growth rate of the trees is 8 m^3/ha/year, with a mean diameter at breast height of around 40 cm and 254 stems/ha.

The other two stands, MED and HIGH, are situated in the Fiemme Valley at an elevation of around 1,300 m a.s.l. (46° 17′ 32″N, 11° 3 6′ 49″E; MED) and 1,900 a.s.l. (46° 15′ 0″N, 11° 29′ 43″E; HIGH). The distance between the areas is 10 km. The slopes range from moderately inclined to steep (25–50 %) and are north-facing, and the bedrock is porphyric partially covered by morainic material, with podsol soils. Both sites are quite close to forest roads and are mainly composed of mature *P. abies*. These stands are dense and more heterogeneous than LOW stand. The MED stand has a regular and continuous canopy, and the mean diameter at breast height is around 40 cm. At HIGH, the stand structure is more heterogeneous and the forest is less productive than in the MED. At MED stand, the vegetation is classified as *Piceetum montanum myrtilletosum,* with sporadic *Abies alba* (less than 10 %) while HIGH is a typical pure subalpine Norway spruce forest classified as *Rhodoreto-Vaccinietum cembretosum* (Weber et al. 2000).

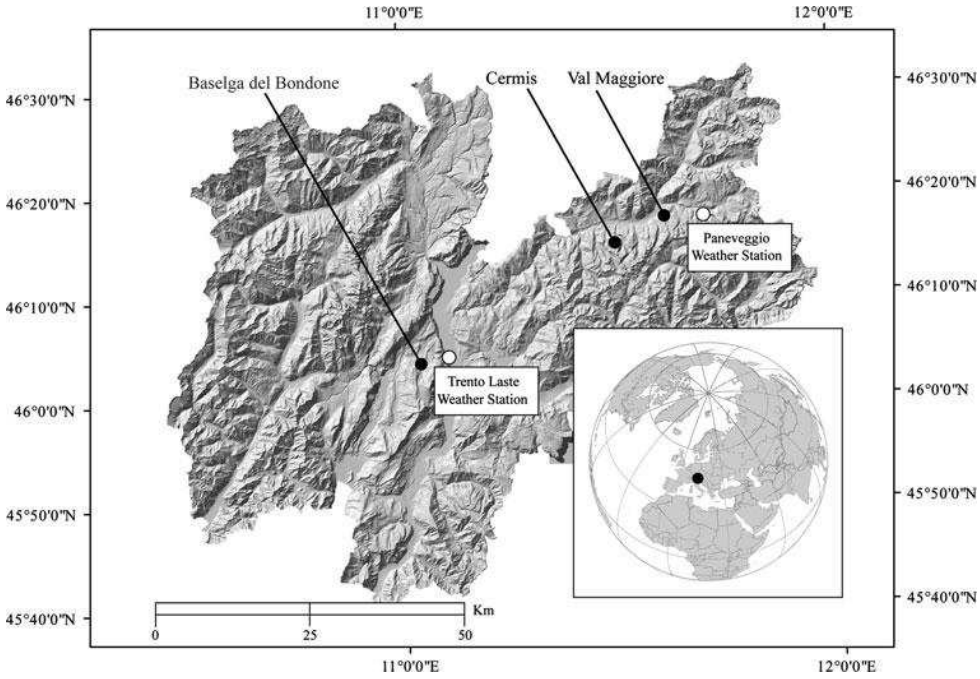

Fig. 1 Location of the study sites. White dots represent the two weather stations at Trento Laste and Paneveggio

All the forests are characterised by several large, even-aged groups of trees, resulting in stands that can be considered to be uneven-aged as a whole. Silvicultural treatments were similar at all the sites, with pre-commercial thinning occurring on average every 20 years at LOW and every 30–40 years at the other sites.

The climatic features are typical of the south-eastern Alpine region, with cold winters, mild summers and precipitation mostly concentrated during the summer months (June to September). Mean annual precipitation at the two meteorological stations was 1,196 mm (Paneveggio weather station: 1,415 m a.s.l.; 46° 18′ 33″N, 11° 44′ 50″E, about 5 km from MED and 15 km from HIGH) and 931 mm (Trento Laste weather station: 312 m a.s.l.; 46° 04′ 19″N, 11° 08′ 8″E, about 6 km from LOW stand) at its maximum in summer; mean annual temperature is 6 °C at Paneveggio and 12 °C at Trento Laste, while the coolest and warmest months are, respectively, January and July.

For dendroclimatic analysis, we used two alpine-wide meteorological datasets: (a) the HISTALP database (Auer et al. 2007) of monthly homogenised instrumental temperature and precipitation measurement and (b) the gridded self-calibrating Palmer Drought Severity Index (scPDSI) for the greater alpine region developed by the Climatic Research Unit of the University of East Anglia at Norwich, United Kingdom (van der Schrier et al. 2007a, b). The scPDSI uses monthly surface air temperature and precipitation data to generate a relative measure of water contained in the soil and therefore represents the water available for vegetation (Palmer 1965).

Sampling and pathological analysis

In October 2009, 10 healthy *P. abies* (control, 'CON') and 10 infected *P. abies* (infected, 'INF') were selected at the three sites located at different elevation. We took care to sample only the dominant trees, to reduce the influence of competition on ring-width growth, thus reflecting the growth dynamics of the whole stand with more precision (Cook and Kairiukstis 1990). Two cores, at 180° from each other, were extracted with a 0.5-cm-diameter Pressler increment borer from each of the 60 trees (10 + 10 at 3 sites), perpendicular to the slope direction to avoid possible wood compression and minimise stem eccentricity.

At all sites, trees were previously classified as CON or INF on the basis of wood samples taken from the roots and at stump height, 20–30 cm above ground as described by Dobbertin et al. (2001). Only trees with a rotten surface over 80 % were selected. We selected only individuals with a rot surface covering almost the whole stump by means of 4 radial cores taken at 90° from each other at stump level. Since tree-ring width at different heights below the crown base commonly shares the same pattern (LeBlanc 1990; van der Maaten-Theunissen and Bouriaud 2012), CON cores were taken at breast height in standing trees while INF cores were taken on felled trees, where the wood was not rotten (between 2 and 4 m height). Decayed wood piece samples taken from each INF were flame-sterilised and incubated at 20–22 °C in a dark humid chamber. After 15 days, wood samples were inoculated onto Benomyl streptomycin malt agar dishes for two weeks

following Maloy's protocol, (1974). The occurrence of *Heterobasidion* was confirmed by the presence of the imperfect state *Spininger meineckellus* (A.J. Olson) Stalpers, according to the methods described by Stalpers (1978). Confirmation of *Heterobasidion* as the cause of decay in each sample tree was done with the aid of the Buller phenomenon (Korhonen 1978) in which each field isolate was pairing with at least three tester strains representing *H. annosum*, *H. parviporum* and *H. abietinum*.

Isolation methods and mating tests were described by Dai et al. (2003). In compatible pairing, the homokaryotic tester strain turns to heterokaryotic; this was indicated by the appearance of clamp connections and by a change in the mycelial morphology of the tester. To avoid uncertainty about the rot root pathogen, trees that had signs of rot that could not be attributed to by *H. parviporum* were excluded.

Ring-width measurement and dendroecological analyses

The cores of each tree were prepared with a core microtome (Gärtner and Nievergelt 2010) to make the ring's features clearly visible under magnification. Ring-width measurement was taken to the nearest 0.01 mm on each core, using the time series analysis programme (TSAP) measurement equipment, coupled to a Leica MS5 stereoscope (Frank Rinn, Heidelberg, Germany). The raw tree-ring widths (TRW) of each curve were plotted, cross-dated visually and then cross-dated statistically using the *Gleichläufigkeit*, which is the percentage agreement in the signs of first difference of two time series. Cross-dating quality was checked using the COFECHA program version 6.06 (Holmes 1983) as a standard dendrochronological protocol for quality control.

Once cross-dating had been verified, the original measurement time series were detrended to remove the decreasing trend and long-term noise caused by *H. parviporum*. Data-adaptive power transformation (PT) was first applied to each raw TRW series (Cook and Peters 1997). The purpose of PT is to stabilise the variance (the ratio between growth rate and inter-annual variance) in heteroscedastic TRW series (Helama et al. 2004). These transformed records were then detrended with a 32-year smoothing spline with 50 % frequency cut-off using the ARSTAN program version 4.1 (Cook and Holmes 1984; Grissino-Mayer et al. 1996). Flexible cubic spline curves are more suitable for removing both the long-term trend and the effect of localised disturbance events. The indexed series of both CON and INF trees within each site were averaged using a bi-weight robust mean (Cook 1985); their variance was stabilised using mean correction as in Frank et al. (2007); and the record was truncated at a minimum replication of five series. In this way, we obtained two indexed chronologies (one for both INF and CON trees) at each site. The analysis was performed using R statistical software with 'dplR' (Dendrochronology Programme Library in R) and 'Mass' packages (Bunn et al. 2008; Venables et al. 2010).

The periods obtained were 1829–2009 at HIGH, 1916–2009 at MED and 1937–2009 at the LOW stand. To compare different chronologies with each other, we considered only the common period 1937–2009.

Several descriptive statistics were calculated for each CON and INF standardised chronology: (a) mean sensitivity measures the relative difference in width between consecutive rings (Fritts 1976); (b) standard deviation indicates the variability of measurements of all the TRWs; (c) the first order of serial autocorrelation, to detect eventual persistence, retained after standardisation and (d) Interseries correlation to measure the strength of the common signal in the chronology and check for chronology quality.

High values of both standard deviation and mean sensitivity indicate the presence of considerable high-frequency variance and are indicative of more climatically responsive chronologies (Fritts 1976).

To assess suppressions (growth reduction) in INF, a running calculation of per cent growth change for a 4-year period was applied to each raw ring width and mean ring-width master chronology. This 'suppression index' was progressively shifted by 1 year and calculated as (A1-A2)/A2 where A1 equals average growth over the prior 4 years and A2 equals average growth over the subsequent four years (Schweingruber et al. 1990). In this way, we also detected abrupt growth reduction when the average ring width of the four rings was at least 40 % smaller than the previous one.

Pointer years were used as additional ecological indicators recording the reactions of trees to environmental factors limiting radial growth (Schweingruber 1996). A given year was defined as a pointer, when more than 80 % of at least 10 trees reacted with a growth increase (positive pointer years) or decrease (negative pointer years) compared to the previous year (Schweingruber et al. 1990). All calculations of pointer years were performed on tree-ring width using the WEISER program (Gonzalez 2001).The hypothesis analysed in this study was that drier years would have a more pronounced effect on INF tree growth, in comparison with CON trees, because root pathogens would limit water availability, as the supply capacity of decayed root xylem is limited (Joseph et al. 1998; Korhonen and Stenlid 1998).

In order to estimate volume losses caused by *H. parviporum* at each site, the mean cumulative basal area (e.g. the average cross-sectional area produced by trees at each year) was also calculated from each raw ring-width master chronology. As the distribution was not normal (R statistical software), we applied a Wilcoxon rank sum test to test the growth difference between CON and INF.

Tree–growth climate relationship

To test the differences in climate–growth response between INF and CON trees, we used the six indexed master chronologies (e.g. two indexed chronologies at each site, one for both CON and INF). We used correlation function analysis (Fritts 1976) for a common period (1937–2009), comparing each CON and INF tree-ring index with the gridded monthly temperature and precipitation anomalies from the HISTALP dataset (Auer et al. 2007) and the gridded scPDSI. Monthly analysis was performed using eight independent climate variables sequenced from January to August in the year of growth.

To test stationarity and any change of the correlation function over time, we also computed a moving correlation function with the software package DENDROCLIM2002 (Biondi and Waikul 2004). For this purpose, a 48-year interval, which was progressively shifted by 1 year over time, was used to compute the correlation coefficients over the common period (Biondi 1997, 2000) for the same variables used in correlation function analysis.

Pearson correlation coefficients were calculated in both analyses using the bootstrapping method, with 1,000 iterations. Each correlation coefficient was considered significant if the mean value was at least twice the standard deviation of its 1,000 replications (Guiot 1991). Since the moving correlation function was calculated on non-independent intervals, the significance of the correlation coefficient was assessed by means of the Bonferroni correction method. This is an adjustment made on confidential levels when multiple statistical tests are evaluated simultaneously (Snedecor and Cochran 1989).

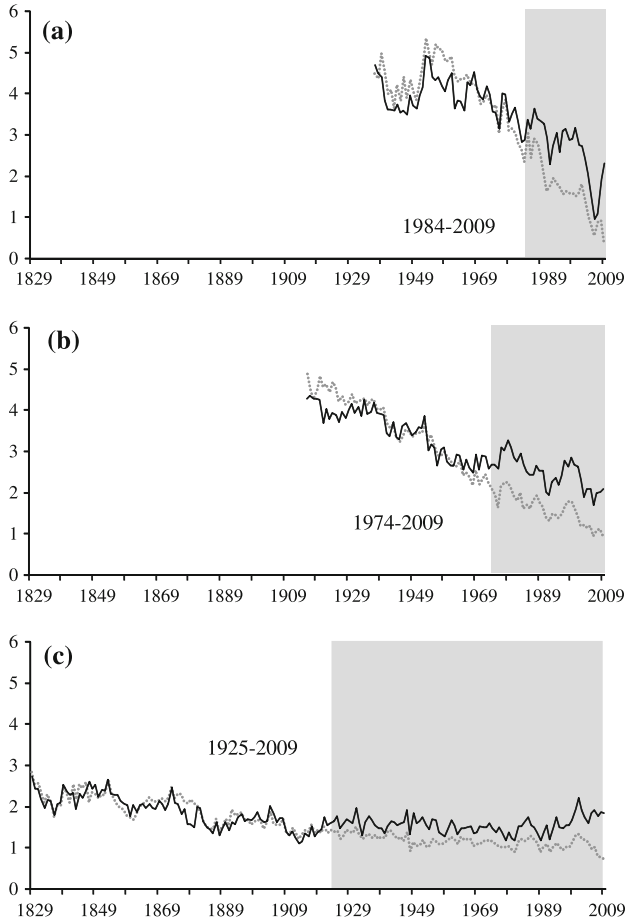

Fig. 2 Mean ring-width chronologies of the infected trees by *Heterobasidion parviporum* (*grey line*) and healthy trees (*black line*), for **a** LOW, **b** MED and **c** HIGH. *Shaded* areas mark intervals in which infected tree growth is significantly lower than for healthy trees ($p < 0.05$). Ordinate axis indicates mean ring width in mm

Results

Ring-width chronologies

Raw ring-width master chronologies for each CON and INF at each site are shown in Fig. 2.

The highest *Gleichläufigkeit* (GLK) values relative to INF series were found at HIGH, with a mean value of 79 %, while at LOW-INF and MED-INF lower values were found, respectively, 70 % and 68 %, although still very high and statistically significant. Cross-dating was verified by COFECHA and no dating errors were identified. After cross-dating, it was found that at LOW, five out of 10 INF trees had ceased cambial activity before sampling (one in 2004, 2005, 2006 and two in 2008), although these trees still had green needles at the time of sampling in 2009, whereas all trees at MED and HIGH still produce new tree rings.

The highest interseries correlation was found at HIGH and the lowest at LOW (Table 1). The highest mean sensitivity, measurement of the relative change in ring width from 1 year to the next in a given series, was found at LOW. At all the sites, the mean sensitivity was higher in INF. The highest autocorrelation values were found at each INF series.

Abrupt growth reduction

At each site, all the series infected by *H. parviporum* showed a decreasing growth trend and clear abrupt growth reductions (Fig. 3). Furthermore, growth reduction increased over time. To test the hypothesis that the differences in radial growth between INF and CON were significant, we performed a Wilcoxon rank sum test. Mean LOW-INF ring width was significantly lower ($p < 0.05$)

Table 1 Descriptive statistics of the infected and healthy Norway spruce tree-ring chronologies

Site code	Altitude (m)	Chronology code	Number of trees[a]	Age[b]	Chrono time span (number of years)	Mean ring width (mm)	SD[c]	Interseries correlation[d]	MS[e]	AC[f]
LOW	850	LOW-CON	10	73 ± 3/80	1937–2009 (72)	2.936	1.14	0.446	0.183	0.805
		LOW-INF	10	70 ± 3/75	1937–2009 (72)	2.673	1.51	0.447	0.185	0.910
MED	1,300	MED-CON	10	97 ± 11/115	1914–2009 (95)	2.746	0.97	0.467	0.115	0.877
		MED-INF	10	94 ± 8/110	1916–2009 (93)	2.140	1.23	0.420	0.129	0.955
HIGH	1,900	HIGH-CON	10	183 ± 21/231	1827–2009 (182)	1.372	0.46	0.638	0.135	0.844
		HIGH-INF	10	184 ± 29/231	1829–2009 (180)	1.099	0.51	0.568	0.136	0.911

[a] Each tree was cored radially from opposite sides

[b] Mean values ± SD/maximum

[c] Standard deviation of mean ring width

[d] Mean correlation between each detrended time series and the detrended site master chronologies, COFECHA output

[e] Mean sensitivity computed on the raw tree-ring series, COFECHA ouput

[f] First-order serial autocorrelation computed on the raw tree-ring series, COFECHA output

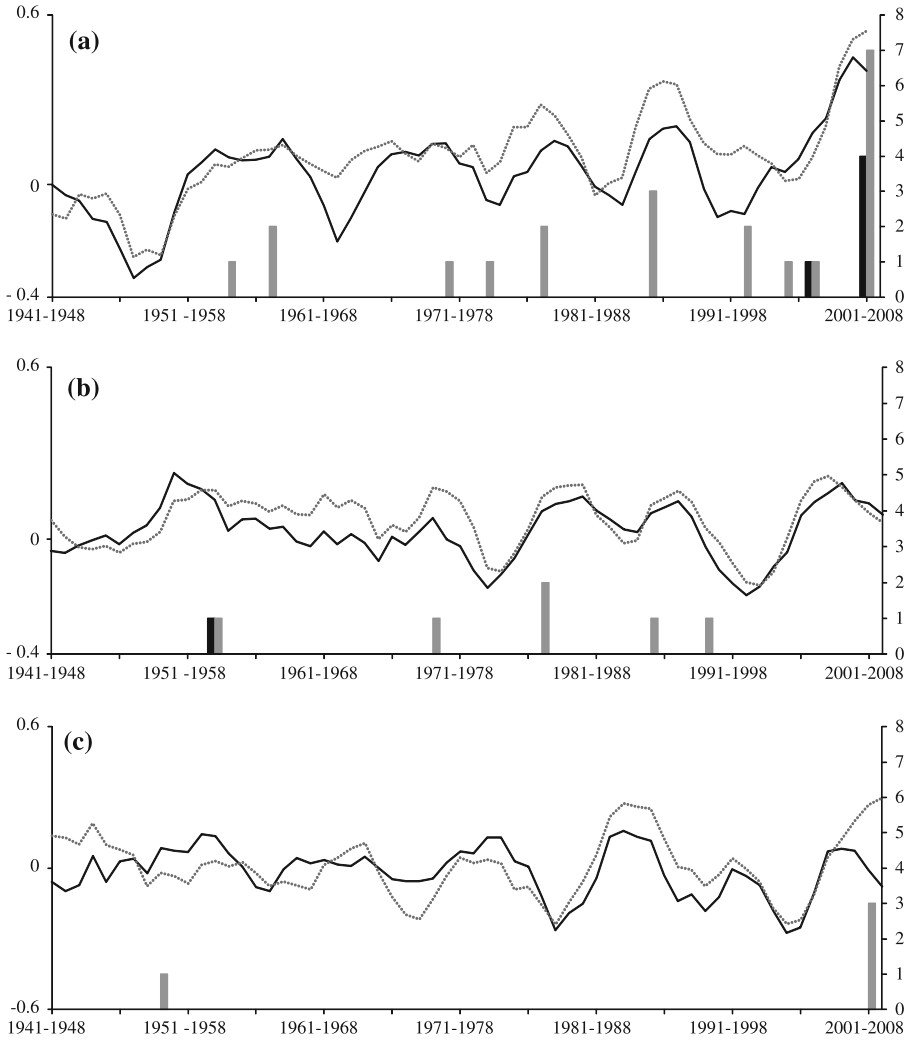

Fig. 3 Growth reduction index of infected trees (*grey line*) and healthy trees (*black line*) for **a** LOW, **b** MED and **c** HIGH, for the common period from 1937 to 2009. The growth reduction index was calculated for each mean chronology as a running calculation of per cent growth change between the average width of four rings with the average width of the four previous rings. Values from 0 to 0.4 indicate a moderate reduction, values above 0.4 a substantial reduction. Bars show the number of abrupt growth reductions for healthy and infected trees. The ordinate axis on the left indicates the suppression index and the second ordinate axis on the right side shows the number of abrupt growth reductions

than LOW-CON after 1984, while INF ring-width chronologies at MED and HIGH were significantly lower after 1974 and 1925, respectively.

Abrupt growth reductions and suppression index analysis, between the INF and CON of each tree, showed other differences in growth between sites (Fig. 2). Each INF

master chronology displayed periods of growth reduction which were not specific to the sites and which could be interpreted on the basis of the weakening caused by fungi. Both INF and CON showed fewer abrupt growth reductions in their juvenile period in every stand, but the intensity and frequency of abrupt growth reductions changed with time. LOW-INF had the highest suppression index and the largest number of abrupt growth reductions (10 periods with at least one tree showing a suppression period) while MED-INF showed five of these periods and HIGH-INF only two. The abrupt growth reductions frequency increased with increasing tree age for all INF trees at LOW (Fig. 3). For each of these trees, a substantial reduction was found in the last decade.

Pointer years

Analysis of negative pointer year (narrow rings) series showed that dry conditions were the main environmental factor limiting tree-ring growth for LOW-INF (1 year in LOW-CON, 4 years in LOW-INF). All four pointer years (1950, 1970, 1976 and 1991) noticed in LOW-INF occurred in dry growing seasons (Table 2). At MED and HIGH, no relationship was found between pointer years and extreme climatic events. At these sites, limiting factors may be both drought and cold conditions and it is more difficult to ascertain clearly the cause of pointer years.

Basal area

In order to assess the loss of productivity caused by *H. parviporum*, the mean cumulative basal area was also calculated from each raw ring-width series (Figs. 4, 5).

Table 2 Pointer years (1937–2009) in the radial growth of Norway spruce at LOW stand: ±indicate positive and negative pointer years

Years	LOW-CON	LOW-INF	May–August precipitation
1944	+		−4.5
1948		+	26.7
1950		−	−36.8
1953	+	+	3.0
1968	+		30.2
1970		−	−9.5
1976		−	−14.5
1978		+	−2.0
1987		+	26.2
1991		−	−25.0
1992	−		−1.8
2002		+	46.0

May–August mean precipitation is shown as deviation from 1900 to 2009 mean

Using the Wilcoxon test, we found that INF grew significantly less than CON for all series, but these differences started in different years. In 2009, significant mean cumulative basal area differences between INF and CON were observed at LOW (30.2 %; 0.45 % per year at $p < 0.05$), MED (38.7 %; 0.42 % per year at $p < 0.001$) and HIGH (36.9 %; 0.20 % per year at $p < 0.001$). These significant differences started in 2000, 1966 and 1973, respectively, at LOW, MED and HIGH. Furthermore, the most relevant mean cumulative basal area loss was found over the last 10 years (Fig. 5; Table 3).

Taken together, these results confirm the highest growth reductions in INF. Interestingly, these stress signals are more evident at LOW-INF.

The influence of climate on tree growth

To clarify the role of climatic conditions, we analysed the relationships between monthly temperature, precipitation

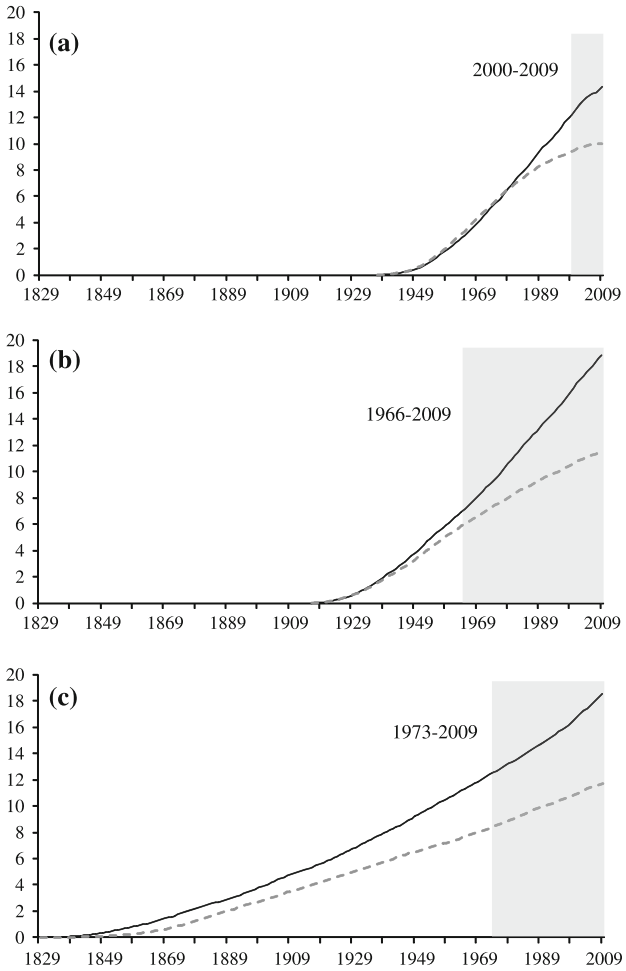

Fig. 4 Mean cumulative basal area of healthy trees (*black line*) and infected trees (*grey line*) at LOW **a**, MED **b** and HIGH **c**. Shaded areas mark intervals in which INF tree growth is significantly lower than for CON trees ($p < 0.05$)

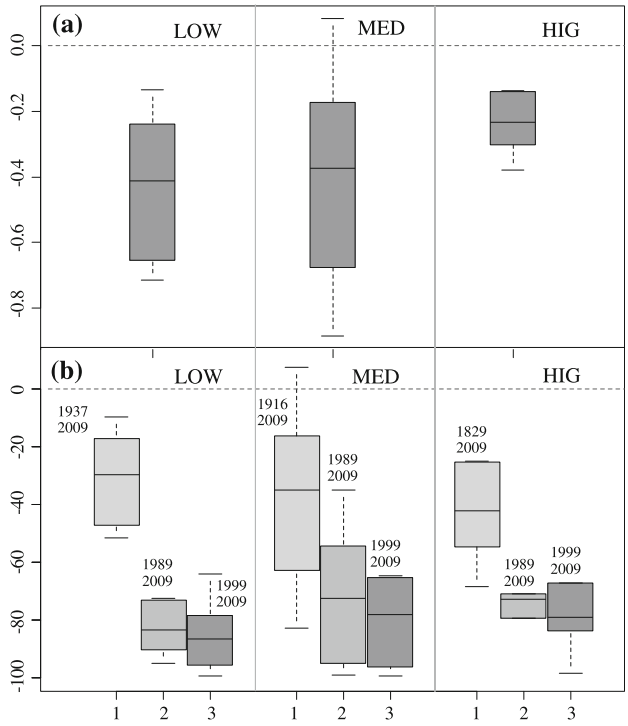

Fig. 5 Box plot of the percentage difference between mean cumulative basal area of INF and CON at each site. Negative values indicate low growth of INF relative to CON. Percentage difference was calculated as the reduction of mean cumulative basal area per year during the whole tree life history (**a**); and as the total reduction of mean cumulative basal area over three periods (**b**), whole tree life history (1), last 20 years (2), last 10 years (3). The first and third quartile are shown

Table 3 Per cent growth differences calculated as mean cumulative basal area of CON minus INF relative to CON during whole tree life at 2009 (1), last 20 years (2) and last 10 years (3)

Site code	Tree life$^{(1)}$	1989–2009$^{(2)}$	1999–2009$^{(3)}$
LOW-INF	30.2 %*	82.6 %***	86.1 %***
MED-INF	38.7 %***	72.6 %***	74.8 %***
HIGH-INF	36.9 %***	63.2 %***	67.7 %***

Different numbers of stars indicate different significance levels at * $p < 0.05$; ** $p < 0.01$; *** $p < 0.001$

and moisture availability (scPDSI) values and tree-ring indexed chronologies.

The correlation function profiles for tree-ring indexed chronologies and climate variables are shown in Fig. 6.

At LOW and MED, tree-ring growth was positively correlated with precipitation in January, June and March, while for scPDSI positive correlations were found from May to August only at LOW-INF, and from January to April for both INF and COR at MED. Moreover, negative correlation with temperature was found in June at LOW-INF and in July for both INF and CON. On the contrary, both CON and INF chronologies at HIGH showed a negative correlation with precipitation in June and a positive influence of summer temperatures with both June and July temperatures. Monthly scPDSI seemed to be a more important factor for tree-ring growth than temperature and precipitation at LOW and MED while at HIGH, the dominant climatic factors controlling tree-ring widths were temperature and precipitation in July.

INF at low elevation was more sensitive to January precipitation and arid conditions in summer than CON trees. In contrast, at both medium and high elevation sites, no significant correlation function differences between CON and INF trees were found.

The stationarity and consistency of climate–growth relationships over time were further analysed using the Pearson correlation coefficient for running windows of 48 years, progressively shifted by 1 year. While climate–growth relationships changed throughout the life of the trees, with a synchronous pattern for both INF and CON at MED and HIGH (Fig. 6), significant differences were found at LOW (Figs. 6, 7).

At LOW, the relationship between INF tree growth and monthly mean scPDSI is higher than CON trees, with a long-term increase in correlation coefficient values from February to May and more stationary or decreasing values in the other months (Fig. 7). INF showed stronger correlation coefficient values in June and July scPDSI over time with stationary responses. On the contrary, the correlation coefficient values of CON were always lower and not significant. The relationship with summer temperature decreased (i.e. lower negative correlation coefficient was found). In addition to this decrease, precipitation in June and July became less correlated with growth. Significant differences in correlation coefficient values were noticed for January precipitation, in particular synchronous variations were found for both CON and INF at LOW, with an increasing positive trend, although INF trees showed higher values.

Discussion

Our findings reflect a stress signal in INF trees, which seems to be more sensitive to climatic variability.

Our results show a strong relationship between *H. parviporum* infection and growth reductions in *P. abies* at each site, confirming the results of several other studies (Arvidson 1975; Bloomberg and Hall 1986; Benz-Hellgren and Stenlid 1995; Oliva et al. 2010).

A significant basal area reduction for all INF trees at each site was observed (Figs. 4, 5). However, different results were found at the three stands. The mean ring-width chronologies of INF were significantly lower than CON only during the last 25 years at LOW (10 years considering the

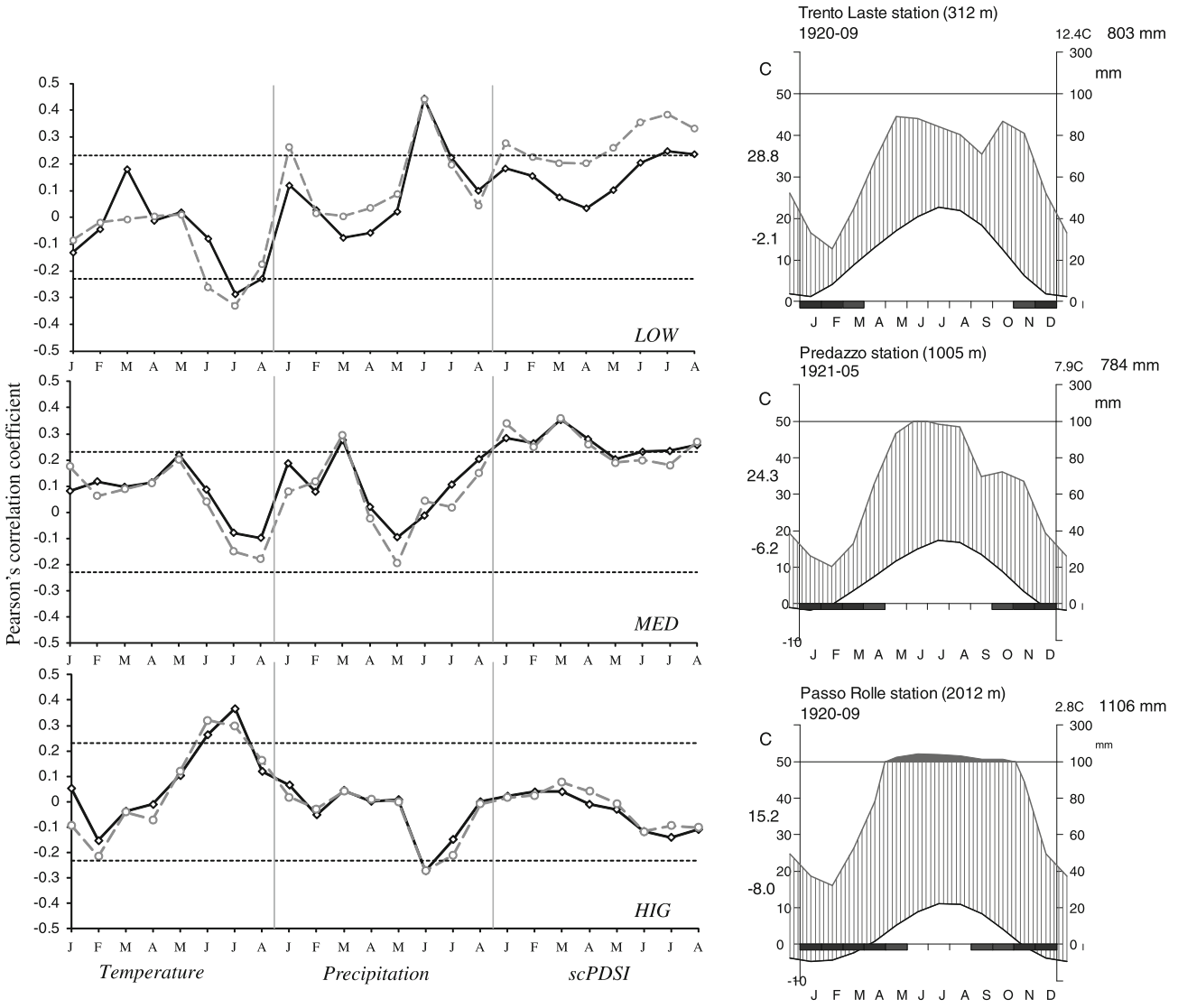

Fig. 6 Pearson correlation coefficient computed between tree-ring index of healthy trees (*black line*) and infected trees (*grey line*) and monthly variables (temperature, precipitation and scPDSI) from January to August of the year of growth during the common period 1937–2003. *Horizontal dotted lines* are statistical critical values ($p < 0.05$) after bootstrap replications. The three small plots on the right show the climatic diagram of the typical average course of mean monthly temperatures and precipitation regimes linked to the three regional chronologies, according to Walter and Lieth (1967)

mean cumulative basal area), while MED-INF and HIGH-INF showed a gradual decline in growth from 1974 and 1925, respectively. Even though the onset of infection cannot be exactly dated for each tree, it seems clear that the infection has been present in the trees at higher elevations for a considerably longer period than in the trees at low elevation. Most likely, INF trees at HIGH became infected since 1925 reporting longest infection for *H. parviporum*. Moreover, all sampled trees were dominant and codominant and since we found the same tree-ring-width patterns before decline, we assumed that the trees had always been dominant during their lifetime and therefore concluded that the effects of competition on growth patterns were negligible.

The higher first order of serial correlation at each INF series over all sites strongly suggests that INF trees not only use stored reserves more than CON trees, but they also profit less when growing conditions are most favourable.

As shown by tree-ring-width analysis, INF trees at LOW and MED were bigger than CON trees (Fig. 2) in the juvenile period. A similar phenomenon, with infected trees having faster growth rates than healthy trees early in their development, has been observed in several other studies, either with *Heterobasidion* sp. (Benz-Hellgren and Stenlid 1995; Oliva et al. 2008; Oliva et al. 2010) or other root diseases, including *Phellinus weirii* (Bloomberg and Reynolds 1985), *Armillaria ostoyae* (Bloomberg and

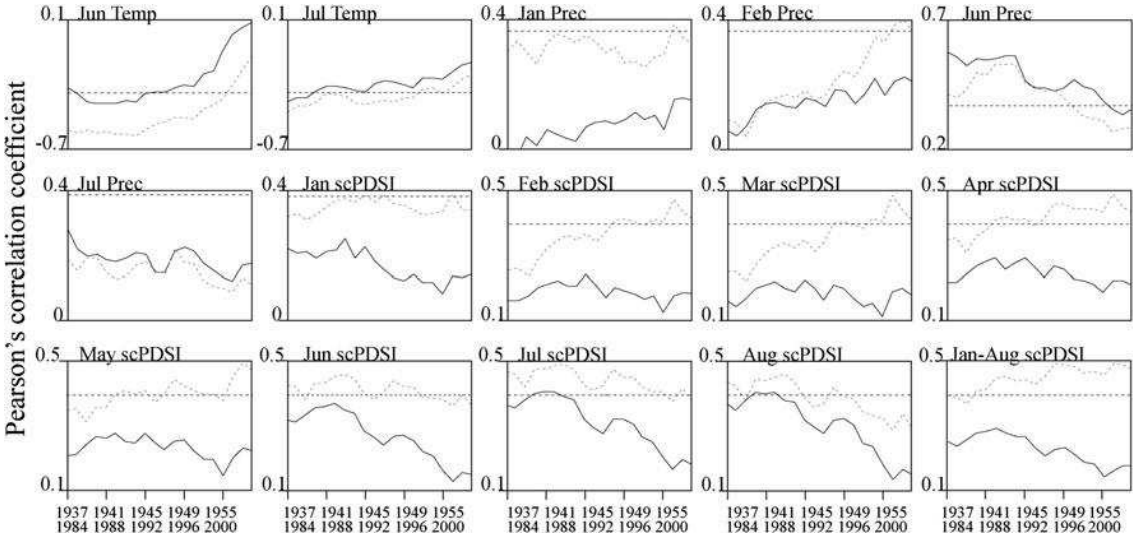

Fig. 7 The 48-year moving correlation function computed between the tree-ring index of healthy trees (*black line*) and infected trees (*grey line*) and the most important climate variable during the period 1937–2003 at LOW stand. *Horizontal dotted lines* indicate the adjusted significance limit ($p < 0.05$), according to the Bonferroni correction. The *x*-axis range is the same for all plots, but the ordinate *axis scale* changes according to absolute values

Morrison 1989) and *Inonotus tomentosus* (Lewis 1997). As suggested by Lewis (1997), dominant trees, having larger root systems, are more likely to be colonized by root pathogens. On the contrary, we did not find this phenomenon at HIGH, because here INF and CON had similar trends in their juvenile development. The results from HIGH may be related to lower competition for resources among trees and a lower juvenile growth rate than at the other two stands.

This paper focuses on tree-ring chronologies to study the long-term effects of fungal attack in different environmental conditions. In terms of basal area, assuming this to be one of the best indicators of volume, MED-INF showed the highest growth reduction, in as much as cumulative basal area was 38.7 % lower than CON trees, while values for LOW and HIGH were 30.2 and 36.9 %, respectively (Table 3). However, considering only the last 10 years, probably at a more advanced stage of infection, LOW-INF showed the highest losses, as mean cumulative basal area was 86 % lower than in CON tree. This trend could reflect behavioural variability and different tree–pathogen interactions. A final rapid decline during the last 10 years could indicate more aggressive behaviour of the fungus at the warmer and drier LOW site than at the other two sites. MED and HIGH showed a slow decline over many decades, reflecting long-term stress and a likely weak pathogen behaviour. Tsanova (1974) reported that damage tends to be smaller at higher elevations due to low temperature. In central Europe, the severity of the disease decreases above 600–700 m (Korhonen and Stenlid 1998). However, the long-term effects of root rot disease on tree growth in southern Europe are not satisfactorily documented in the literature (Oliva et al. 2008).

Furthermore, at the time of sampling in 2009 at LOW, five out of 10 INF trees had ceased cambial activity (one in 2004, 2005 and 2006, and two in 2008). These findings are in agreement with Cherubini et al. (2002), who found a difference (1–31 years) between the year of cessation of cambial activity and the year of cessation of photosynthetic activity. Even though there is no clear evidence, the presence of advanced rot surface (even 90 % in some cases) suggests that the tree, to assure water supply, could use systems other than xylem, such as air humidity (Cherubini et al. 2002).

The mean cumulative basal area losses of 30–38 % observed in our trees are higher than in earlier investigations. Arvidson (1975) estimated volume losses of 14 % in one Norway spruce stand located in Sweden affected by *Heterobasidion* spp. Benz-Hellgren and Stenlid (1995) reported average volume losses of 23 % due to *H. annosum* infection. Moreover, Kimberley et al. (2002) reported volume losses of 21 % for *Armillaria* root disease on *Pinus radiata*. We argue that these differences may be induced by sampling methods, as we selected only heavily rotted trees including those where cambial activity had ceased, while infected trees in these previous studies were not seriously rotted.

From a methodological point of view, our results demonstrate that abrupt growth reductions are good indicators of fungal attack, as reported by other authors (Cherubini et al. 2002; Schweingruber et al. 1990). Moreover, pointer years (Table 2) show tree reaction to past dry conditions for INF at LOW. Indeed, each pointer year detected in INF at LOW occurred in dry growing season, highlighting that

drought was the main environmental factor limiting tree growth. This was shown by correlation functions between tree-ring width and climate variables (Fig. 6). Positive relationships with the scPDSI of the growing season (from May to August) in INF trees at LOW confirm a strong water stress signal in these trees. Our results show that dry conditions occurring at low elevation play a key role in trees that are already stressed by fungal infection. We hypothesise that water deficit in trees infected by *H. parviporum* and possible different allocation patterns (e.g. reaction zone) could induce stronger growth reduction at low elevation than at upper elevations. Due to a shallow root system (Puhe 2003), *P. abies* is often reported to be particularly sensitive to soil water-deficit conditions in summer, especially at lower elevations (Battipaglia et al. 2009; Levanic et al. 2009), because at lower elevation drought is more frequent. At the LOW site, representing the lowest elevation limit for *P.abies* in this region, fungal infection may have further limited the ability of trees to withstand water stress, causing their rapid mortality. Furthermore, an increase in mortality induced by *H. parviporum* at warmer sites is well known (La Porta et al. 2008; Korhonen and Stenlid 1998; Puddu et al. 2003; Sànchez et al. 2005; Scherm and Chakraborty 1999). Similar results have been confirmed by several authors. In the Balkan mountains, both *H. parviporum* and *H. abietinum* showed an higher infection for *Picea abies* and *Abies alba* at lower and warmer sites (La Porta et al. 1998).

An increasing sensitivity to summer drought in infected trees has been reported by Linares et al. (2010) for *Abies pinsapo* affected by *H. abietinum* at low elevation stands in Mediterranean mountains in Spain. They concluded that drought is likely to be an inciting factor causing growth reduction and a sharp rise in the mortality of trees that are already stressed by root rot damage. However, Waldboth and Oberhuber (2009) observed an inverse relationship between summer mean temperature and the radial growth of *Castanea sativa* affected by *Cryphonectria parasitica*, suggesting that fungal infection increases the susceptibility of *C. sativa* to drought stress. On the contrary, at the MED and HIGH stands, both INF and CON trees showed the same climate correlation patterns, suggesting that favourable climatic factors and suitable site conditions for *P. abies* would increase the host's ability to tolerate infection and colonization (Korhonen and Stenlid 1998).

Moreover, moving correlation functions were used to provide a more detailed and dynamic perspective of climate signals over time (Fig. 7). As expected, INF trees at the LOW stand showed a strong stepwise increase in sensitivity to the scPDSI, especially in the early growing season, while the MED and HIGH forests showed similar patterns for both CON and INF trees. This confirms that fungal attack makes *P. abies* more susceptible to drought stress in dry Alpine valleys. Furthermore, a consistent negative relationship between mean temperature in June and July and radial growth was found in INF trees at LOW. Since high temperature increases evaporation rates, we hypothesise that *P. abies* could maintain lower stomatal conductance to reduce water loss. This also slows down plant photosynthesis, respiration and growth.

On the other hand, we point out that trees with *H. parviporum* at MED and HIGH showed a slow long-term decline.

Conclusions

Our tree-ring results and the climate correlation analyses highlight different growth patterns in INF *P. abies* depending on the different environmental site conditions. In our study, *P. abies* affected by *H. parviporum* showed a slow decline in growth over many decades at medium and high elevation, whereas at lower elevation trees infected by *H. parviporum* showed a final rapid decline and stopped cambial activity, some years before the sampling.

Our results show that the INF stand at LOW had a reduced ability to withstand soil water deficit. Instead, at MED and HIGH, the ability to overcome drought stress was the same for both infected and uninfected trees. These findings indicate that the infection at low elevations makes trees more susceptible to drought stress. We suggest that this higher tolerance of Norway spruce to the fungus at high elevations could be likely related to suboptimal growth conditions for the pathogen (such as a shorter growing season, lower temperature and a higher water availability) rather than genetic differences in host tree tolerance. It should be borne in mind that optimum growth of *H. parviporum* takes place in thermally isolated tissues and at temperatures above 20C°. Even though we need further investigations, we speculate that, given the predicted increase in air temperature in the next decades, *H. parviporum* could be more aggressive even at higher and colder sites. We understand that the considerable differences in the climatic sensitivity of INF trees observed at LOW may be caused by interactive effects. Contrasting and synergic environmental factors influence tree-ring growth; therefore, the question of whether drought stress acts as a predisposing or contributing stress factor in INF trees is still open. Accordingly, to evaluate these complex mechanisms, future ecophysiological studies integrated with dendrochronological analyses would be of assistance.

Even though the time of infection can be hypothesised but not measured with any precision, we assume that infection has been present at higher elevation for a considerably long period reported, never shown for *H. parviporum* (ca. 80 years).

From a management point of view, our results contribute to improve control methods, silvicultural treatments could include thinning to enhance water availability, and promoting the presence of native broad-leaved trees that are relatively less susceptible (such as some deciduous trees of the genera *Quercus*, *Carpinus*, *Ostrya* and *Acer*). Since thinning operations could also increase the risk of stump infection, urea treatment or other chemical and biological control are therefore recommended.

In conclusion, our study demonstrates that tree-ring data are useful tools for assessing tree health, host resistance and physiological changes in the pathogen–host system. However, we are aware that history of tree disease cannot be fully reconstructed, for example, the onset of infection can only be estimate.

Acknowledgments This study was supported and co-funded by the 'Fondazione CARITRO—Cassa di Risparmio di Trento e Rovereto' with the project ISOCHANGE. The authors wish to thank Magdalena Nötzli and Anne Verstege (WSL, Birmensdorf, Switzerland) for valuable laboratory assistance, Luca Ziller (FEM-IASMA, S. Michele a/Adige, Italy), Vivienne Frankell for correcting the English text and the 'Magnifica Comunità di Fiemme' for allowing us to sample the trees. The authors wish to thank two anonymous reviewers for their insightful and helpful comments on a previous version of the manuscript.

References

Arvidson B (1975) A study of the economic effects of root rot (*Polyporus annosus*) in the Norway Spruce. Translation, Environment Canada

Auer I, Boehm R, Jurkovic A et al (2007) HISTALP: historical instrumental climatological surface time series of the Greater Alpine Region RID C-8718-2009 RID A-2447-2011. Int J Climatol 27:17–46. doi:10.1002/joe.1377

Battipaglia G, Saurer M, Cherubini P et al (2009) Tree rings indicate different drought resistance of a native (*Abies alba* Mill.) and a nonnative (*Picea abies* (L.) Karst.) species co-occurring at a dry site in Southern Italy RID D-4121-2009. For Ecol Manag 257:820–828. doi:10.1016/j.foreco.2008.10.015

Benz-Hellgren M, Stenlid J (1995) Long-term reduction in the diameter growth of butt rot affected Norway spruce, *Picea abies*. For Ecol Manag 74:239–243. doi:10.1016/0378-1127(95)03530-N

Biondi F (1997) Evolutionary and moving response functions in dendroclimatology. Dendrochronologia 15:139–150

Biondi F (2000) Are climate-tree growth relationships changing in North-Central Idaho, USA RID G-2536-2010. Arct Antarct Alp Res 32:111–116. doi:10.2307/1552442

Biondi F, Waikul K (2004) DENDROCLIM2002: a C++ program for statistical calibration of climate signals in tree-ring chronologies RID G-2536-2010. Comput Geosci 30:303–311. doi:10.1016/j.cageo.2003.11.004

Bloomberg W, Hall AA (1986) Effects of laminated root rot on relationships between stem growth and root-system size, morphology, and spatial distribution in Douglas-fir. For Sci 32:202–219

Bloomberg W, Morrison D (1989) Relationship of growth reduction in Douglas-fir to infection by *Armillaria* root disease in southeastern British-Columbia. Phytopathology 79:482–487. doi:10.1094/Phyto-79-482

Bloomberg W, Reynolds G (1985) Growth loss and mortality in laminated root-rot infection centers in 2nd-growth Douglas-fir on Vancouver-island. For Sci 31:497–508

Bunn AG (2008) A dendrochronology program library in R (dplR). Dendrochronologia 26:115–124. doi:10.1016/j.dendro.2008.01.002

Capretti P, Korhonen K, Mugnai L, Romagnoli C (1990) An intersterility group of *Heterobasidion annosum* specialized to *Abies alba*. Eur J For Pathol 20:231–240

Cherubini P, Fontana G, Rigling D et al (2002) Tree-life history prior to death: two fungal root pathogens affect tree-ring growth differently. J Ecol 90:839–850. doi:10.1046/j.1365-2745.2002.00715.x

Cook ER (1985) A time series approach to tree-ring standardization. Thesis dissertation, University of Arizona, Arizona

Cook ER, Holmes RL (1984) Program ARSTAN users manual. Laboratory of tree ring research. University of Arizona, Arizona

Cook ER, Kairiukstis LA (1990) Methods of dendrochronology: applications in the environmental sciences. Kluwer, Dordrecht

Cook E, Peters K (1997) Calculating unbiased tree-ring indices for the study of climatic and environmental change. Holocene 7:361–370. doi:10.1177/095968369700700314

Dai Y, Vainio E, Hantula J et al (2003) Investigations on *Heterobasidion annosum* s. lat. in central and eastern Asia with the aid of mating tests and DNA fingerprinting. For Pathol 33:269–286. doi:10.1046/j.1439-0329.2003.00328.x

Desprez-Loustau ML, Marcais B, Nageleisen LM et al (2006) Interactive effects of drought and pathogens in forest trees. Ann For Sci 63:597–612. doi:10.1051/forest:2006040

Dobbertin M, Baltensweiler A, Rigling D (2001) Tree mortality in an unmanaged mountain pine (*Pinus mugo var. uncinata*) stand in the Swiss National Park impacted by root rot fungi. For Ecol Manag 145:79–89. doi:10.1016/S0378-1127(00)00576-4

Fischlin A, Midgley GF, Price J et al (2007) Ecosystems, their properties, goods and services. In: Parry ML, et al. (eds) Climate change 2007: impacts, adaptation and vulnerability. Contrib. Working group II to the 4th assessment rep. Intergovernmental panel on climate change, Cambridge, pp 211–272

Frank D, Esper J, Cook ER (2007) Adjustment for proxy number and coherence in a large-scale temperature reconstruction. Geophys Res Lett. doi:10.1029/2007GL030571

Fritts HC (1976) Tree rings and climate. Academic Press, London

Gärtner H, Nievergelt D (2010) The core-microtome: a new tool for surface preparation on cores and time series analysis of varying cell parameters. Dendrochronologia 28:85–92. doi:10.1016/j.dendro.2009.09.002

Gonzalez IG (2001) WEISER: a computer program to identify event and pointer years in dendrochronological series. Dendrochronologia 19:239–244

Grissino-Mayer HD, Holmes RL, Fritts HC (1996) The international tree ring data bank program library version 2.0. Users's manual. Laboratory of Tree Ring Research, Arizona

Guiot J (1991) The bootstrapped response function. Tree-Ring Bull 51:39–41

Helama S, Lindholm M, Timonen M, Eronen M (2004) Detection of climate signal in dendrochronological data analysis: a comparison of tree-ring standardization methods. Theor Appl Climatol 79:239–254. doi:10.1007/s00704-004-0077-0

Henry DA, Guardiola-Claramonte M, Barron-Gafford GA et al. (2009) Temperature sensitivity of drought-induced tree mortality portends increased regional die-off under global change-type drought. Proceedings of the national academy of sciences, 2009. doi:10.1073/pnas.0901438106

Hietala AM, Nagy NE, Steffenrem A et al (2009) Spatial patterns in hyphal growth and substrate exploitation within Norway spruce stems colonized by the pathogenic white-rot fungus *Heterobasidion parviporum* RID C-5536-2008. Appl Environ Microbiol 75:4069–4078. doi:10.1128/AEM.02392-08

Holmes RL (1983) Computer-assisted quality control in tree-ring dating and measurement. Tree-Ring Bull 43:69–78

Joseph G, Kelsey R, Thies W (1998) Hydraulic conductivity in roots of ponderosa pine infected with black-stain (*Leptographium wageneri*) or annosus (*Heterobasidion annosum*) root disease. Tree Physiol 18:333–339

Kimberley MO, Hood IA, Gardner JF (2002) Armillaria root disease of *Pinus radiata* in New Zealand. 6: growth loss. N Z J For Sci 32:148–162

Korhonen K (1978) Intersterility groups of *Heterobasidion annosum*. Commun Inst For Fenniae 94:1–25

Korhonen K, Stenlid J (1998) Biology of *Heterobasidion annosum*. In: Woodward S, Stenlid J, Karjalainen R, Hüttermann A (eds) Heterobasidion annosum: biology, ecology, impact and control. CAB International, Wallingford, pp 43–70

Kozlowski TT (1969) Tree physiology and forest pests. J For 67:118–123

Kozlowski TT, Kramer PJ, Pallardy SG (1991) The physiological ecology of woody plants. Academic Press, London

La Porta N, Capretti P, Kammiovirta K et al (1997) Geographical cline of DNA variation within the F intersterility group of *Heterobasidion annosum* in Italy. Plant Pathol 46:773–784. doi:10.1046/j.1365-3059.1997.d01-65.x

La Porta N, Apostolov K, Korhonen K (1998) Intersterility groups of *Heterobasidion annosum* and their host specificity in Bulgaria. Eur J For Pathol 28:2–9

La Porta N, Capretti P, Thomsen IM, Kasanen R, Hietala AM, Von Weissenberg K (2008) Forest pathogens with higher damage potential due to climate change in Europe. Can J Plant Pathol 30:177–195

LeBlanc DC (1990) Relationships between breast-height and whole-stem growth indices for red spruce on Whiteface Mountain, New York. Can J For Res 20:1399–1407. doi:10.1139/x90-185

Levanic T, Gricar J, Gagen M et al (2009) The climate sensitivity of Norway spruce [*Picea abies* (L.) Karst.] in the southeastern European Alps. Trees-Struct Funct 23:169–180. doi:10.1007/s00468-008-0265-0

Lewis K (1997) Growth reduction in spruce infected by *Inonotus tomentosus* in central British Columbia. Can J For Res 27:1669–1674. doi:10.1139/cjfr-27-10-1669

Linares CJ, Camarero JJ, Bowker MA et al (2010) Stand-structural effects on *Heterobasidion abietinum*-related mortality following drought events in *Abies pinsapo*. Oecologia 164:1107–1119. doi:10.1007/s00442-010-1770-6

Lonsdale D, Gibbs JN (1996) Effects of climate change on fungal diseases of trees. In: Frankland JC, Magan N, Gadd GM (eds) Fungi and environmental change. Cambridge University Press, Cambridge

Maloy OC (1974) Benomyl-malt agar for the purification of cultures of wood decay fungi. Plant Dis Rep 58:902–904

Manion PD (1991) Tree disease concepts, 2nd edn. Prentice Hall, Inc., Englewood

Niemelä T, Korhonen K (1998) Taxonomy of the genus *Heterobasidion*. In: Woodward S, Stenlid J, Karjalainen R, Hüttermann A (eds) Heterobasidion annosum: biology, ecology, impact and control. CAB International, Wallingford, pp 27–33

Oliva J, Samils N, Johansso U, Bendz-Hellgren M, Stenlid J (2008) Urea treatment reduced *Heterobasidion annosum* s.l. root rot in *Picea abies* after 15 years. For Ecol Manag 255:2876–2882

Oliva J, Thor M, Stenlid J (2010) Reaction zone and periodic increment decrease in *Picea abies* trees infected by *Heterobasidion annosum* s.l. For Ecol Manag 260:692–698. doi:10.1016/j.foreco.2010.05.024

Palmer WC (1965) Meteorological drought. Research paper, 45. US Weather Bureau, Washington

Pedersen B, McCune B (2002) A non-invasive method for reconstructing the relative mortality rates of trees in mixed-age, mixed-species forests. For Ecol Manag 155:303–314. doi:10.1016/S0378-1127(01)00567-9

Puddu A, Luisi N, Capretti P, Santini A (2003) Environmental factors related to damage by *Heterobasidion abietinum* in *Abies alba* forests in Southern Italy. For Ecol Manag 180:37–44. doi:10.1016/S0378-1127(02)00607-2

Puhe J (2003) Growth and development of the root system of Norway spruce (*Picea abies*) in forest stands: a review. For Ecol Manag 175:253–273. doi:10.1016/S0378-1127(02)00134-2

Sànchez ME, Capretti P, Calzado C et al. (2005) Root rot disease on *Abies pinsapo* in southern Spain. In: Manka M, Lakomy P (eds) Proceedings of the 11th international conference on root and butt rots, 16–22 August 2004, IUFRO. The August Ciezuowski, Agricultural University, Poznan, pp 220–223

Scherm H, Chakraborty S (1999) Climate change and plant disease. Annu Rev Phytopathol 37:399–426

Schmitt C, Parmeter J, Kliejunas J (2000) Annosus root rot disease of western conifers. For Pest Leafl US Department of Agriculture, Forest Service

Schweingruber FH (1996) Tree rings and environment: dendroecology. Paul Haupt Verlag, Berne

Schweingruber FH, Eckstein D, Serre-Bachet F, Braker OU (1990) Identification, presentation and interpretation of event years and pointer years in dendrochronology. Dendrochronologia 8:9–38

Shain L (1979) Dynamic responses of differentiated sapwood to injury and infection. Phytopathology 69:1143–1147

Snedecor GW, Cochran WG (1989) Statistical methods, 8th edn. Iowa State University

Stalpers JA (1978) Identification of wood-inhabiting *Anphyllophorales* in pure culture. Studies in mycology no. 16. Centraal bureau voor Schimmelcultures, Baarn

Stenlid J, Johansson M (1987) Infection of roots of Norway spruce (Picea abies) by Heterobasidion annosum.2. early changes in phenolic content and toxicity. Eur J For Pathol 17:217–226

Tsanova P (1974) The distribution of *Fomes annosus* and factors affecting its development in some natural Spruce forests. Gorskostopanska Nauka 11:59–70

van der Maaten-Theunissen M, Bouriaud O (2012) Climate–growth relationships at different stem heights in silver fir and Norway spruce. Can J For Res 42:958–969. doi:10.1139/x2012-046

van der Schrier G, Efthymiadis D, Briffa KR, Jones PD (2007a) European Alpine moisture variability for 1800–2003. Int J Biometeorol 27:415–427. doi:10.1002/joc.1411

van der Schrier G, Efthymiadis D, Briffa KR et al (2007b) European Alpine moisture variability for 1800–2003. Int J Biometeorol 27:415–427. doi:10.1002/joc.1411

Venables R, Hornik K, Albrecht G (2010) Main package of Venables and Ripley's MASS, Ver. 7.3.7. Repository CRAN, Licence GPL

Waldboth M, Oberhuber W (2009) Synergistic effect of drought and chestnut blight *(Cryphonectria parasitica)* on growth decline of European chestnut (*Castanea sativa*). For Pathol 39:43–55. doi:10.1111/j.1439-0329.2008.00562.x

Walter H, Lieth H (1967) Klimadiagramm-Weltatlas. 3 Bande. Fischer, Jena

Weber H, Moravec J, Theurillat JP (2000) International code of phytosociological nomenclature. 3rd edn. J Veg Sci 11:739–768

Woodward S, Stenlid J, Karjalainen R et al (1998) *Heterobasidion annosum*: biology, ecology, impact and control. Cab International, Wallingford

Section 3

Tree-ring isotope analysis of Norway spruce suffering from long-term infection by the pathogenic white-rot fungus *Heterobasidion parviporum*.

Forest Pathology 2013. DOI: 10.1111/efp.12089

Forest Pathology WILEY-BLACKWELL

For. Path. doi: 10.1111/efp.12089

SHORT COMMUNICATION

Tree-ring isotope analysis of Norway spruce suffering from long-term infection by the pathogenic white-rot fungus *Heterobasidion parviporum*

By Y. Gori[1,2], N. La Porta[1] and F. Camin[1]

[1]IASMA Research and Innovation Centre - Fondazione Edmund Mach, Via E. Mach 1, 38010, San Michele all' Adige, Italy;
[2]E-mail: yuri.gori@fmach.it (for correspondence)

Summary

We report for the first time a tree-ring isotopic analysis on host trees infected with *Heterobasidion parviporum*. By measuring carbon and oxygen stable isotope ratios in tree rings over ca. 150 years of forest growth, we obtained evidence that stomatal conductance increases in *Picea abies* affected by *H. parviporum*. We put forward this approach as a novel way of providing an insight into plant–pathogen relationships during tree life.

1 Introduction

Since first being described, biology and ecology of *Heterobasidion* spp. have received considerable attention, but much less attention has been paid to the physiological responses of host plants infected by *Heterobasidion* spp. as well as other root pathogens.

Host plants can modify their physiological processes in different ways (e.g. by altering water relations or photosynthetic capacity), responses which are thought to be defensive mechanisms of resistance (Little et al. 2003). For example, previous studies have reported significant variations in photosynthetic rate and stomatal activity as a consequence of insect defoliation (Little et al. 2003). Indeed, most research has focussed on the physiological responses of plants during insect outbreak, and so far, very few studies have looked at the adaptive mechanisms of plants infected by fungi at the ecosystem level (Little et al. 2003). We expected the physiological responses of trees infected with fungi to be similar to insect outbreaks in terms of photosynthetic activity and stomatal regulation, but we did not know which mechanism would be altered (i.e. stomatal conductance or photosynthetic activity) and whether different environmental conditions would affect responses.

The link between physiological responses and isotope discrimination is well known (see McCarroll and Loader 2004 for a review). According to the Scheidegger's qualitative model, simultaneous measurement of carbon and oxygen isotopes in tree rings allows us to estimate changes in stomatal conductance and photosynthetic rate during the tree life and under different ecological conditions (Scheidegger et al. 2000).

This study examines the variations in carbon and oxygen isotope values in the tree rings of healthy and *H. parviporum*-infected Norway spruce (*Picea abies* (L.) Karst.) in three stands at different elevations in a south-eastern Alpine region (Trentino, Italy). Our hypothesis was that presence of the fungus would trigger physiological alterations in infected trees.

2 Methods

Two cores per tree of 10 healthy (control) and 10 infected *P. abies* were collected in October 2009 from three stands at different altitudes. Cores were taken at 3 m above stump level to avoid rotten wood, and all trees were alive at sampling time. The stands were located at: Baselga, a low-altitude stand (850 m.asl; 46°4′48″N, 11°3′3″E), Val Maggiore, a medium-altitude stand (1300 m.asl; 46°17′32″N, 11°36′49″E) and Cermis, a high-altitude stand (1900 m.asl; 46°15′0″N, 11°29′43″E). All the stands were located within an area having a 25 km radius in the eastern Alps (Trentino, Italy). All were even-aged stands of predominantly Norway spruce with a northerly exposure and managed under similar silvicultural systems. Trees were classified as control or infected on the basis of a previous study and only heavily rotten trees (trees with rot covering at least 80% of the entire surface of the stump 20–30 cm above ground) were selected as infected samples. A more detailed description of the sites and the pathological analysis is given in Gori et al. (2013a).

Each core was prepared according to standard dendrochronological procedures (Phipps 1985). Wood samples were ground according to Lamuer et al. (2009). The $\delta^{13}C$ and $\delta^{18}O$ analyses were performed using isotope ratio mass spectrometry (IRMS) according to the procedure described in Gori et al. (2013b). All $\delta^{13}C$ series measurements were corrected to pre-industrial atmospheric $\delta^{13}C$ values.

Agreement between series was assessed with the *Gleichläufigkeit* (GLK) statistic, a measure of high-frequency coherence between series.

Finally, an ANOVA (analysis of variance) was performed to assess whether there was a significant pathogen effect on the $\delta^{13}C$ and $\delta^{18}O$ values.

Received: 28.6.2013; accepted: 5.11.2013; editor: S. Woodward

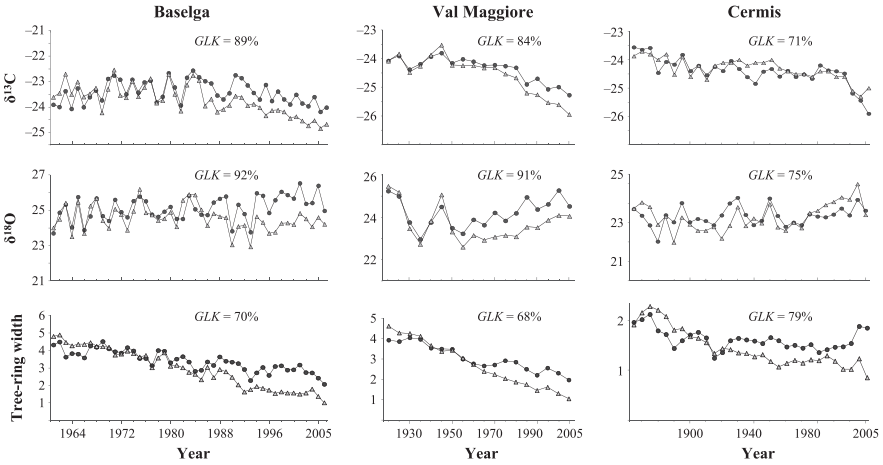

Fig. 1. Tree-ring width and Carbon and oxygen stable isotope chronologies in tree rings from the three spruce stands. Chronologies span from 1960 to 2005 at Baselga, 1920 to 2005 at Val Maggiore and 1860 to 2005 at Cermis. Infected Norway spruce, light grey triangle line; control Norway spruce, dark grey circle line. The Gleichläufigkeit (GLK) between control and infected trees is reported for each stand ($p < 0.01$). [Correction added on 11 December 2013, after first online publication: The first part of the figure has been removed]

3 Results and discussion

The periods dated by dendrochronological analysis were 1960–2005 at Baselga, 1920–2005 at Val Maggiore and 1860–2005 at Cermis. The time series of $\delta^{13}C$ and $\delta^{18}O$ and tree-ring width values at each site are given in Fig. 1. The high degree of synchronicity (GLK values ≥70%, Fig. 1) between the isotope series of control and infected trees suggests that environmental factors affect plant physiological processes (e.g. stomatal conductance and the rate of photosynthesis) irrespective of the presence of fungal infection. The GLK of $\delta^{13}C$ and $\delta^{18}O$ series revealed a high degree of synchronicity between control and infected trees in each stand with values ranging from 70% to 92% ($p < 0.01$, Fig. 1). Nevertheless, with the exception of the first period, $\delta^{13}C$ and $\delta^{18}O$ values at Baselga (after 1984) and Val Maggiore (after 1950) were always lower in infected trees than in controls (Fig. 1) ($p < 0.001$), while during the first period, the $\delta^{13}C$ and $\delta^{18}O$ chronologies in infected and control trees have comparable mean values ($p < 0.001$).

The ANOVA for Cermis, on the other hand, showed that the mean stable isotope ratios of both isotope series did not differ significantly between infected and control trees.

Stable isotope analysis was successfully used to investigate physiological mechanisms. Analyses of both $\delta^{13}C$ and $\delta^{18}O$ suggest different physiological responses in infected and control trees in stands at low and medium elevations.

According to the conceptual model of Scheidegger et al. (2000), a depletion in $\delta^{13}C$ and $\delta^{18}O$ values is expected to result in stomatal opening. It can therefore be assumed that infection in the trees at Baselga and Val Maggiore increased stomatal conductance, which should not be surprising. *H. annosum* s.l. causes the death of most major roots, and as a consequence, fungal infection may have restricted the trees' capacity to take up water from the soil; increased stomatal conductance could be a compensatory mechanism to improve water uptake. Moreover, an increase in stomatal conductance could compensate for the reduced foliage commonly found in infected trees.

We found a significant relationship between tree-ring $\delta^{13}C$ and $\delta^{18}O$ and fungal infection at two of the three sites, but it remains unclear why infected and control trees at Cermis (the high-altitude stand) exhibited similar isotope patterns. According to Scheidegger's model (Scheidegger et al. 2000), a similar tree-ring isotope signature may be explained by similar stomatal regulation. One explanation, therefore, could be that suboptimal growth conditions at a higher elevation (i.e. a shorter growing season, lower temperatures and higher water availability) make the fungus less aggressive. In a previous study (Gori et al. 2013a), we reported very gradual tree-ring reduction over many decades in Norway spruce infected with *H. parviporum* at a high elevation. While there was a clear temporal correlation between the decrease in $\delta^{13}C$ and $\delta^{18}O$ values and the reduction in tree-ring width in infected trees at Baselga and Val Maggiore, no such correlation was found at the high-altitude stand (Fig. 1). We hypothesize that stomatal conductance in infected trees at high altitude has remained unchanged, despite the prolonged presence of the fungus having caused a gradual reduction in growth over many decades. These findings are consistent with the higher tolerance of Norway spruce to the fungus at high elevations (Gori et al. 2013a).

Other studies have reported that damage tends to be less severe at higher elevations due to low temperatures Korhonen and Stenlid 1998). However, stomatal regulation of trees infected with *H. annosum* s.l. is not documented in the literature, and our isotope analysis confirms weak pathogen behaviour at high elevation.

We are aware that our assumption is no doubt a simplification as many other factors could influence stomatal response; nevertheless, the increase in stomatal conductance at low elevations confirms the hypothesis that fungal infection makes Norway spruce more susceptible to water availability in these environments (Gori et al. 2013a).

Acknowledgements

This study was supported and co-funded by the Fondazione CARITRO (Cassa di Risparmio di Trento e Rovereto) with the project ISO-CHANGE. The authors wish to thank Anne Verstege (WSL, Birmensdorf, Swiss) for assistance with measuring, Tessa Say for revision of the English text and the Magnifica Comunità di Fiemme for allowing us to sample the trees.

References

Gori, Y.; Cherubini, P.; Camin, F.; La Porta, N., 2013a: Fungal root pathogen (*Heterobasidion parviporum*) increases drought stress in Norway spruce stand at low elevation in the Alps. Eur. J. For. Res. **132**, 607–619.

Gori, Y.; Wehrens, R.; Greule, M.; Keppler, F.; Ziller, L.; La Porta, N.; Camin, F., 2013b: Carbon, hydrogen and oxygen stable isotope ratios of whole wood, cellulose and lignin methoxyl groups of *Picea abies* as climate proxies. Rapid Commun. Mass Spectrom. **27**, 265–275.

Korhonen, K.; Stenlid, J., 1998: Biology of *Heterobasidion annosum*. In: Heterobasidion annosum: biology, ecology, impact and control. Ed. by Woodward, S.; Stenlid, J.; Karjalainen, R.; Hütterman, A. Wallingford: CAB International, pp. 43–70.

Laumer, W.; Andreu, L.; Helle, G.; Schleser, G. H.; Wieloch, T.; Wissel, H., 2009: A novel approach for the homogenization of cellulose to use micro-amounts for stable isotope analyses. Rapid Commun. Mass Spectrom. **23**, 1934–1940.

Little, C. H. A.; Lavigne, M. B.; Ostaff, D. P., 2003: Impact of old foliage removal, simulating defoliation by the balsam fir sawfly, on balsam fir tree growth and photosynthesis of current-year shoots. For. Ecol. Manage. **186**, 261–269.

McCarroll, D., Loader, N. J., 2004: Stable isotopes in tree rings. Quat. Sci. Rev. **23**, 771–801.

Phipps, R., 1985: Collecting, preparing, cross-dating, and measuring tree increment cores. US Geological Survey Water Resource Investigations Report. pp. 85–4148.

Scheidegger, Y.; Saurer, M.; Bahn, M.; Siegwolf, R., 2000: Linking stable oxygen and carbon isotopes with stomatal conductance and photosynthetic capacity: a conceptual model. Oecologia **125**, 350–357.

Section 4

Tree rings and stable isotopes reveal the short- and long-term effects of insect defoliation on Norway spruce (*Picea abies*).

Submitted to *Forest Ecology and Management* on 27 October 2013.

Tree rings and stable isotopes reveal the short- and long-term effects of insect defoliation on Norway spruce (*Picea abies*)

Yuri Gori[1*], Federica Camin[1], Nicola La Porta[1], Marco Carrer[2], Andrea Battisti[3]

[1]FEM-IASMA Edmund Mach Foundation, Via E. Mach, 1, 38010 San Michele all'Adige, Italy; [2]Università degli Studi di Padova, Dip. TeSAF, Treeline Ecology Research Unit, Agripolis, I-35020 Legnaro Italy; [3]Università degli Studi di Padova, Dip. DAFNAE, Agripolis, I-35020 Legnaro Italy.

Corresponding author. E-mail: yuri.gori@fmach.it

Abstract

This paper focuses on carbon and oxygen stable isotopes in conjunction with tree-ring chronologies to investigate the short- and long-term effects of *Cephalcia arvensis* defoliation on *Picea abies*. We found massive growth loss and significantly different carbon and oxygen stable isotope patterns associated with insect feeding; while carbon isotope values increased, oxygen isotope values decreased in the defoliated trees. We hypothesized that a period of severe drought in the outbreak area before the insect attack may have caused the trees to mobilise reserves, which made trees more susceptible to *Cephalcia* attack as a result of increased soluble sugars and amino acids concomitant with the direct effect of high temperature and dry weather on the insect populations. Moreover, the carbon and oxygen isotope patterns could be explained by both an increase in photosynthetic rate and a resort to starch reserves following insect feeding. Overall, these findings contribute to our understanding of how trees respond to insect attack.

Key-words: Dendroecology, Farquhar model, insect defoliation, isotope analysis, photosynthetic capacity, web-spinning sawfly.

Introduction

Heavy defoliation is one of the main disturbances affecting forest ecosystems. Insect feeding usually brings about an abrupt reduction in tree growth during the outbreak, which can severely diminish forest productivity. Moreover, defoliation may provoke a variety of physiological responses in a wide range of plants (Chen et al., 2001; Ozaki et al., 2004a; Pataki et al., 1998; Quentin et al., 2011), yet, although the impact of insect feeding in terms of biomass loss has been extensively studied (Kozlowski, 1969; Kulman, 1971; Mayfield et al., 2005; Simard et al., 2012; VanderKlein and Reich, 2000), less attention has been paid to physiological responses.

As a consequence of insect defoliation, host plants can change their physiology by altering water relations, and modifying photosynthate allocation and photosynthetic capacity (Kozlowski, 1969). However, conflicting interpretations are often put forward, mainly as a result of the different functional groups of insects and host tree species investigated (Barbosa and Wagner, 1988; Trumble et al., 1993). While many studies have highlighted an increase in photosynthetic activity as a compensatory mechanism during insect feeding, other researches have focussed on contrasting responses in stomatal activity (Chen et al., 2001; Lavigne et al., 2001; Little et al., 2003; VanderKlein and Reich, 1999). Some authors have observed that the response of stomata varies according to past stress, suggesting that stomatal behaviour may be dependent on previous conditions (Hinckley et al., 1978; Pill et al., 1978; Schulte et al., 1987). However, it is important to point out that an adaptive mechanism of this sort cannot be generalized, as stomatal behaviour is the result of a complex interaction between environmental and

genetic factors (Larcher, 1995) and is often species-specific (Mansfield and Davies, 1981).

Compensation against herbivory was reported in older trees (*Pinus sylvestris* L. *nevadensis*) under full sunlight availability (Hódar et al., 2008) and in herbaceous plants (*Solidago altissima*) grown under high-resource treatments (Wise and Abrahamson, 2008).

While most studies have dealt with gas-exchange and physiological responses during the few years of the outbreak, much less attention has been given to adaptive mechanisms in the long-term. For example, it is well known that an increase in photosynthetic activity may offset biomass loss and the metabolic cost of producing defensive chemicals, which requires large amounts of carbohydrates (Kozlowski, 1969; Kozlowski et al., 1991; Waring and Pitman, 1985), although it is still unclear whether this adaptive mechanism persists after defoliation and full recovery of the tree. A comprehensive study to assess the long-term effects of defoliation on plant physiology is therefore required to resolve these issues.

Physiological changes (e.g. changes in stomatal conductance and photosynthetic rate) are known to result in differences in carbon and oxygen isotope discriminations (Farquhar et al., 1982; Scheidegger et al., 2000; Voncaemmerer and Farquhar, 1984). For example, an increase in the carbon isotope value ($\delta^{13}C$) may be the result of either a decrease in stomatal conductance or an increase in photosynthetic rate, whereas a decrease in the oxygen isotope value ($\delta^{18}O$) may coincide with an increase in stomatal conductance (McCarroll and Loader, 2004; Scheidegger et al., 2000). Although the link between stable isotopes and physiological responses is well known, few studies have been carried out on the impact of defoliation on stable isotope composition. Leavitt and Long (1986),

for example, found an increase in $\delta^{13}C$ values in tree rings during the period of most severe defoliation of *Abies concolor* and *Pseudotsuga menziesii* by the spruce budworm *Choristoneura fumiferana* (Clem.).

Tree-ring analysis has proven to be a suitable tool for measuring growth reduction and as an indicator of past environmental stress or insect attack (Schweingruber, 1996; Swetnam et al., 1985). In addition, dendrochronology and stable isotopes in tree rings can be used to analyse tree history at an annual resolution, making them suitable for assessing tree reaction in the long-term (Gori et al., 2013a; McCarroll and Loader, 2004).

The web-spinning sawfly *Cephalcia arvensis* is a monophagous defoliator of the *Picea* genus and endemic to the spruce range in Eurasia, where a few outbreaks have been recorded (Battisti et al. 2000). In one case, between 1986 and 1992 in the Southern Alps, hundreds of hectares of mature stands of Norway spruce (*Picea abies* (L.) Karst.) were severely defoliated, although some of the trees were salvage harvested (Marchisio et al., 1994). Total loss of needle biomass was recorded in 1988-1989 at the core of the outbreak area, but the population has returned to latent phase since 1992 (Battisti et al., 2000).

We combined tree-ring and C and O stable isotope analyses of Norway spruce trees, defoliated and non-defoliated by *C. arvensis*, to study the impact of defoliation on tree growth in the long-term. Given that defoliation was triggered by exceptional water deficit in the trees in the most productive stands of the forest (Marchisio et al. 1994) and growth was not affected at the beginning of the outbreak, we hypothesized that trees reacted to the stress by maintaining high metabolic activity. We examined the characteristics of these changes by measuring tree rings and assessing the yearly variability of C and O stable isotopes in the wood. In addition, we used the same approach to investigate the

possibility that defoliation triggers a compensatory mechanism in the uneaten needles, which persist for a few years.

Materials and methods

Study site

The study was carried out on the Cansiglio plateau, about 30 km east of the town of Belluno, Italy (Fig. 1). It is part of the Venetian Pre-Alps and is located at an elevation ranging from 900 to 1200 m. The prevailing geological substrate is limestone and the soil is deep and rich in clay on the flat part of the plateau, the site of the core of the outbreak, while it is shallow and less fertile on the surrounding slopes (Marchisio et al. 1994). The forest stand was a mature plantation of Norway spruce (about 90 years old) with sporadic European silver fir (*Abies alba*) and beech (*Fagus sylvatica*), and was dense (602-624 trees/ha) and fairly homogeneous characterized by about the same silvicultural parameters (Marchisio et al. 1994).

Mean annual precipitation at the Cansiglio meteorological station of is 1700 mm (1960-2003) with maximum rainfall in June and November; mean annual temperature is 5.1°C for the same period, the coolest month being January and the warmest July.

The outbreak was detected in 1986 at Tramezzere (Fig. 1). It then expanded to the east (Cornesega sites) in 1987-88, but was over by 1992 as a result of control methods and an increase in natural mortality (Battisti et al. 2000). The areas surrounding the outbreak have been carefully surveyed since detection and no evidence of high population density has been found.

Field sampling

Field sampling was carried out on mature Norway spruce trees located inside and outside the outbreak area. In October 2004, ten trees were selected at each of 21 randomly

selected sites, 13 unaffected (control) and 8 previously defoliated (Fig. 1). Care was taken to select only mature spruce trees with similar stem diameters, growing in similar light conditions and with no visible mechanical damage. Two increment cores were extracted at 180° from each other at breast height using a Pressler increment borer. Two of the 21 sites (control site 19, previously defoliated site 22) were selected for isotope analysis (Fig. 1). No lubricants, markers or other materials were used during field sampling at these 2 sites in order to prevent isotopic contamination.

Ring-width measurement

Each core was prepared in the laboratory following standard dendrochronological procedures (Phipps, 1985). The increment cores were air dried, mounted on grooved wooden mounts, then sanded with progressively finer grade abrasive paper until optimal surface resolution allowed annual rings to be detected under magnification. Care was taken to avoid contamination of the samples from the two sites (i.e. 19 and 22) selected for isotopic analysis (Fig. 1) by preparing each core with a core-microtome (Gaertner and Nievergelt, 2010) to make the features of the rings clearly visible under magnification. Ring width on each core was measured to the nearest 0.001 mm using a linear table coupled to a Leica MS5 stereoscope and then assigned to calendar year. Tree-ring widths of each curve were plotted, cross-dated visually, then statistically checked for cross-dating and measurement errors using the COFECHA computer program (Holmes, 1983) as a standard dendrochronological protocol for quality control.

In order to remove the effect of decreasing ring width with age, each tree-ring series was first standardized by fitting a negative exponential curve to the measured data series and by dividing observed values by expected values. These dimensionless indices were then processed with a second standardization to emphasize inter-annual high-frequency

variations by fitting a spline function with 50% frequency response of 35 years to each tree-ring series and calculating the indices as the observed versus the expected ratios. Flexible cubic spline curves are very effective at removing both the long-term trend and the effect of localized disturbance events, which are always present in the tree's history, while conserving inter-annual frequency variations (Cook and Peters, 1997).

Standardization and mean tree-ring chronologies were calculated using the ARSTAN program (Cook and Holmes, 1984), which was specifically developed for processing tree-ring series from closed-canopy forests. Mean tree-ring chronologies for each site were computed by (1) averaging the two standardized ring-width series for each tree to obtain a tree chronology, and (2) averaging all the tree chronologies within a site for each of the 21 sites using a biweight robust mean.

Several statistical analyses were carried out to determine the key features of each site chronology: a) mean sensitivity (MS), a measure of the relative change in ring width from one year to the next in a given series calculated over the whole tree-ring series (Fritts, 1976); b) standard deviation (SD): MS and SD are used to assess high-frequency variation in the series; c) first order of serial autocorrelation (AC), a measure of the previous year's influence on the current year's growth, typically varying from 0.300 to 0.800, which is useful for detecting potential persistence before and after standardisation; d) mean interseries correlation (rbar), a measure of the strength of the signal (typically the climate signal) common to all sampled trees at the site; and e) the expressed population signal (EPS) (Wigley et al., 1984), a measure of the correlation between the mean chronology derived from the samples and the population from which they were extracted, which allows the degree of variation in year-by-year growth of trees at the same site to be estimated. EPS indicates to what extent the sample size is representative

of a theoretically infinite population. Higher rbar values indicate greater synchronization in the annual growth patterns among sampled trees, while EPS is commonly adopted as a criterion for assessing chronology reliability. An EPS value above 0.85 is widely recognized in dendrochronological studies as indicating that the mean growth series is well replicated (Wigley et al., 1984).

Radial-growth reduction

In order to estimate the reduction in growth induced by defoliation, the effects of common environmental factors on defoliated and control chronologies were removed using the procedure described by Swetnam et al. (1985):

$PRI = SD_{(D)}/SD_{(C)} * [index_{(C)} - mean_{(C)}]$

$CI = index_{(D)} - PRI$

The procedure allows residuals from the control chronology (C) to be scaled to the same variance as the defoliated chronology (D). The scaled residuals are known as the Predicted Residual Indices (*PRI*). Finally, corrected indices (*CI*) were obtained by subtracting PRI from the D index.

Isotope analysis

After dating, all the cores taken from sites 19 (control) and 22 (previously defoliated) were prepared for isotopic analysis. As the trees which had been defoliated during the outbreak presented very narrow tree rings with indistinguishable latewood, all the samples were whole annual tree-rings (Gori et al., 2013b; Hill et al., 1995; Naurzbaev et al., 2002; Schleser et al., 1999). Annual rings from the period 1975-2003 were split with a razor under a binocular microscope, and those from the two radii were pooled to reduce isotope variability around the circumference of the tree (Leavitt and Long, 1984). Finally, all rings from a given year from the same site (ten trees per site) were pooled.

Wood samples of annual rings were assumed to be homogeneous. In fact, isotopic composition varies considerably within a single year due to different isotopic signatures over the season (Laumer et al., 2009; Loader et al., 2003; Verheyden et al., 2004). In order to obtain wood samples that were as homogeneous as possible, coarse wood samples were ground according to the method described by Laumer et al. (2009). Firstly, they were twice cooled (-196°C) in liquid nitrogen in order to convert them to a highly brittle state. In a second step, each cooled sample was placed in an iron cylinder (25 ml) with a 10 mm grinding ball and pulverized by radial oscillation (1800 Hz min^{-1}) for 4 minutes using a freezer-mill (CryoMill, Retsch®, Hann, Germany). Liquid nitrogen circulated through the system to keep the temperature at -196°C. The procedure was repeated twice to obtain a final sample size of between 5 and 20 µm.

Samples of about 0.30±0.5 mg of the dried, ground wood were placed in tin capsules for $\delta^{13}C$ analysis and in silver capsules for $\delta^{18}O$ analysis. All samples were then oven dried (80°C) to remove water vapour, then stored in a desiccator until analysis.

For carbon isotopic analysis, the tin capsules were placed in an Elemental Analyser (Flash EA™1112, Thermo Scientific) to convert the contents to CO_2 and H_2O (H_2O removed using a $Mg(ClO_4)_2$ filter). The CO_2 was flushed into the Isotopic Ratio Mass Spectrometer (Finnigan DELTA XP, Thermo Scientific, Bremen, Germany) via the ConFlo III device (Conflo III, Thermo Scientific), where the content of the different isotopomers (m/z 44 and 45) was determined.

For oxygen isotopic analysis, the samples in the silver capsules were converted to CO and H_2 at a temperature of 1450°C using a Pyrolyser (Finnigan™ TC/EA, High Temperature Conversion Elemental Analyser, Thermo Scientific), then flushed into the IRMS.

Values are reported in δ‰ relative to the Vienna Peedee Belemnite (VPDB) standard for $\delta^{13}C$ and the Vienna Standard Mean Ocean Water (VSMOW) for $\delta^{18}O$ according to the equation:

$$\delta‰ = [(R_{sample} - R_{standard})/R_{standard}] * 1000$$

where δ‰ is the isotope value of interest and R is the ratio between the heavier isotope and the lighter one.

Analytical precision (1 standard deviation) was 0.2 ‰ for $\delta^{13}C$ and 0.4 for $\delta^{18}O$.

Statistical analyses

Principal component analysis (PCA) was performed as a clustering and dimension-reducing technique to identify site chronologies with similar patterns and to check for differences between control and defoliated trees in tree-growth patterns. PCA was performed using mean-centred and autoscaled data on the correlation matrix of the 21 (13 control and 8 defoliated) standardized site chronologies. We distinguished three different periods: a) before the *C. arvensis* outbreak (1965-1985); b) the outbreak (1986-1991); c) post-outbreak (1992-2003).

In order to check whether radial growth reduction persisted after defoliation and to assess full tree recovery, a year by year ANOVA (analysis of variance) was performed on the defoliated and control sites. In addition, a simple Pearson's correlation coefficient was calculated to determine the relationships between the control and defoliated chronologies during the three above-mentioned periods.

The relationship between the isotope values of control and defoliated trees was investigated by *t*-test.

Results

Tree-ring analysis

Tree-ring chronologies showed there to be a large difference in tree growth between infested and uninfested trees, as shown in Table 1. Some rings were missing from two of

the eight defoliated site chronologies (sites 1 and 4) during the outbreak period, but none was missing from the control site chronologies. The chronologies of the defoliated trees had the highest mean sensitivity, the highest first-order of serial autocorrelation, and the highest mean interseries correlation. All site chronologies exceeded the minimum EPS value of 0.85: defoliated tree-ring chronologies had a value of 0.98, controls 0.97. Defoliated and control series had comparable standard deviations, and their mean ring widths were 3 and 3.6 mm, respectively.

Growth patterns were similar in control and defoliated trees during the period 1965 to 1986. In 1987 (the second year after onset of defoliation) tree growth of the defoliated trees began to drop below that of control trees (Fig. 2), the mean radial growth loss being 8%. During the heaviest defoliation period (1988-1990), radial growth loss amounted to 65% (Table 2), but there was a slight recovery in growth from 1992. It is remarkable that after full recovery (1992-1993), defoliated trees grew by 20-34% more than control trees over the following 7 years (1994-2000).

The year by year ANOVA confirms that growth was higher in defoliated trees ($p<0.05$) for several years following the outbreak.

The principal component analysis (PCA) shows no distinct groups appearing prior to defoliation (Fig. 3a), while there is a clear-cut discrimination between two clusters during defoliation (Fig. 3b). It is worth noting that the separation into two clusters persists after defoliation (Fig. 3c) and full recovery of tree growth, although it is less clear-cut. Following the outbreak, dispersion on both PCs was greater for defoliated sites than for the control stands.

Isotope analysis

Tree-ring carbon and oxygen isotope values have similar patterns and a high degree of synchronicity during the period before defoliation (Fig. 4b, c). However, while $\delta^{13}C$ and $\delta^{18}O$ values of defoliated and control trees do not differ significantly during the period prior to defoliation ($p<0.001$), defoliated trees had higher $\delta^{13}C$ values and lower $\delta^{18}O$ values ($p<0.01$) both during and after the outbreak .

In 1985 (one year before the outbreak) the $\delta^{13}C$ values in defoliated trees started to increase, reaching their peak in 1987. Surprisingly, ^{13}C enrichment in defoliated trees began two years prior (1985) to any noticeable reduction in radial growth (Fig. 4), whereas the year it reached its peak, 1987, coincided with the onset of a slight reduction in radial growth. Of note is the finding that ^{18}O depletion reached its peak (-22.8‰) in 1989 coinciding with the year of highest growth loss, while the values in defoliated trees were close to those in control trees in 1990, two years earlier than complete growth recovery in 1992.

During the first three years of the outbreak (1986-1988), $\delta^{18}O$ values in defoliated trees decreased to a minimum of 21.9‰ in 1988. In addition, ^{18}O depletion started one year ahead of growth reduction, whereas ^{18}O enrichment started one year before growth recovery.

We point out that both the $\delta^{13}C$ and the $\delta^{18}O$ values seem to precede tree-ring trends by one (oxygen series) or two years (carbon series).

Discussion

Carbon and oxygen stable isotope ratios and tree-ring analyses were carried out in order to evaluate the short- and long-term effects of heavy defoliation on a Norway spruce stand.

We found a time lag between substantial growth reduction and the reported onset of defoliation, which occurred in 1986. A delay between the appearance of the insect and the presence of narrow tree-rings is rather common. In this study, we found that a slight reduction in tree-ring growth in defoliated chronologies occurred during the second consecutive year of heavy defoliation.

Comparable radial growth losses in association with other conifer-feeding sawflies of the same taxonomic group have also been found. The pine false webworm (*Acantholyda erythrocephala*(L.)) caused radial growth reduction of 40% to 70% in white pine (*Pinus strobus* L.) stands after 2 years of heavy defoliation (Mayfield et al., 2005), while the larch web-spinning sawfly (*Cephalcia lariciphila*) caused a reduction in radial growth of 67% in the same year as defoliation (Vejpustková and Holuša, 2006). The difference is probably due to the leaf type of the host plant, with deciduous species responding more quickly than evergreens.

Plants under stress rely on reserves stored in the roots or stem functioning as a resilience mechanism (Kozlowski et al., 1991; Lopez et al., 2009). In our study, full needle loss was observed during peak insect feeding activity in 1988, when plants maintained slight radial growth despite the absence of photosynthetic biomass. Yet we found missing rings in only two of the eight affected sites in 1989, i.e. during the second year of complete defoliation. This is consistent with expectations (Waring and Pitman, 1985), as the defoliated trees had probably been using their reserves during the outbreak. As stem diameter growth has lower priority than the formation of new shoots and roots and the production of protective chemicals (Mayfield et al., 2005; Waringand Pitman, 1985), fewer reserves are expended on new ring formation. This appears to be what happened in 1989 when we found maximum growth loss and missing rings, suggesting that fewer

reserves were available for xylem production as they were most likely directed to new shoot and root formation (Waring and Pitman, 1985).

Although severe defoliation was observed over at least six consecutive years, all defoliated site chronologies showed recovery to control chronology values in 1992, when the *C. arvensis* populations returned to latent phase, after which there was a resumption in normal radial growth, as shown in table 2.

Moreover, the annual growth of defoliated trees was significantly greater than control trees after the outbreak (Tab. 2). This was confirmed by the PCA analysis (Fig. 3), which revealed no growth differences between the sites prior to outbreak (Fig. 3a), whereas there is a clear-cut discrimination between defoliated and control sites during the outbreak (Fig. 3b), which persists even after defoliation (Fig. 3c). Since climatic conditions were the same at both the control and the defoliated sites (Marchisio et al., 1994), other factors probably caused the growth differences after the outbreak period. It is well known that, when damaged by insects, several plant species increase the photosynthetic rate in the remaining foliage as a compensatory mechanism (Barry and Pinkard, 2013; Chen et al., 2001; Ozaki et al., 2004a; Quentin et al., 2011; Trumble et al., 1993; VanderKlein and Reich, 1999). In our study, an increase in photosynthetic rate could have been triggered by the onset of *C. arvensis* feeding, and, even though gas-exchange measurements would be needed to confirm this, the persistence of two different groups even after the outbreak suggests that a change in plant physiology of this sort persisted at the defoliated sites after feeding (Trumble et al., 1993), a hypothesis that is supported by the stable isotope analysis.

There was a clear increase in the $\delta^{13}C$ values at the defoliated sites from 1985, i.e. one year before any visible damage by *C. arvensis*. On the other hand, the $\delta^{18}O$ values at the

defoliated sites depleted to their minimum in 1988, when total needle loss was recorded, then increased to close to control values as the outbreak gradually came to an end. Nevertheless, lower $\delta^{18}O$ values persisted after the outbreak at damaged sites (Fig. 4c). In light of the large body of evidence supporting a relationship between stable isotopes and physiological change reported in the literature (Scheidegger et al., 2000), we offer here a plausible interpretation of our results.

According to the Farquhar model (Farquhar et al., 1982), an increase in $\delta^{13}C$ in plants can be the result of either 1) reduced stomatal conductance, 2) increased photosynthetic capacity, or 3) a change in both. In Scheidegger's conceptual model (Scheidegger et al., 2000), the inverse relationship between stomatal opening and $\delta^{18}O$ values can be used to identify the most likely case among the three aforementioned possibilities. The pattern of increased $\delta^{13}C$ values and decreased $\delta^{18}O$ values before the outbreak occurred (two years for carbon and one year for oxygen) does not seem to be related to defoliation but instead to the severe water deficit which affected the trees between 1983 and 1985, especially in the outbreak area owing to the nature of the soil (Marchisio et al. 1994). During the dry period ,the trees in the outbreak area may have mobilized their starch reserves in order to increase osmotic potential and prevent water loss. It is, in fact, well-known that starch reserves have a richer carbon isotopic composition than tree-ring wood (Brugnoli et al., 1988; Helle and Schleser, 2004; Le Roux et al., 2001). The resulting combination of higher soluble sugars and aminoacids concomitant with the direct effect of high temperatures and dry weather on the insect populations (Marchisio et al. 1994; Ozaki et al., 2004b) may have contributed to the outbreak.

Once the outbreak had started, the increase in $\delta^{13}C$ values and decrease in $\delta^{18}O$ values continued and persisted after defoliation. According to Scheidegger's model

(Scheidegger et al., 2000) “the most likely case” is that the trees increased their photosynthetic capacity.

It is clear, however, that our interpretation is something of a simplification and we are aware that no gas-exchange measurements were made in this study. Nevertheless, ^{13}C enrichment occurred simultaneously with an increase in radial growth at the onset of the outbreak, and continued after defoliation during the period 1994-2000 (Fig. 4), supporting the hypothesis that the increase in photosynthetic rate induced by insect activity persists even after defoliation. Photosynthetic upregulation following defoliation is thought to be related to carboxylation efficiency and ribulose-1,5-bisphosphate (RuBP) regeneration capacity (Layne and Flore, 1995; von Caemmerer and Farquhar, 1984). Simard et al. (2008) reported ^{13}C enrichment in *Abies balsama* and *Picea mariana* following defoliation by the spruce budworm *Choristoneura fumiferana*. However, they found no differences in $\delta^{18}O$ values during and after the outbreak and concluded that enriched ^{13}C could be explained by both an increase in photosynthetic rate and a resort to starch reserves during severe defoliation.

Overall, the results of our isotope and tree-ring analyses suggest tree growth to have been affected by a combination of weather and associated insect-induced defoliation.

Conclusions

Several studies have found a clear reduction in growth between one and four years after the onset of insect-induced defoliation (Krause et al., 2003; Mayfield et al., 2005; Simard et al., 2008). In our study, we found a significant reduction in growth only from the second year onwards. The carbon isotope results indicate that in the drought period before the outbreak (1983-1985) starch reserves may have been mobilised making the trees more susceptible to *Cephalcia* attack in 1986. Tree-ring and stable isotope patterns

also suggest that defoliation may have triggered an increase in photosynthetic capacity. Moreover, carbon and oxygen isotope values confirm the onset of insect attack as 1986, i.e. two years before a noticeable reduction in growth. In agreement with Simard et al. (2008), we conclude that carbon and oxygen isotope values are a more immediate indicator of the onset of defoliation than tree-ring width.

Our findings represent a significant contribution to the understanding of how trees respond to severe defoliation and point the way to future research focussed on long-term investigation of plant-physiology and plant-insect interactions.

References

Barbosa, P., Wagner, M.R., 1988. Introduction to forest and shade tree insects. Academic Press, Inc., San Diego, California, USA.

Barry, K.M., Pinkard, E.A., 2013. Growth and photosynthetic responses following defoliation and bud removal in eucalypts. For. Ecol. Manag. 293, 9.

Battisti, A., Boato, A., Masutti, L., 2000. Influence of silvicultural practices and population genetics on management of the spruce sawfly, *Cephalcia arvensis*. For. Ecol. Manage. 128, 159–166.

Brugnoli, E., Hubick, K., Voncaemmerer, S., Wong, S., Farquhar, G., 1988. Correlation Between the Carbon Isotope Discrimination in Leaf Starch and Sugars of C-3 Plants and the Ratio of Intercellular and Atmospheric Partial Pressures of Carbon-Dioxide. Plant Physiol. 88, 1418–1424.

Chen, Z., Kolb, T.E., Clancy, K.M., 2001. Mechanisms of Douglas-fir resistance to western spruce budworm defoliation: bud burst phenology, photosynthetic compensation and growth rate. Tree Physiology 21, 1159–1169.

Cook, E., Holmes, R.L., 1984. Program ARSTAN user manual. Laboratory of tree ring research. University of Arizona, Arizona.

Cook, E., Peters, K., 1997. Calculating unbiased tree-ring indices for the study of climatic and environmental change. Holocene 7, 361–370.

Farquhar, G., O'Leary, M., Berry, J., 1982. On the Relationship Between Carbon Isotope Discrimination and the Intercellular Carbon Dioxide Concentration in Leaves. Functional Plant Biol. 9, 121–137.

Fritts, H.C., 1976. Tree rings and climate. Academic Press.

Gaertner, H., Nievergelt, D., 2010. The core-microtome: A new tool for surface preparation on cores and time series analysis of varying cell parameters. Dendrochronologia 28, 85–92.

Gori, Y., Cherubini, P., Camin, F., Porta, N.L., 2013a. Fungal root pathogen (*Heterobasidion parviporum*) increases drought stress in Norway spruce stand at low elevation in the Alps. Eur. J. For. Res. 132, 607–619.

Gori, Y., Wehrens, R., Greule, M., Keppler, F., Ziller, L., La Porta, N., Camin, F., 2013b. Carbon, hydrogen and oxygen stable isotope ratios of whole wood, cellulose and lignin methoxyl groups of *Picea abies* as climate proxies. Rapid Commun. Mass Spectrom. 27, 265–275.

Helle, G., Schleser, G.H., 2004. Beyond CO_2-fixation by Rubisco - an interpretation of $^{13}C/^{12}C$variations in tree rings from novel intra-seasonal studies on broad-leaf trees. Plant Cell Environ. 27, 367–380.

Hill, S., Waterhouse, J., Field, E., Switsur, V., Aprees, T., 1995. Rapid Recycling of Triose Phosphates in Oak Stem Tissue. Plant Cell Environ. 18, 931–936.

Hinckley, T., Aslin, R., Aubuchon, R., Metcalf, C., Roberts, J., 1978. Leaf Conductance and Photosynthesis in 4 Species of Oak-Hickory Forest Type. For. Sci. 24, 73–84.

Hódar, J.A., Zamora, R., Castro, J., Gómez, J.M., García, D., 2008. Biomass allocation and growth responses of Scots pine saplings to simulated herbivory depend on plant age and light availability. Plant Ecol. 197, 229–238.

Holmes, R.L., 1983. Computer-assisted quality control in tree-ring dating and measurement. Tree-Ring Bulletin 43, 69–78.

Kozlowski, T.T., 1969. Tree Physiology and Forest Pests. Journal of Forestry 67, 118–123.

Kozlowski, T.T., Kramer, P.J., Pallardy, S.G., 1991. The physiological ecology of woody plants. Academic Press, Inc., San Diego, California, USA.

Krause, C., Gionest, F., Morin, H., MacLean, D.A., 2003. Temporal relations between defoliation caused by spruce budworm (*Choristoneura fumiferana* Clem.) and growth of balsam fir (*Abies balsamea* (L.) Mill.). Dendrochronologia 21.

Kulman, H.,M., 1971. Effects of insect defoliation on growth and mortality of trees. Ann. Rev. Entomol. 16, 289-324.

Larcher, W., 1995. Physiological plant ecology. Ecophysiology and stress physiology of functional groups. Springer-Verlag, Berlin, Germany.

Laumer, W., Andreu, L., Helle, G., Schleser, G.H., Wieloch, T., Wissel, H., 2009. A novel approach for the homogenization of cellulose to use micro-amounts for stable isotope analyses. Rapid Commun. Mass Spectrom. 23, 1934–1940.

Lavigne, M.B., Little, C.H.A., Major, J.E., 2001. Increasing the sink : source balance enhances photosynthetic rate of 1-year-old balsam fir foliage by increasing allocation of mineral nutrients. Tree Physiol. 21, 417–426.

Layne, D., Flore, J., 1995. End-Product Inhibition of Photosynthesis in Prunus-Cerasus L in Response. J. Am. Soc. Hortic. Sci. 120, 583–599.

Le Roux, X., Bariac, T., Sinoquet, H., Genty, B., Piel, C., Mariotti, A., Girardin, C., Richard, P., 2001. Spatial distribution of leaf water-use efficiency and carbon isotope discrimination within an isolated tree crown. Plant Cell Environ. 24, 1021–1032.

Leavitt, S., Long, A., 1984. Sampling Strategy for Stable Carbon Isotope Analysis of Tree Rings in Pine. Nature 311, 145–147.

Leavitt, S., Long, A., 1986. Influence of site disturbance on $\delta^{13}C$ isotopic time series from tree rings. In: Jacoby, G.C., Hornbeck, J.W. Proceedings of the international symposium on ecological aspects of tree-ring analysis, 1986, Marymount College, Tarrytown, New York.

Little, C.H.A., Lavigne, M.B., Ostaff, D.P., 2003. Impact of old foliage removal, simulating defoliation by the balsam fir sawfly, on balsam fir tree growth and photosynthesis of current-year shoots. For. Ecol. Manage. 186, 261–269.

Loader, N.J., Robertson, I., McCarroll, D., 2003. Comparison of stable carbon isotope ratios in the whole wood, cellulose and lignin of oak tree-rings. Paleogeogr. Paleoclimatol. Paleoecol. 196, 395–407.

Lopez, B.C., Gracia, C.A., Sabate, S., Keenan, T., 2009. Assessing the resilience of Mediterranean holm oaks to disturbances using selective thinning. Acta Oecol.-Int. J. Ecol. 35, 849–854.

Mansfield, T.A., Davies, W.J., 1981. Stomata and stomatal mechanisms. The physiology and biochemistry of drought resistance in plants.

Marchisio, C., Cescatti, A., Battisti, A., 1994. Climate, soils and *Cephalcia arvensis* outbreaks on *Picea abies* in the Italian Alps. For. Ecol. Manage. 68, 375–384.

Mayfield, A.E., Allen, D.C., Briggs, R.D., 2005. Radial growth impact of pine false webworm defoliation on eastern white pine. Can. Rech. For. 35, 1071–1086.

McCarroll, D., Loader, N.J., 2004. Stable isotopes in tree rings. Quat. Sci. Rev. 23, 771–801.

Naurzbaev, M., Vaganov, E., Sidorova, O., Schweingruber, F., 2002. Summer temperatures in eastern Taimyr inferred from a 2427-year late-Holocene tree-ring chronology and earlier floating series. Holocene 12, 727–736.

Ozaki, K., Fukuyama, K., Isono, M., Takao, G., 2004(a). Simultaneous outbreak of three species web-spinning sawflies: influence of weather and stand structure. For. Ecol. Manage. 187, 75-84.

Ozaki, K., Saito, H., Yamamuro, K., 2004(b). Compensatory photosynthesis as a response to partial debudding in ezo spruce, *Picea jezoensis* seedlings. Ecol. Res. 19, 225–231.

Pataki, D.E., Oren, R., Phillips, N., 1998. Responses of sap flux and stomatal conductance of *Pinus taeda* L. Trees to stepwise reductions in leaf area. J. Exp. Bot. 49, 871–878.

Phipps, R.L., (U.S.), G.S., 1985. Collecting, preparing, crossdating, and measuring tree increment cores. U.S. Dept. of the Interior, Geological Survey.

Pill, W., Lambeth, V., Hinckley, T., 1978. Effects of Nitrogen Form and Level on Ion Concentrations, Water Stress, and Blossom-End Rot Incidence in Tomato. J. Am. Soc. Hortic. Sci. 103, 265–268.

Quentin, A.G., O'Grady, A.P., Beadle, C.L., Worledge, D., Pinkard, E.A., 2011. Responses of transpiration and canopy conductance to partial defoliation of *Eucalyptus globulus* trees. Agric. For. Meteorol. 151, 356–364.

Scheidegger, Y., Saurer, M., Bahn, M., Siegwolf, R., 2000. Linking stable oxygen and carbon isotopes with stomatal conductance and photosynthetic capacity: a conceptual model. Oecologia 125, 350–357.

Schleser, G.H., Frielingsdorf, J., Blair, A., 1999. Carbon isotope behaviour in wood and cellulose during artificial aging. Chem. Geol. 158, 121–130.

Schulte, P., Hinckley, T., Stettler, R., 1987. Stomatal Responses of Populus to Leaf Water Potential. Can. J. Bot.-Rev. Can. Bot. 65, 255–260.

Schweingruber, F.H., 1996. Tree rings and environment: dendroecology. Paul Haupt AG Bern, Berne, Switzerland.

Simard, S., Elhani, S., Morin, H., Krause, C., Cherubini, P., 2008. Carbon and oxygen stable isotopes from tree-rings to identify spruce budworm outbreaks in the boreal forest of Quebec. Chem. Geol. 252, 80–87.

Simard, S., Morin, H., Krause, C., Buhay, W.M., Treydte, K., 2012. Tree-ring widths and isotopes of artificially defoliated balsam firs: A simulation of spruce budworm outbreaks in Eastern Canada. Environ. Exp. Bot. 81, 44–54.

Swetnam, T.W., Thompson, M.A., Sutherland, E.K., 1985. Using dendrochronology to measure radial growth of defoliated trees. USDA Forest Service Agricultural Handbook, 639, 1–39.

Trumble, J., Kolodnyhirsch, D., Ting, I., 1993. Plant Compensation for Arthropod Herbivory. Annu. Rev. Entomol. 38, 93–119.

Vanderklein, D.W., Reich, P.B., 2000. European larch and eastern white pine respond similarly during three years of partial defoliation. Tree Physiol. 20, 283–287.

Vanderklein, D.W., Reich, P.B., 1999. The effect of defoliation intensity and history on photosynthesis, growth and carbon reserves of two conifers with contrasting leaf lifespans and growth habits. New Phytol. 144, 121–132.

Vejpustková, M., Holuša, J., 2006. Impact of defoliation caused by the sawfly *Cephalcia lariciphila* (Hymenoptera: Pamphilidae) on radial growth of larch (*Larix decidua* Mill.). Eur J Forest Res 125, 391–396.

Verheyden, A., Helle, G., Schleser, G.H., Dehairs, F., Beeckman, H., Koedam, N., 2004. Annual cyclicity in high-resolution stable carbon and oxygen isotope ratios in the wood of the mangrove tree Rhizophora mucronata. Plant Cell Environ. 27, 1525–1536.

Voncaemmerer, S., Farquhar, G., 1984. Effects of Partial Defoliation, Changes of Irradiance During Growth, Short-Term Water-Stress and Growth at Enhanced P(CO_2) on the Photosynthetic Capacity of Leaves of Phaseolus-Vulgaris L. Planta 160, 320–329.

Waring, R., Pitman, G., 1985. Modifying Lodgepole Pine Stands to Change Susceptibility to Mountain Pine-Beetle Attack. Ecology 66, 889–897.

Wigley, T.M.L., Briffa, K.R., Jones, P.D., 1984. On the Average Value of Correlated Time Series, with Applications in Dendroclimatology and Hydrometeorology. Journal of Climate and Applied Meteorology 23, 201–213.

Wise, M.J., Abrahamson, W.G., 2008. Applying the limiting resource model to plant tolerance of apical meristem damage. Am. Nat. 172, 635–647.

Acknowledgements

This study was supported and co-funded by the ISOCHANGE project, and by the University of Padova grant 60%. The authors wish to thank Luca Ziller (FEM, San Michele all'Adige) for valuable laboratory assistance, Anna Rova (Università degli Studi di Padova) for the collection of data in Cansiglio, and Tessa Say for revision of the English text.

Table 1. Descriptive statistics of defoliated and non-defoliated tree-ring chronologies

Parameter	Defoliated *P. abies*	Non-defoliated *P. abies* (control)
Chronology time span	1901-2003 (103)	1903-2003 (100)
No. of trees/No. of cores	80/160	130/260
Mean ring width (mm)	3.00	3.62
Standard deviation	1.15	1.26
Mean sensitivity (MS)	0.20	0.17
First-order of serial autocorrelation (AC)	0.61	0.42
Mean interseries correlation (rbar)	0.83	0.74
Expressed population signal (EPS)	0.98	0.97
No. of missing rings	12	0

Mean ring width and standard deviation were computed on the raw tree-ring chronologies.

MS, AC, rbar and EPS were computed on the indexed tree-ring chronologies.

Table 2. ANOVA comparing the 8 defoliated chronologies with the 13 control chronologies. Years with significant growth differences are shown ($p<0.05$).

Year	ANOVA test	MRW Def.*	MRW Con. †	Growth differences between control and defoliated chronologies (%)‡
1978	*	1.024	0.929	9
1984	**	1.191	1.029	14
1985	***	1.104	0.979	12
1986	*	1.089	0.974	15
1988	***	0.545	0.823	-8
1989	***	0.304	0.964	-65
1990	***	0.366	0.972	-56
1991	***	0.602	0.946	-30
1994	*	1.056	0.921	19
1995	*	0.967	0.812	34
1996	*	1.079	0.941	15
1997	**	1.262	1.112	22
1998	*	1.162	1.062	2

* $p<0.05$; ** $p<0.01$; *** $p<0.001$

*Mean ring width of the 8 defoliated site chronologies.
† Mean ring width of the 13 control site chronologies.
‡Radial growth differences after Swetnam et al. (1985) correction are reported.

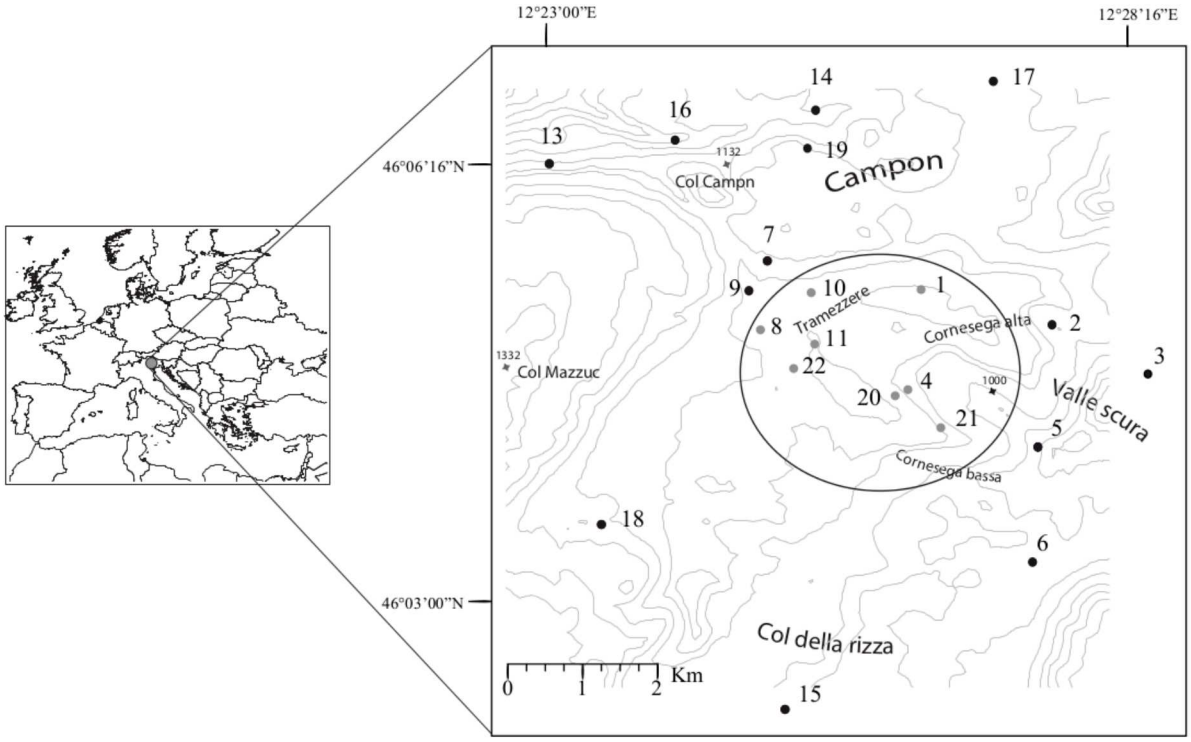

Fig. 1 Location of the study sites. Grey dots, defoliated sites; black dots, control sites. The circle indicates the outbreak area. Sites 19 and 22 were selected for isotopic analysis.

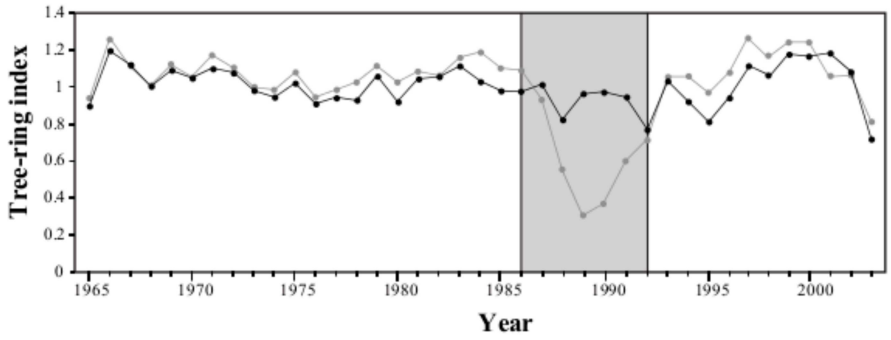

Fig. 2 Tree-ring indices of *Picea abies* for the period 1965-2003. Defoliated chronology, grey line; control chronology, dotted line. The shaded area indicates the outbreak period.

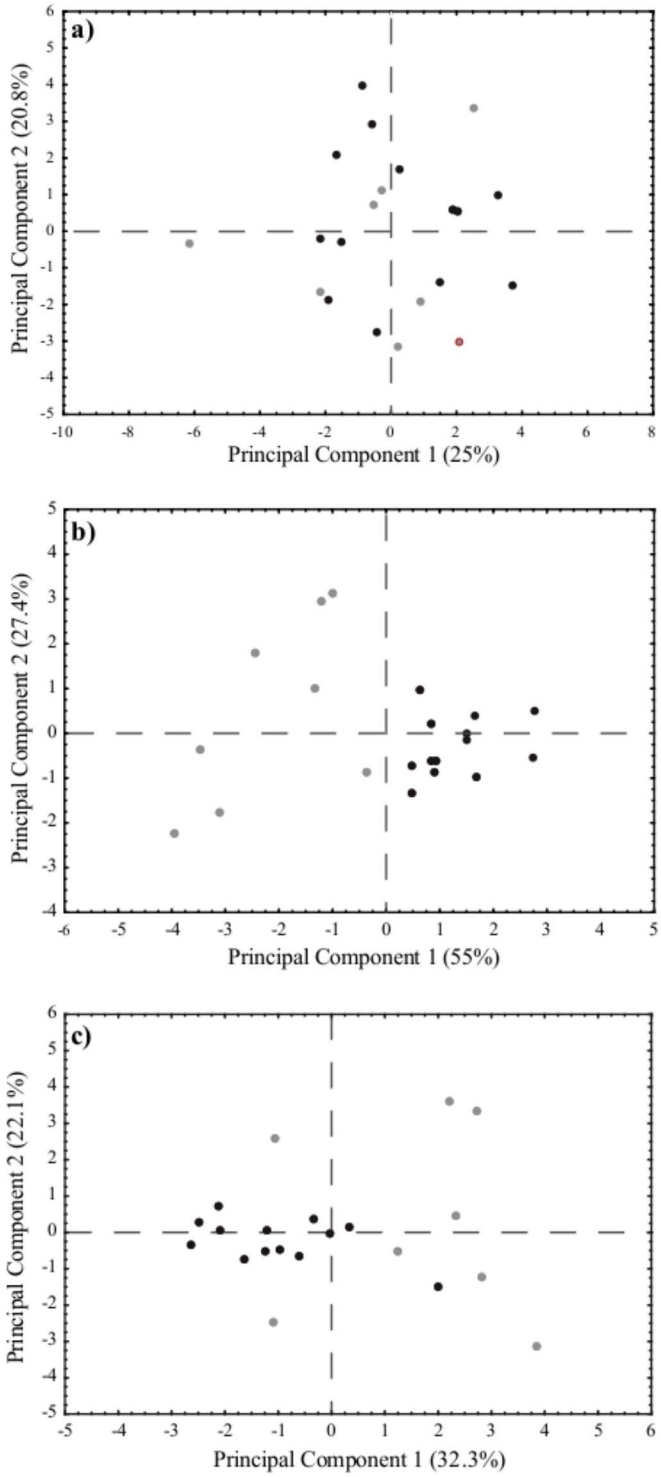

Fig. 3 Scatter plots of weighting coefficients for the first two principal components for the periods 1965-1985 (a), 1986-1992 (b), 1993-2003 (c). Grey dots, defoliated stand chronologies; black dots, control stand chronologies.

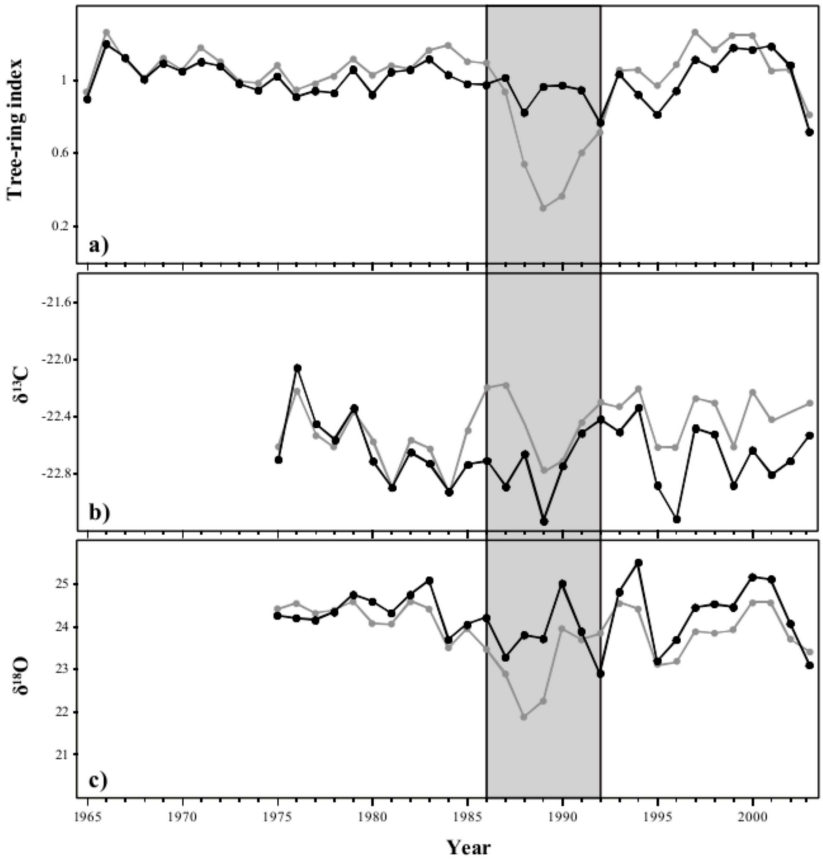

Fig. 4 Tree-ring indices (a), carbon (b) and oxygen (c) isotope values of control (black line) and defoliated trees (grey line) during the period 1975-2003. Tree-ring indices are reported as in Fig. 2. The shaded area indicates the outbreak period.

General conclusions

I combined tree-ring and stable isotope analyses of Norway spruce (Picea abies (L.) Karst.) to investigate the impact of a white-rot fungus and a defoliating insect on tree growth and physiological responses in the long term.

Climatic signals from stable isotope ratios

I analyzed eight different isotope proxies in different wood components ($\delta^{13}C$, $\delta^{18}O$ and $\delta^{2}H$ in whole wood, cellulose and lignin methoxyl groups) in order to discover the best proxy to provide the strongest climate signal at different elevations and climate conditions. Except for the highest site, no correlation was found ($p<0.01$) with precipitation (Table 2; section 1). This is consistent with the findings of other researchers, who showed $\delta^{13}C$ values to be closely related with precipitation only at very dry sites. I found that stable isotope values in whole wood samples preserve the best climatic signal (Table 3; section 1). Combining the stable isotope ratios of whole wood and cellulose doesn't improve climate prediction, so it is not necessary to extract cellulose (Table 4; section 1). These results appear to disagree with those of many other researches which report that $\delta^{18}O$ values of cellulose yield the best climate signal. Finally, I found that lignin methoxyl groups are not closely related with climate (Table 5; section 1). This results are useful for selecting the appropriate wood components for palaeoclimatological research. This saves a considerable amount of time, but the model may, of course, be applied only in the case of temperature reconstruction with Norway spruce in the south-eastern Alps.

Stable isotope dendrochronologies in infected trees

Tree-ring patterns and stable isotope chronologies of *Picea abies* affected by *Heterobasidion parviporum* were analysed in three mature stands located at different elevations (Fig. 1; section 2). The aim was to clarify the role of climatic conditions on infected trees. I found evidence that infection by *H. parviporum* at low elevations makes trees more susceptible to drought stress (Fig. 6-7; section 2). Moreover, infection at the lowest site (Baselga, 900 m asl) resulted in a final rapid decline, indicating lower tolerance of Norway spruce to the fungus. Conversely, infected stands at high elevations showed a slow decline over many decades, reflecting long-term stress and likely weak pathogen behaviour (Fig 2;

section 2). Finally, infected stands at low elevations showed the greatest growth reduction during the last 10 years, reporting a final growth loss of 86%, while infected stands at high elevations reported a growth reduction of 68% (Table 3; section 2). The higher tolerance of Norway spruce to the fungus at highest elevations could be related to suboptimal growth conditions for this pathogen. While, at low elevations, the more aggressive behaviour of the fungus could be due to optimal ecological factors such as: long growing season and high temperature. In fact, optimal growth conditions of *H. parviporum* takes place at temperature above 20°C and these climate conditions are typical for low elevation in the southern Alps.

Stable isotope analyses were successfully used to investigate physiological mechanisms. Analyses of both $\delta^{13}C$ and $\delta^{18}O$ suggest physiological responses caused by fungal infection at low and medium elevations. With respect to isotope theory, stomatal conductance increases in *Picea abies* affected by *H. parviporum* at low and medium elevations (Fig. 1; section 3). On the other hand, despite the prolonged presence of the fungus, stomatal conductance seems remained unchanged in infected trees at high altitude. These results are consistent with the higher tolerance of Norway spruce to the fungus at high elevations and confirm that fungal infection makes Norway spruce more susceptible to water availability at low elevation.

Although the onset of the fungal attack may be only hypothesised, it seem likely that infection had been present at a higher elevation for about 80 years; such a long period has never before been reported in the literature for *H. parviporum*.

Stable isotope dendrochronologies in defoliated trees

Tree-ring patterns and stable isotope chronologies of *P. abies* defoliated by *Cephalcia arvensis* were analysed to investigate the short- and long-term effects of an heavy defoliation. By tree-ring analysis I found a clear growth reduction only in the second year after the onset of insect-induced defoliation. Stable isotope ratios indicate that in the drought period before the outbreak (1983-1985) starch reserves may have been mobilised making the trees more susceptible to *Cephalcia* attack in 1986. Moreover, the combination of tree-ring and stable isotope patterns suggest that defoliation may have triggered an increase in photosynthetic capacity and confirm the onset of insect attack as 1986, i.e. two years before a

noticeable reduction in growth. These results provide a significant contribution to the understanding of how trees respond to severe defoliation and point the way to future research focussed on long-term investigation of plant physiology and plant-insect interactions.

As an overall conclusion, I give a substantial contribution to demonstrated that by combining tree-ring and stable isotope analyses it is possible to reconstruct the history of stressed trees, at least with respect to the physiological processes involved during and after *H. parviporum* infection and *C. arvensis* defoliation. Moreover, I found that a combination of tree-ring and stable isotope patterns may be helpful in estimating the onset of infection or insect attack. Finally, I should point out that some of the hypotheses I have put forward in this research may only be confirmed by physiological analyses (e.g. gas-exchange and stomatal conductance measurements, RuBisCo activity, chlorophyll fluorescence), which, I hope, could be specific topics for future research.

References

Anderson, W.T., Bernasconi, S.M., McKenzie, J.A., 1998. Oxygen and carbon isotopic record of climatic variability in tree ring cellulose (*Picea abies*): an example from central Switzerland (1913–1995). Journal of Geophysical Research 103/D24, 31625–31636.

Anderson, W.T., Bernasconi, S.M., McKenzie, J.A., Saurer, M., Schweingruber, F., 2002. Model evaluation for reconstructing the oxygen isotopic composition in precipitation from tree ring cellulose over the last century. Chemical Geology 182, 121–137.

Asiegbu F.O. 2005. Conifer root and butt rot caused by *Heterobasidion annosum* (Fr.) Bref. s.l. Molecular Plant Pathology. 6, 395-409.

Barbour M.M. 2001. Correlations between oxygen isotope ratios of wood constituents of *Quercus* and *Pinus* samples from around the world. Aust. J. Plant Physiol. 28, 335-348.

Barszczowka Lidia, Jedrysek Mariusz-Orion. 2005. Carbon isotope distribution along pine needles (*Pinus nigra* Arnold). Acta Societatis Botanicorum Poloniae. 74, 93-98.

Battipaglia G. et al. 2008. Climatic sensitivity of $\delta^{18}O$ in the wood and cellulose of tree rings: Results from a mixed stand of *Acer pseudoplatanus* L. and *Fagus sylvatica* L. Palaeogeography, Palaeoclimatology, Palaeoecology. 261,193–202.

Battipaglia G. et al. 2010. Traffic pollution affects tree-ring width and isotopic composition of *Pinus pinea*. Science of the Total Environment, 408, 586-593.

Battipaglia G. et al. 2013. Elevated CO_2 increases tree-level intrinsic water use efficiency: insights from carbon and oxygen isotope analyses in tree rings across three forest FACE sites. New Phytologist. 197. 544-554.

Battipaglia, Saurer, M., Cherubini, P., Siegwolf, R., Cotrufo, M., 2009. Tree rings indicate different drought resistance of a native (*Abies alba* Mill.) and a nonnative (*Picea abies* (L.) Karst.) species co-occurring at a dry site in Southern Italy. For. Ecol. Manag. 257, 820–828.

Battisti, A. and Stergulc, F., 1988. Notizie preliminari su pullulazioni di *Cephalcia arvensis* Panzer (Hym. Pamphiliidae) in peccete delle Prealpi Orientali. Atti Congr. Naz. Ital. Entomol., XV: 431-438. Battisti, A., Boato, A., Masutti, L., 2000. Influence of silvicultural practices and population genetics on management of the spruce sawfly, *Cephalcia arvensis*. For. Ecol. Manage. 128, 159–166.

Battisti, A., Stastny, M., Buffo, E., Larsson, S., 2006. A rapid altitudinal range expansion in the pine processionary moth produced by the 2003 climatic anomaly. Global Change Biology 12, 662–671 .

Becker, B., Kromer, B., Trimborn, P., 1991. A stable isotope tree-ring timescale of the Late Glacial/Holocene boundary. Nature 353, 647–649. Bert, D., Leavitt, S.W., Dupouey, J.-L., 1997. Variations of wood $\delta^{13}C$ and water use efficiency of *Abies alba* during the last century. Ecology 78 (5), 1588–1596.

Benz-Hellgren M., Stenlid J. 1995. Long-term reduction in the diameter growth of butt rot affected Norway spruce, *Picea abies*. For Ecol Manag 74:239–243. doi:10.1016/0378-1127(95)03530-N

Boas, J.E.V., 1934. Ein ernster Angriff von *Lyda arvensis* Panz. Z. Angew. Entomol., 20: 268-280.

Borella, S., Leuenberger, M., Saurer, M., 1999. Analysis of $\delta^{18}O$ in tree rings: Wood-cellulose comparison and method dependent sensitivity. J. Geophys. Res. Atmospheres 104, 19267–19273.

Briffa, K., Schweingruber, F.H., Jones, P.D., Osborn, T.J., Shiyatov, S.G., Vaganov, E.A., 1998. Reduced sensitivity of recent tree growth to temperature at high northern latitudes. Nature 391, 678–682.

Buhay, W.M., Edwards, T.W.D., 1995. Climate in southwestern Ontario, Canada, between AD 1610 and 1885 inferred from oxygen and hydrogen isotopic measurements of wood cellulose from trees in different hydrologic settings. Quaternary Research 44, 438–446.

Burk, R.L., Stuiver, M., 1981. Oxygen isotope ratios in trees reflect mean annual temperature and humidity. Science 211, 1417–1419.

Capecki, 2., 1982. Masowe wystapienie zasnui wysokogorskiej Cephalcia fallen (Dalm.)(Pamphiliidae, Hymenoptera) w Gorcach. Sylwan, 126:41-50.

Capretti P, Korhonen K, Mugnai L, Romagnoli C. 1990. An intersterility group of *Heterobasidion annosum* specialized to *Abies alba*. Eur J For Pathol 20:231–240.

Chen, Z., Kolb, T.E., Clancy, K.M., 2001. Mechanisms of Douglas-fir resistance to western spruce budworm defoliation: bud burst phenology, photosynthetic compensation and growth rate. Tree Physiol. 21, 1159–1169.

Cherubini P, Fontana G, Rigling D et al. 2002. Tree-life history prior to death: two fungal root pathogens affect tree-ring growth differently. J Ecol 90:839–850. doi:10.1046/j.1365-2745.2002.00715.x

Chevillat V.S. et al. 2005. Tissue-specific variation of $\delta^{13}C$ in mature canopy trees in a temperate forest in central Europe. Basic and Applied Ecology. 6, 519-534.

Cook E.R, Holmes R.L. 1986. Users manual for program ARSTAN. In 'Tree-ring chronologies of Western North America: California, eastern Oregon and northern Great Basin'. (Eds RL Holmes, RK Adams, and HC Fritts) pp. 50-65. (Laboratory of Tree-Ring Research, University of Arizona).

Cook E.R., Peters K. 1981. The smoothing spline: a new approach to standardizing forest interior tree-ring width series for dendroclimatic studies. Tree ring Bulletin 41.

Cook, E.R., Briffa, K.R., Meko, D.M., Graybill, D.A., Funkhouser, G., 1995. The “segment length curse” in long tree-ring chronology development for palaeoclimatic studies. The Holocene 5, 229–237.

Cook, E.R.. K. (Ed.), 1990. Methods of dendrochronology: applications in the environmental sciences.

Coplen, T.B., 1995. Discontinuance of SMOW and PDB. Nature 375, 285–285.

Craig, H., 1954. Carbon-13 variations in Sequoia rings and the atmosphere. Science 119, 141–144.

Cullen L.E., Grierson F.E. 2006. Is cellulose extraction necessary for developing stable carbon and oxygen isotopes chronologies from *Callitris glaucophylla*? Palaeogeography, Palaeoclimatology, Palaeoecology 236, 206 – 216.

Cullen L.E., Macfarlane C. 2005. Comparison of cellulose extraction methods for analysis of stable isotope ratios of carbon and oxygen in plant material. Tree Physiology 25, 563-569

Dansgaard, W., 1964. Stable isotopes in precipitation. Tellus 16, 436–468.

De Micco V. 2007. Variations of wood anatomy and $\delta^{13}C$ within-tree rings of coastal *Pinus pinaster* showing intra-annual density fluctuations . IAWA Journal, 28, 61-74

Dellus, V., Mila, I., Scalbert, A., Menard, C., Michon, V., Herve du Penhoat, C.L.M., 1997. Douglas-fir polyphenols and heartwood formation. Phytochemistry 45, 1573–1578.

Desprez-Loustau, M.-L., Marcais, B., Nageleisen, L.-M., Piou, D., Vannini, A., 2006. Interactive effects of drought and pathogens in forest trees. Ann. For. Sci. 63, 597–612.

Dubois, A.D., 1984. On the climatic interpretation of the hydrogen isotope ratios in recent and fossil wood. Bulletin de la Société Belge de Géologie 93, 267–270.

Dupouey, J.-L., Leavitt, S.W., Choisnel, E., Jourdain, S., 1993. Modeling carbon isotope fractionation in tree-rings based upon effective evapotranspiration and soil-water status. Plant, Cell and Environment 16, 939–947.

Duquesnay, A., Br! eda, N., Stievenard, M., Dupouey, J.L., 1998. Changes of tree-ring $\delta^{13}C$ and water-use efficiency of beech (*Fagus sylvatica* L.) in north-eastern France during the past century. Plant, Cell and Environment 21, 565–572.

Edwards, T.W.D., Graf, W., Trimborn, P., Stichler, W., Payer, H.D., 2000. $\delta^{13}C$ response surface resolves humidity and temperature signals in trees. Geochimica et Cosmochimica Acta 64, 161–167.

Eichhorn, O., I 990. Untersuchungen über die Fichtengespinstblattwespen Cephalcia spp. Panz. (Hym., Pamphiliidae). III. Populationsdynamische Faktorcn und Gesamtschau. J. Appl. Entomol., I l0: 321-345.

Epstein, S., Krishnamurthy, R.V., 1990. Environmental information in the isotopic record in trees. Philosophical Transactions of the Royal Society 330A, 427–439.

Epstein, S., Yapp, C.J., 1976. Climatic implications of the D/H ratio of hydrogen in C–H groups in tree cellulose. Earth and Planetary Science Letters 30, 252–261.

Farmer, J.G., Baxter, M.S., 1974. Atmospheric carbon dioxide levels as indicated by the stable isotope record in wood. Nature 247, 273–275.

Farquhar, G., O'Leary, M., Berry, J., 1982. On the Relationship Between Carbon Isotope Discrimination and the Intercellular Carbon Dioxide Concentration in Leaves. Funct. Plant Biol. 9, 121–137.

Farquhar, G.D., Henry, B.K., Styles, J.M., 1997. A rapid on-line technique for the determination of oxygen isotope composition of nitrogen containing organic compounds and water. Rapid Communications in Mass Spectrometry 11, 1554–1560.

Farquhar, G.D., Lloyd, J., 1993. Carbon and oxygen isotope effects in the exchange of carbon dioxide between terrestrial plants and the atmosphere. In: Ehleringer, J.R., Hall, A.E., Farquhar, G.D. (Eds.), Stable Isotopes and Plant Carbon–Water Relations. Academic Press, New York, pp. 47–70.

February, E.C., Stock, W.D., 1999. Declining trends in the $^{13}C/\ ^{12}C$ ratio of atmospheric carbon dioxide from tree rings of South AfricanWiddringtonia cedarbergensis. Quaternary Research 52, 229–236.

Ferrio J.P., 2005. Reconstruction of climatic and crop conditions in the past based on the isotope signature of archaeobotanical remains. PhD dissertation. Departament de Producció Vegetal i Ciència forestal.

Ferrio, J.P., Voltas, J., 2005. Carbon and oxygen isotope ratios in wood constituents of *Pinus halepensis* as indicators of precipitation, temperature and vapour pressure deficit. Tellus B 57, 164–173.

Fischlin A, Midgley G.F, Price J. et al. 2007. Ecosystems, their properties, goods and services. In: Parry ML, et al. (eds) Climate change 2007: impacts, adaptation and vulnerability. Contrib. Working group II to the 4th assessment rep. Intergovernmental panel on climate change, Cambridge, pp 211–272 Forestry and Forest Products Research Institute Scientific Meeting.

Francey, R.J., Allison, C.E., Etheridge, D.M., Trudinger, C.M., Enting, I.G., Leuenberger, M., Langenfelds, R.L., Michel, E., Steele, L.P., 1999. A 1000-year high precision record of $\delta^{13}C$ in atmospheric CO_2. Tellus 51B, 170–193.

Freyer, H.D., 1979a. On the ^{13}C record in tree rings. Part 1. ^{13}C variations in Northern Hemispheric trees during the last 150 years. Tellus 31, 124–137.

Freyer, H.D., 1979b. On the ^{13}C record in tree rings. Part 2. Registration of microenvironmental CO_2 and anomalous pollution effect. Tellus 31, 308–312.

Freyer, H.D., Belacy, N., 1983. 12 C/ 13 C records in Northern Hemispheric trees during the past 500 years: anthropogenic impact and climatic superpositions. Journal of Geophysical Research 88, 6844–6852.

Gagen M. et al. 2006. Combining ring width, density and stable carbon isotope proxies to enhance the climate signal in tree-rings: an example from the southern French Alps. Climatic Change, 78: 363-379.

Gärtner, H., Nievergelt, D., 2010. The core-microtome: A new tool for surface preparation on cores and time series analysis of varying cell parameters. Dendrochronologia 28, 85–92.

Gori Y., La Porta N., Camin F., 2013c. Tree ring isotope analysis of Norway spruce suffering from long-term infection by the pathogenic white-rot fungus Heterobasidion parviporum. Forest Pathology doi: 10.1111/efp.12089 1–13.

Gori, Y., Cherubini, P., Camin, F., Porta, N.L. 2013b. Fungal root pathogen (*Heterobasidion parviporum*) increases drought stress in Norway spruce stand at low elevation in the Alps. Eur. J. For. Res. 132 (4), 607–619.

Gori, Y., Wehrens, R., Greule, M., Keppler, F., Ziller, L., La Porta, N., Camin, F., 2013a. Carbon, hydrogen and oxygen stable isotope ratios of whole wood, cellulose and lignin methoxyl groups of Picea abies as climate proxies. Rapid Commun. Mass Spectrom. 27, 265–275.

Gray, J., Se, J.S., 1984. Climatic implications of the natural variation of D/H ratios in tree-ring cellulose. Earth and Planetary Science Letters 70, 129–138.

Gray, J., Thompson, P., 1976. Climatic information from 18 O/ 16 O ratios of cellulose in tree-rings. Nature 262, 481–482.

Gray, J., Thompson, P., 1977. Climatic information from 18 O/ 16 O analysis of cellulose, lignin and wholewood from tree-rings. Nature 270, 708–709.

Guerrieri et al. 2009. Impact of different nitrogen emission sources on tree physiology as assessed by a triple stable isotope approach. Atmospheric Environment. 43, 410-418

Hartmann, G., Blank, R. 1992. Winterfrost, Kahlfrass und Prachtkäpferbefall als Faktoren im Ursachenkomplex des Eichensterbens in Norddeutschland. Summary in English: winter frost, insect defoliation and *Agrilus biguttatus* Fabr. as causal factors of oak decline in northern Germany. Forst Holz, 47, pp. 443-452.

Hemming, D.L., Switsur, V.R., Waterhouse, J.S., Heaton, T.H.E., Carter, A.H.C., 1998. Climate and the stable carbon isotope composition of tree ring cellulose: an intercomparison of three tree species. Tellus 50B, 25–32.

Henry DA, Guardiola-Claramonte M, Barron-Gafford GA et al. 2009. Temperature sensitivity of drought-induced tree mortality portends increased regional die-off under

global change-type drought. Proceedings of the national academy of sciences, 2009. International Workshop on Asian and Pacific Dendrochronology.

Hietala A.M., Nagy N.E., Steffenrem A. et al. 2009. Spatial patterns in hyphal growth and substrate exploitation within Norway spruce stems colonized by the pathogenic white-rot fungus *Heterobasidion parviporum*. RID C-5536-2008. Appl Environ Microbiol 75:4069–4078. doi:10.1128/AEM.02392-08

Impa S.M. 2005. Carbon Isotope Discrimination Accurately Reflects Variability in WUE Measured at a Whole Plant Level in Rice. Crop Science. 45, 2517-2522.

Jedrysek, M.O., Krapiec, M., Skrzypek, G., Kaluzny, A., Halas, S., 1998. An attempt to calibrate carbon and hydrogen isotope ratios in oak tree rings cellulose: the last millennium. RMZ Materials and Geoenvironment 45, 82–90.

Keppler, F., Harper, D.B., Kalin, R.M., Meier-Augenstein, W., Farmer, N., Davis, S., Schmidt, H.-L., Brown, D.M., Hamilton, J.T.G., 2007. Stable hydrogen isotope ratios of lignin methoxyl groups as a paleoclimate proxy and constraint of the geographical origin of wood. New Phytol. 176, 600–609.

Kitagawa, H., Matsumoto, E., 1995. Climatic implications of $\delta^{13}C$ variations in a Japanese cedar (*Cryptomeria japonica*) during the last two millenia. Geophysical Research Letters 22, 2155–2158.

Korhonen K, Stenlid J. 1998. Biology of *Heterobasidion annosum*. In: Woodward S, Stenlid J, Karjalainen R, Hüttermann A (eds). *Heterobasidion annosum*: biology, ecology, impact and control. CAB International, Wallingford, pp 43–70

Korhonen K. 1978. Intersterility groups of *Heterobasidion annosum*. Commun Inst For Fenniae 94:1–25

Krishnamurthy, R.V., 1996. Implications of a 400 year tree ring based $^{13}C/^{12}C$ chronology. Geophysical Research Letters 23, 371–374.

Krishnamurthy, R.V., Epstein, S., 1985. Treering D/H ratio from Kenya, East Africa and its palaeoclimatic significance. Nature 317, 160–162.

La Porta N, Capretti P, Kammiovirta K et al. 1997.Geographical cline of DNA variation within the F intersterility group of *Heterobasidion annosum* in Italy. Plant Pathol 46:773–784.

La Porta, N., Capretti, P., Thomsen, I.M., Kasanen, R., Hietala, A.M., Von Weissenberg, K., 2008. Forest pathogens with higher damage potential due to climate change in Europe. Can. J. Plant Pathol.-Rev. Can. Phytopathol. 30, 177–195.

Lawrence, J.R., White, J.W.C., 1984. Growing season precipitation from D/H ratios of Eastern White Pine. Nature 311, 558–560.

Leavitt, S., Long, A., 1984. Sampling Strategy for Stable Carbon Isotope Analysis of Tree Rings in Pine. Nature 311, 145–147.

Leavitt, S., Long, A., 1986. Stable-Carbon Isotope Variability in Tree Foliage and Wood. Ecology 67, 1002–1010.

Leavitt, S.W., Danzer, S.R., 1993. Method for batch processing small wood samples to holocellulose for stable-carbon isotope analysis. Anal. Chem. 65, 87–89.

Libby, L.M., Pandolfi, L.J., 1974. Temperature dependence of, isotope ratios in tree rings. Proceedings of the National Academy of Science 71, 2482–2486.

Libby, L.M., Pandolfi, L.J., Payton, P.H., Marshall III, J., Becker, B., Giertz-Siebenlist, V., 1976. Isotopic tree thermometers. Nature 261, 284–290.

Linares C.J., Camarero J.J., Bowker M.A. et al. 2010. Stand-structural effects on *Heterobasidion abietinum*-related mortality following drought events in *Abies pinsapo*. Oecologia 164:1107–1119. doi: 10.1007/s00442-010-1770-6

Lindberg, M., Johansson, M., 1992. Resistance of Picea abies seedlings to infection by *Heterobasidion annosum* in relation to drought stress. Eur. J. For. Pathol. 22, 115–124.

Lipp, J., Trimborn, P., 1991. Long-term records and basic principles of tree-ring isotope data with emphasis on local environmental conditions. Pal. aoklimaforschung 6, 105–117.

Little, C.H.A., Lavigne, M.B., Ostaff, D.P., 2003. Impact of old foliage removal, simulating defoliation by the balsam fir sawfly, on balsam fir tree growth and photosynthesis of current-year shoots. For. Ecol. Manag. 186, 261–269.

Loader, N.J., Switsur, V.R., 1996. Reconstructing past environmental change using stable isotopes in tree-rings. Botanical Journal of Scotland 48, 65–78.

Lonsdale D., Gibbs J.N. 1996. Effects of climate change on fungal diseases of trees. In: Frankland JC, Magan N, Gadd GM (eds) Fungi and environmental change. Cambridge University Press, Cambridge

Manion, P.D., 1991. Tree disease concepts. Prentice-Hall, Englewood Cliffs, New Jersey, USA.

Marchisio, C., Cescatti, A., Battisti, A., 1994. Climate, Soils and *Cephalcia-Arvensis* Outbreaks on Picea-Abies in the Italian Alps. For. Ecol. Manag. 68, 375–384.

Martinek, V., 1987. Premnozemí ploskohrbetky cerné vevrcholovych smrcinach Orlickjch. hor. Lesn. Pr., 66: 11-18.

McCarroll, D., Loader, N.J., 2004. Stable isotopes in tree rings. Quat. Sci. Rev. 23, 771–801.

McCarroll, D., Pawellek, F., 1998. Stable carbon isotope ratios of latewood cellulose in Pinus sylvestrisfrom northern Finland: variability and signal strength. The Holocene 8, 693–702.

McCarroll, D., Pawellek, F., 2001. Stable carbon isotope ratios of *Pinus sylvestris* from northern Finland and the potential for extracting a climate signal from long Fennoscandian chronologies. The Holocene 11, 517–526.

McCormac, F.G., Baillie, M.G.L., Pilcher, J.R., Brown, D.M., Hoper, S.T., 1994. $\delta^{13}C$ measurement from the Irish oak chronology. Radiocarbon 36, 27–35.

Monserud R.A. 1986. Time-series analyses of tree-ring chronologies. Forest Science 32,349-372.

Niemelä T, Korhonen K. 1998. Taxonomy of the genus *Heterobasidion*. In: Woodward S, Stenlid J, Karjalainen R, Hüttermann A (eds) *Heterobasidion annosum*: biology, ecology, impact and control. CAB International, Wallingford, pp 27–33

Okada, N., Fujiwara, T., Ohta, S., Matsumoto, E., 1995. Stable carbon isotopes *of Chamaecyparis obtusa* grown at a high altitude region in Japan: within and among-tree variations. In: Ohta, S., Fujii, T., Okada, N., Hughes, M.K., Eckstein, D. (Eds.), TreeRings: From the Past to the Future.

Oliva J., Thor M., Stenlid J. 2010. Reaction zone and periodic increment decrease in *Picea abies* trees infected by Heterobasidion annosum s.l. For Ecol Manag 260:692–698. doi:10.1016/ j.foreco.2010.05.024

Ozaki, K., Saito, H., Yamamuro, K., 2004. Compensatory photosynthesis as a response to partial debudding in ezo spruce, *Picea jezoensis* seedlings. Ecol. Res. 19, 225–231.

Pataki, D.E., Oren, R., Phillips, N., 1998. Responses of sap flux and stomatal conductance of *Pinus taeda* L. Trees to stepwise reductions in leaf area. J. Exp. Bot. 49, 871–878.

Pendall, E., 2000. Influence of precipitation seasonality on pine cellulose $\delta^{2}H$ values. Global Change Biology 6, 287–301.

Pollastrini M. et al. 2013. Intra-annual Pattern of Photosynthesis, Growth and Stable Isotope Partitioning in a Poplar Clone Subjected to Ozone and Water Stress. Water, Air, Soil, Pollution. 224:1761

Quentin, A.G., O'Grady, A.P., Beadle, C.L., Worledge, D., Pinkard, E.A., 2011. Responses of transpiration and canopy conductance to partial defoliation of Eucalyptus globulus trees. Agric. For. Meteorol. 151, 356–364.

Ramesh, R., Bhattacharya, S.K., Gopalan, K., 1985. Dendroclimatological implications of isotope coherence in trees from Kashmir Valley, India. Nature 317, 802–804.

Ramesh, R., Bhattacharya, S.K., Gopalan, K., 1986. Climatic correlations in the stable isotope records of silver fir (Abies pindrow) tree from Kashmir, India. Earth and Planetary Science Letters 79, 66–74. Report 1, pp. 165–169.

Robertson, I., Rolfe, J., Switsur, V.R., Carter, A.H.C., Hall, M.A., Barker, A.C., Waterhouse, J.S., 1997. Signal strength and climate relationships in $^{13}C/\ ^{12}C$ ratios of tree ring cellulose from oak in southwest Finland. Geophysical Research Letters 24, 1487–1490.

Roden, J.S., Lin, G., Ehleringer, J.R., 2000. A mechanistic model for interpretation of hydrogen and oxygen isotope ratios in tree-ring cellulose. Geochimica et Cosmochimica Acta 64, 21–35.

Saurer, M., Borella, S., Schweingruber, F., Siegwolf, R., 1997. Stable carbon isotopes in tree rings of beech: climatic versus site-related influences. Trees 11, 291–297.

Saurer, M., Cherubini, P., Siegwolf, R., 2000. Oxygen isotopes in tree rings of Abies alba: The climatic significance of interdecadal variations. J. Geophys. Res. Atmospheres 105, 12461–12470.

Saurer, M., Schweingruber, F.H., Vaganov, E.A., Shiyatov, S.G., Siegwolf, R., 2002. Spatial and temporal oxygen isotope trends at northern tree-line Eurasia. Geophysical Research Letters 29, 10–14.

Saurer, M., Siegenthaler, U., 1989. $^{13}C/\ ^{12}C$ isotope ratios in tree rings are sensitive to relative humidity. Dendrochronologia 7, 9–13.

Saurer, M., Siegenthaler, U., Schweingruber, F., 1995. The climate– carbon isotope relationship in tree rings and the significance of site conditions. Tellus 47B, 320–330.

Saurer, M., Siegwolf, R., Borella, S., Schweingruber, F., 1998. Environmental information from stable isotopes in tree rings of *Fagus sylvatica*. In: Beniston, M., Innes, J.L. (Eds.), The Impacts of Climate Variability on Forests. Springer, Berlin, pp. 241–253.

Scheidegger, Y., Saurer, M., Bahn, M., Siegwolf, R., 2000. Linking stable oxygen and carbon isotopes with stomatal conductance and photosynthetic capacity: a conceptual model. Oecologia 125, 350–357.

Schiegl, W.E., 1974. Climatic significance of deuterium abundance in growth rings of *Picea*. Nature 251, 582–584.

Schleser, G.H., Helle, G., L. ucke, A., Vos, H., 1999. Isotope signals as climate proxies: the role of transfer functions in the study of terrestrial archives. Quaternary Science Reviews 18, 927–943.

Schmidt-Vogt, H., 1977. Die Fichte, Bd. I. Parey, Hamburg

Schweingruber, F.H., 1996. Tree rings and environment: dendroecology. Paul Haupt AG Bern, Berne, Switzerland.

Schwenke, W., 1963. über die Beziehungen zwischen dem Wasserhaushalt von Bàumen und der Vermehrung blattfressender Insekten. Z. Angew. Entomol., 51: 371-376.

Shain L. 1979. Dynamic responses of differentiated sapwood to injury and infection. Phytopathology. 69:1143–1147

Sheu, D.D., Kou, P., Chiu, C.-H., Chen, M.-J., 1996. Variability of tree-ringd 13 C in Taiwan fir: growth effect and response to May–October temperatures. Geochimica et Cosmochimica Acta 60, 171–177.

Simard, S., Elhani, S., Morin, H., Krause, C., Cherubini, P., 2008. Carbon and oxygen stable isotopes from tree-rings to identify spruce budworm outbreaks in the boreal forest of Quebec. Chem. Geol. 252, 80–87.

Simard, S., Morin, H., Krause, C., Buhay, W.M., Treydte, K., 2012. Tree-ring widths and isotopes of artificially defoliated balsam firs: A simulation of spruce budworm outbreaks in Eastern Canada. Environ. Exp. Bot. 81, 44–54.

Sonninen, E., Jungner, H., 1995. Stable carbon isotopes in tree-rings of a Scots pine (*Pinus sylvestris* L.) from northern Finland. Pal. aoklimaforschung 15, 121–128.

Stalpers J.A. 1978. Identification of wood-inhabiting *Anphyllophorales* in pure culture. Studies in mycology no. 16. Centraal bureau voor Schimmelcultures, Baarn

Stuiver, M., Braziunas, T.F., 1987. Tree cellulose $^{13}C/\ ^{12}C$ C isotope ratios and climate change. Nature 328, 58–60.

Switsur, V.R., Waterhouse, J.S., Field, E.M., Carter, A.H.C., 1996. Climatic signals from stable isotopes in oak tree-rings from East Anglia, Great Britain. In: Dean, J.S., Meko, D.,M., Swetnam, T.W. (Eds.), Tree Rings, Environment and Humanity Radiocarbon, pp. 637–645. Radiocarbon, Arizona.

Switsur, V.R., Waterhouse, J.S., Field, E.M.F., Carter, A.H.C., Hall, M., Pollard, M., Robertson, I., Pilcher, J.R., Heaton, T.H.E., 1994. Stable isotope studies of oak from the English Fenland and Northern Ireland. In: Funnell, B.M., Kay, R.L.F. (Eds.), Palaeoclimate of the Last Glacial/Interglacial Cycle. Natural Environment Research Council Special Publication 94/2, 67–73.

Tardif J.C. et al. 2008. Tree rings, δ13C and climate in Picea glauca growing near Churchill, subarctic Manitoba, Canada.

Thor, M., Bendz-Hellgren, M., Stenlid, J., 1997. Sensitivity of Root Rot Antagonist *Phlebiopsis gigantea* spores to high temperature or pressure. Scand. J. For. Res. 12, 356–361.

Thor, M., Ståhl, G., Stenlid, J., 2005. Modelling root rot incidence in Sweden using tree, site and stand variables. Scand. J. For. Res. 20, 165–176.

Trägårdh, I., 1939. Sveriges Skoginsekter. Gebers, Stockholm.

Ulla Mattila, T.N. Assessing the Incidence of Butt Rot in Norway Spruce in Southern Finland.

Veblen, T.T., Hadley, K.S., Reid, M.S., Rebertus, A.J., 1991. Methods of detecting past spruce beetle outbreaks in Rocky Mountain subalpine forests. Can. J. For. Res. 21, 242–254.

Wershaw, R.L., Friedman, I., Heller, S.J., 1966. Hydrogen isotope fractionation in water passing through trees. In: Hobson, F., Speers, M. (Eds.), Advances in Organic Geochemistry. Pergamon, New York, pp. 55–67.

Wingate L. et al. 2007. Variations in 13C discrimination during CO2 exchange by Picea sitchensis branches in the field. Plant, Cell and Environment. 30, 600-616

Woodward S, Stenlid J, Karjalainen R et al. 1998. *Heterobasidion annosum*: biology, ecology, impact and control. Cab International, Wallingford

Acknowledgements

First of all I thank prof. Andrea Battisti, dr. Federica Camin and dr. Nicola La Porta for the valuable comments to the manuscripts and for the great support during these years.

I wish to thank Magdalena Nötzli and Anne Verstege (WSL, Birmensdorf, Switzerland) for their assistance with measuring and dr. Paolo Cherubini who allowed me to work in a wonderful "dendroLAB", thank for the great support and help during my staying at Zurich.

I have to thank the great dr. Ari Hietala (Norwegian Forest and Landscape Institute, Ås, Norway), thank for the kind hospitality in the beautiful Ås (Norway).

I would like to thank dr. Ron Wehrens (FEM, S. Michele all'Adige, Italy) for a valuable help in statistical analysis, prof. Marco Carrer (Padova University) and dr. Patrick Fonti (WSL, Birmensdorf, Switzerland) for the course in Dendrochronology.

Andrea Bertagnolli, Giorgio Behaman and Rino Braito (Magnifica Comunità di Fiemme, Italy) for allowing me to sample the trees.

Emanuele Eccel, Annalisa Piazzi and Luca Delucchi (FEM, S. Michele all'Adige, Italy) for their suggestions concerning the meteorological analysis. Luca Ziller (FEM, S. Michele all'Adige, Italy) for valuable laboratory assistance.

I really thank my colleagues and friends for their support and, above all, for their companionship.

...and,

"tantissimi baci alle mie ragazze Martina e Caterina!"